Delft University of Technology

Sensitivity Analysis of Vehicle-to-Grid based Ancillary Services

Marcel E. Otte

TU Delft

PORSCHE

Sensitivity Analysis of Vehicle-to-Grid based Ancillary Services

by

Marcel Eckhard Otte

to obtain the degree of Master of Science
at the Delft University of Technology,
to be defended publicly on Monday October 18, 2021 at 1:00 PM.

Student number:	5161215	
Project duration:	February 1, 2021 – October 18, 2021	
Thesis committee:	Prof. Dr. Peter Palensky,	TU Delft, supervisor
	Dr. Miloš Cvetković,	TU Delft, daily supervisor
	Dr. David Dallinger,	Porsche AG, daily supervisor
	Dr. Gautham Ram Chandra Mouli,	TU Delft

This thesis is confidential and cannot be made public until October 18, 2022.

TU Delft

PORSCHE

Sperrvermerk

Die vorliegende Abschlussarbeit enthält zum Teil Informationen, die nicht für die Öffentlichkeit bestimmt sind. Während einer Sperrzeit von 0 Jahren ab dem Abgabedatum liegt das alleinige Recht zur Verwertung, insbesondere zur Verbreitung der Abschlussarbeit, auch auf elektronischen Medien, bei der Dr. Ing. h.c. F. Porsche AG.

Während dieser Sperrzeit darf die Abschlussarbeit - sei es in Teilen oder als Ganzes - nur mit der ausdrücklichen schriftlichen Genehmigung der Dr. Ing. h.c. F. Porsche AG an Dritte weitergegeben werden.

Die vorliegende Abschlussarbeit ist zur Vorlage zur Anerkennung der Prüfungsleistung freigegeben.

Stuttgart, den

Kramer Joachim
VWPKI
69FCA5DE3126164C

Digital unterschrieben von
Kramer Joachim VWPKI
69FCA5DE3126164C
Datum: 2021.10.05
14:50:18 +02'00'

Unterschrift Abteilungsleiter/in

Abstract

In order to decrease carbon emissions of the transport sector, the roll-out of plug-in electric vehicles (PEV) aims a replacement of conventional combustion-based vehicles. Their intended power system integration goes along with increasing the share of renewable energies. Hereby, PEV have the prerequisites for intelligent charging to support grid stability and increasing the utilisation of fluctuating renewable energies. Beside integrating PEV as an intelligent load, the approach using the PEV's battery capacity to serve power system needs can further increase the value of PEV in the power system. Thus, for compensating additional stress on the PEV's components, ancillary services revenues are commonly measured against PEV's wearout for Vehicle-to-Grid (V2G) applications. Depending on the selected driving pattern, location, battery, regulation and revenue of ancillary services, use cases lead to different conclusions. In the scope of this thesis, it is argued that ongoing transitions in the power system and transport sector result in uncertainties how these use case and its dependencies change in the future. However, the technical prerequisites of V2G based ancillary services, which subject to physical, chemical and electrical processes, are known, whereby a broad view on use cases is essential. Hence, in this thesis, the sensitivity of these services is measured against vehicle characteristics from a technical point of view. This work identifies more than 30 technical dependencies that affect the PEV's degradation and total discharging costs. With respect to the Dutch energy market, the results demonstrate that Vehicle-to-Grid costs can lead to a significant market potential loss. However, operation conditions exists, which lead not only to a high market potential in the balancing and day-ahead market, but also in a reduction of battery degradation. Based on the sensitivity results, implications that cover the regulation, business, user and technical layers of Vehicle-to-Grid are given based on an architecture model. The presented work allows identifying use case related dependencies and therefore helps to clarify the reasons for the different results/conclusions on V2G research.

Acknowledgements

Herewith, I want to express my deepest thanks to
Prof. Dr. Peter Palensky
Dr. Miloš Cvetković and
Dr. Gautham Ram Chandra Mouli
for the excellent supervision at
the Delft University of Technology.

Furthermore, I am extremely grateful for the exceptional support of
Dr. David Dallinger and
the Porsche AG.

Finally, a special thanks to my lovely family and friends.

Marcel Eckhard Otte
Delft, 2021

Contents

List of Figures

List of Tables

1 Introduction

Driven by the decarbonisation of the transport sector, plug-in electric vehicles intend to replace combustion based engines. Their integration into the power system provides opportunities for grid supporting functionalities like Vehicle-to-Grid based ancillary services [50]. Nevertheless, the complexity of both, the power grid and electric vehicles, result in a variety of dependencies that affect the integration approach.

In this chapter, Section 1.1 outlines the impact of electric vehicles on the power grid, first. Secondly, the derived problem definition will be revealed in Section 1.2 to define the research question of the thesis. Thirdly, Section 1.3 presents the methodology applied in this thesis. Finally, the last section defines the scope of the work to complete the theoretical approach behind the research question.

1.1. Electric Vehicles & their Impact on the Power Grid

Before laying focus on electric vehicles, it is necessary to understand how a reduction of carbon emissions foster a paradigm change in the power system. The design of existing power grids is driven by a hierarchical and centralised approach with fossil fuel powered plants at the transmission level and a unidirectional powerflow to the consumers [26]. However, not only combustion engines of vehicles, but also fossil fuel powered plants underlay the usage of limited and carbon based resources like coal or oil. Hence, to meet global emission targets a replacement by sustainable technologies are a key for future power systems.

On the one hand, technologies like windpowerplants and photovoltaic systems foster a carbon emission reduction, but on the other hand, they inject uncertainties due to their weather dependant power output. Hence, increasing the share of renewable energies increases the demand for flexibilities and storage technologies in the grid for balancing supply and demand at any given time. Hereby, it is possible to generate electricity at low cost by using a mix of several technologies [9]. Beside integrating storage technologies, expanding information and communication technologies results in a more intelligent power grid that enables and identifies flexibilities. The so-called smart grids are expected to be ”resilient, “green,” and efficient” [62].

How are electric vehicles influencing the power system? It is expected, that a share of 15 % of electric vehicles in Europe for the year 2030 increases the overall energy consumption by roughly 3 % [90]. Increasing the number of electric vehicles enlarges the role of this technology within the energy market. From a power system perspective a plugged-in electric vehicle can be either integrated as an uncontrolled load, flexible load or as an additional storage unit. Hence, charging and discharging an electric vehicle varies in terms of methodology and power rating, which system design is a key for the large scale penetration.

The rollout of uncontrolled charging methods is simple, but impedes the grid operator to maintain grid stability, power quality and operational efficiency [80]. Mainly large scale fleets following an

uncontrolled charging methods at peak hours can increase the overall system costs. Not only higher energy prices at peak hours, but also the expansion of physical limits towards higher power ratings increases the overall costs. From an information and communication technological perspective, no communication between the grid operator and the vehicle is required.

With controlled charging approaches, the adjustment of the vehicle's charging power is able to reduce costs and stresses on the power system. From a user perspective, intelligent charging is commonly used in combination with a photovoltaic system to promote the usage of carbon emission free and cheap electricity [95]. By enhancing communication infrastructures between the vehicle and grid operator, controlled charging provides opportunities for load shedding, demand response and other services.

By further increasing the role of electric vehicle's in the power system, a bidirectional charging approach allocates the vehicle's battery as an energy storage for the grid. Jochem et al. [36] argue that one million electric vehicles, that provide 10 kWh of their capacity, could replace two large pump storage power plants (10 GWh). Hence, so-called Vehicle-to-Grid approaches enlarge the capabilities for grid service provisions and the stability of the power system. However, bidirectional power electronics are required and discharging the vehicle's battery influences the user and its primary interest of mobility.

Overall, with an increased share of renewable energies at the distribution level, the transportation of energy to the vehicle can be reduced to a few meters. Compared to internal combustion engines in locations like Europe, where the gasoline is imported, electric vehicles can charge the required energy from sustainable energy technologies directly. The decentralised organisation of future power system allows concepts such as Vehicle-to-Home or Vehicle-to-Neighbourhood.

1.2. Problem Definition & Research Question

The increasing share of renewable energy sources and electric vehicles foster the demand for controlled charging methods. It is evidently that with a large scale penetration of vehicles, controlled charging methods are likely to be implemented to accelerate their integration. However, it is not apparent, if bidirectional charging capabilities should be enabled to serve the demand of the grid.

The literature indicates an ambiguous perspective on the economical benefit of Vehicle-to-Grid based services. On the one hand, Noori et al. [58] conclude that Vehicle-to-Grid "is very likely to be profitable for vehicle owners […]". Further examples, which evaluate Vehicle-to-Grid as economical, can be found in references [39, 57]. On the other hand, Bishop et al. [6] argue that it is "likely aggregator revenues are insufficient to cover the additional battery degradation costs […]". References [18, 76] lead to similar results.

Beside economical uncertainties, socio-technical and technical assumptions may have a noticeable impact on the practicability of Vehicle-to-Grid. Because not all driving patterns, user behaviours, types of vehicle and infrastructures may be profitable, a broad view is essential. Moreover, paradigm changes in the power system as well as in the transport sector take place. Hence, it is not known, how further developments like the degree of autonomous driving or market designs influence all above mentioned aspects.

By applying a sensitivity analysis on Vehicle-to-Grid based ancillary services in technical terms, socio-technical and economical uncertainties can be eliminated. Hence, instead of applying a use case driven investigation, this approach can reveal favourable conditions and identifies sensitive parameters. Thus, the research question is defined as:

How sensitive are bidirectional charging capabilities
for Vehicle-to-Grid based ancillary services against vehicle characteristics?

The focus of the thesis intends to rely on a model driven approach. Rather than proving if Vehicle-to-Grid is economical feasible, the primary interest is to reveal which parameter affect these outcomes. Hence, the sensitivity analysis primarily focuses on technical parameter.

1.3. Methodology

To solve the research question, a model based sensitivity analysis forms the core of the thesis. Figure 1.1 highlights the applied methodology. The methodology consists of five steps in a chronological order.

Figure 1.1: Methodology to solve the research question.

Firstly, a literature review emphasises existing and emerging ancillary services. Not only Vehicle-to-Grid suitable, but also existing ancillary services provided by synchronous based generator form the scope of Chapter 2. Besides, with an increased share of direct current based generation and storage units, converter based ancillary services emerge. These emerging services may intersect with future requirements for converter that are used for enabling bidirectional charging capabilities.

Secondly, in order to apply a sensitivity analysis, a model for both, the power grid and vehicle has to be derived. To begin with electric vehicles, Chapter 3 presents a model containing relevant parameters such as degradation, efficiency and state of charge. Subsequently, the power system model in Chapter 4 focuses mainly on limits and capacities of representative grid topologies. Thereafter, Chapter 5 summarises the dependencies of both models and derives the analysis framework.

Thirdly, the analysis in Chapter 6, as the main part of the thesis, extracts the sensitivity of technical dependencies in the context of Vehicle-to-Grid suitable ancillary services. Before analysing the electric vehicle in combination with the grid, the sensitivity of bidirectional charging capabilities from the vehicle's perspective is conducted beforehand. Afterwards, four selected ancillary services are in the scope of interest: peak shaving, active power provision for frequency control, active power ramping and reactive power for voltage regulation. Even if the thesis argues that economical aspects are uncertain, a assessment of costs and market potentials will be conducted based on the Dutch energy market. However, rather than deriving if Vehicle-to-grid is profitable, the economical assessment should give an indicator how the technical sensitivity affects the market potential.

Fourthly, an evaluation reflects on the applied methodology and derived results. Hence, Chapter 7 incorporates a critical review of assumptions and approaches made in the thesis. Besides, within the evaluation the model itself and its parameters will be reviewed. Thus, this chapter facilitates to evaluate the results, which are necessary to solve the research question.

Finally, Chapter 8 summarises the main findings of thesis in order to solve the research question. Based on the sensitivity analysis and its outcome, several conclusions can be drawn that are relevant for different disciplines and stakeholder. Furthermore, by answering the research question, sensitive parameters in the context of Vehicle-to-Grid are revealed.

For non-technical readers, Chapter 3 contains a preliminary conclusion, which summarises the findings of the chapter without going into technical depths. With respect to the scope of the work that will be discussed in Section 1.4, this thesis emphasises the importance of evaluating Vehicle-to-Grid as a multidisciplinary topic. Therefore, Vehicle-to-Grid requires, among other things, an analysis of socio-technical, regulatory and market aspects. The preliminary conclusion should facilitate that other disciplines could align their research on the results made within the thesis.

1.4. Scope of the Work

Previous sections refer to Vehicle-to-Grid as a multidisciplinary topic. Integrating electric vehicles into the power system increases not only the technical complexity, but also the impact of socio-technical, market, regulatory related dependencies. Hence, assessing electric vehicle charging and discharging processes as a multidisciplinary topic, facilitates the identification of uncertainties, stakeholder dependencies and their sensitivities. This thesis relies on an architecture model, which projects these aspects.

Solving the research question requires the identification of parameter that are relevant for the scope of the thesis. For this purpose, Figure 1.2 depicts the developed multidisciplinary architecture model.

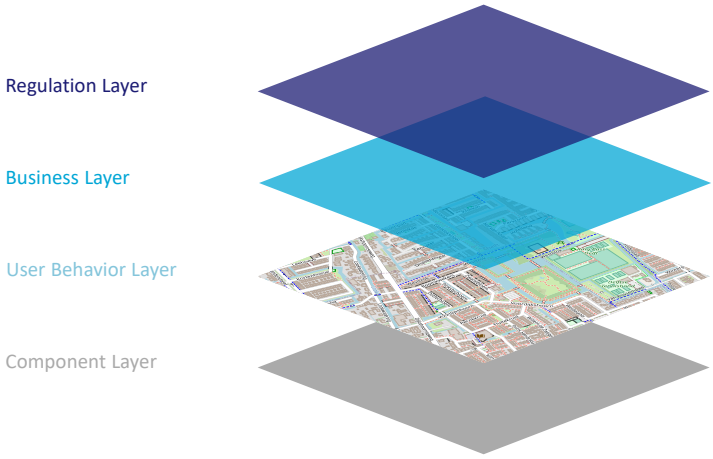

Figure 1.2: Architecture model representing Vehicle-to-Grid as a multidisciplinary topic.

The presented architecture in Figure 1.2 defines electric vehicle studies in four layers: regulation layer, business layer, user behaviour layer and component layer. While the three upper layers portray involved stakeholders, mechanism, design rules and behaviours, the bottom layer mainly describes the physical nature of electric vehicles and their power system integration. Compared to other use case models, like the Smart Grid Architecture Model [73], which can be applied on electric vehicle use cases [44], the presented architecture is stakeholder and disciplinary driven. Hence, the applied architecture model focuses on highlighting layer dependencies and affiliations. Not only use cases can be depicted, but also the identification of parameter are mappable on each layer.

In the scope of this thesis, the sensitivity analysis focuses on the component layer. Compared to the upper layers, the component layer mainly subjects to chemical, physical and electrical phenomena. Hence, those sensitivities lead to favourable and avoidable conditions, which have to be revealed beforehand. In example, the development of suitable business models or selected use case can shift focal points to those conditions. Thus, applying a layer wise analysis allows to extract the sensitivity of each layer individually. Furthermore, in this work it will be assumed that the energy transition as well as the transition of the transport sector lead to uncertainties in the upper layers. To prevent assumptions, which may not be valid in the future, these uncertainties can be reduced by focusing on the component layer.

Shifting the scope on the layered approach facilitates which parameter and dependencies should be addressed in the thesis. Consequently, the layers can be summarised as follows:

The top layer defines the regulation layer, which includes, among other things, grid codes and regulatory frameworks. Along with the increased share of renewable energies and the penetration of electric vehicles, new regulations and political decisions are like to emerge. For a comprehensive integration

of electric vehicles, standards and regulation will need to be expanded [8]. Similar to photovoltaic system and wind power plant regulations, a higher penetration can increase the opportunities for new grid services as it will be explained in later chapters.

The business layer intends to identify a financial benefit for the user behaviour with respect to the regulation framework and technical capabilities. For unidirectional controlled and uncontrolled charging, plugging in the vehicle is a reaction to the interest of mobility. However, for Vehicle-to-Grid, a common approach is to create financial incentives to plug in the vehicle even if it is already charged. Hence, a Vehicle-to-Grid business model primarily has to compensate a lower state of charge and/or battery degradation. Mechanism like flexible tariffs or free charging indicate how a layer has its degrees of freedom but affects other layers, simultaneously. Besides, a higher electric vehicle penetration can lead to an aggregator that participates beyond being a price taker [32].

The user behaviour layer covers all dependencies, that affects how a user interacts with the technology itself. Hereby, the user behaviour covers the charging profile and driving pattern according to the individual user. As an example, parameter like the driving pattern determine the availability of the electric vehicle for Vehicle-to-Grid services.

The technical layer forms the scope of the work that requires a comprehensive analysis of the working principle. Thus, Figure 1.3 represents a simplified representation of Vehicle-to-Grid divided into three subsystems: the AC power grid, the electric vehicle supply equipment (noted as EVSE) and the vehicle's battery.

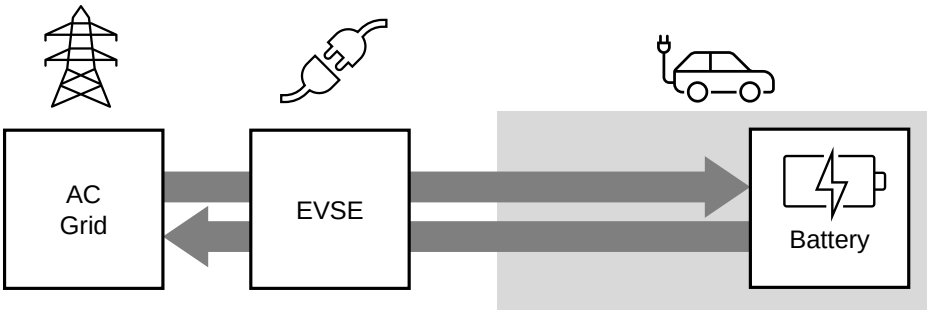

Figure 1.3: Vehicle-to-Grid as a system consisting of the AC grid,
the electric vehicle supply equipment (EVSE), the electric vehicle (EV) and its battery.

The parameter of each subsystem will be revealed in Chapter 3. Without going into depth at this point, the sensitivity of the component layer reveals favourable and avoidable conditions.

1.5. Scientific Contribution

Use-case driven Vehicle-to-Grid research are well presented in literature [6, 11, 58, 64, 91, 92, 97]. To continue research on Vehicle-to-Grid, a multidisciplinary and analytical methodology will be applied. More depth into the sensitivity of the component layer is necessary to reveal favourable and avoidable conditions independent of the user, regulation and business model. This methodology will be applied to consider the individuality of users and the multidisciplinary frame of Vehicle-to-Grid research. Accordingly, this section will elaborate the scientific contribution by taking other disciplines into account. As an example, socio-technical research will be considered to emphasise why it is crucial to provide a sensitivity analysis independent of the user, regulation and business model.

In the scope of this work, it is argued that the use cases subject to several uncertainties induced, among other things, by the user. It is a common research approach to model the user as an optimiser, who minimises or maximises a certain interest. With respect to Vehicle-to-Grid, the objective function can vary significantly. Hence, it is uncertain if a user optimises in terms of: self-sufficiency, costs, lifetime battery, sustainability, vehicle range, technological pioneering or none of them above. Even if a financial driven objective function is likely, it may be possible as well that the optimisation approach of a user is unpredictable. Socio-technical driven research emphasise the role of the user and even criticise the neglected social dimensions in the context of Vehicle-to-Grid. In their review, Sovacool et al. [82] emphasised that the user behaviour in terms of Vehicle-to-Grid research is covered in only 3.7 % of the literature. In addition to that, Harris et al. [32] questioned that Vehicle-to-Grid research commonly assume perfect knowledge about driving patterns and vehicle usage. Furthermore, they criticise the approach to evaluate an aggregator exclusively as a price taker. They refer to the work of Sioshansi et al. [79], who analysed large scale grid storage systems and noted that using such an assumption can lead to an overestimation of income. Furthermore, socio-technical research identified individual acceptance [84, 96] and individual user behaviour [28, 56]. Thus, it is argued that each user should be analysed individually to identify their suitability in the context of Vehicle-to-Grid [7, 27].

How are socio-technical dimensions affecting Vehicle-to-Grid use cases? For a better understanding the architecture model from the previous section will be again taken into account. Figure 1.4 visualises both, how use cases are portrayed and the objective of this sensitivity analysis on the right-hand side.

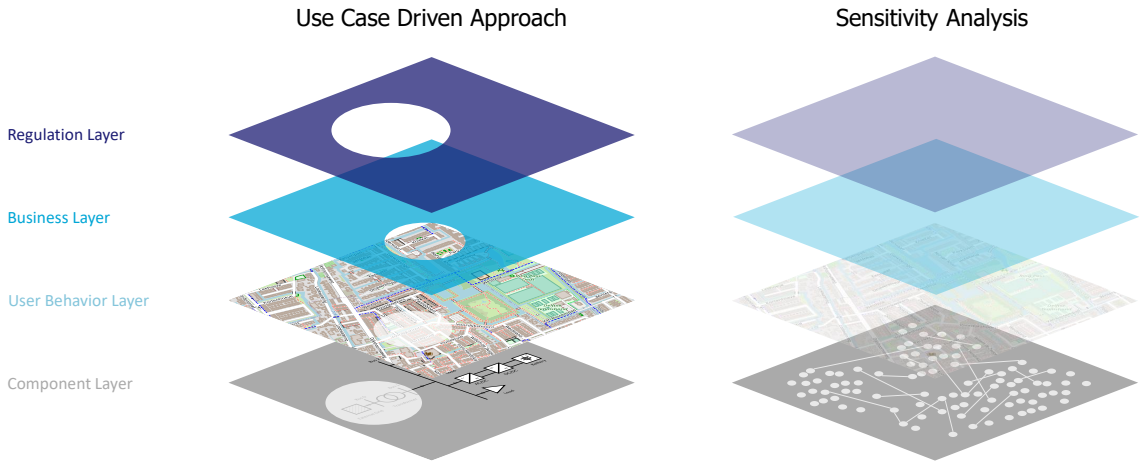

Figure 1.4: The architecture model compares use case driven Vehicle-to-Grid research with the sensitivity analysis of this work.

As the figure emphasises, use cases are able to cover a specific area from each layer, whereby it is possible to evaluate that specific use cases. This methodology allows if the objective of Vehicle-to-Grid is satisfied. For example, if the financial income is high enough to compensate the user. Commonly, a sensitivity analysis enhances the work to discuss how the relevant parameter affect the objective.

However, within this work, it is argued that the sensitivity analysis of the component layer can extract the sensitivities more independent and comprehensively.

How to enhance the research already conducted on Vehicle-to-Grid by considering the social dimensions? Beside the regulation and business layers, the social dimensions of Vehicle-to-Grid are proven to exist leading to uncertainties in the user behaviour layer, as discussed above. Applying a use case driven methodology will tend including assumptions about each layer, which are likely to affect total outcome. Hence, avoiding user, business and regulation induced uncertainties allows extracting sensitivities of Vehicle-to-Grid independent of those assumptions. The right-hand side of Figure 1.4 visualises the approach, which indicate and assumes several relationship and operation conditions at the component layer. Extracting the sensitivity without defining a use case facilitates to identify favourable conditions. Hence, this methodology supports research to sharpen the focus on user behaviours, business models, regulation approaches, which are most suitable for Vehicle-to-Grid. Instead of providing results, that are already affected by these uncertainties, one can extract sensitivities, that are from a technical point of view. Therefore, a broader variety of cases can be portrayed, which necessity is raised by Sovacool et al. [81].

2

Existing & Emerging Ancillary Services

The transmission of electrical energy requires an actively controlled power system designed for a stable and secure grid operation. Accordingly, ancillary services have the functionality to intervene supportively in operation conditions guaranteeing those requirements. Thus, this chapter covers existing ancillary services and those who will emerge due to an increased share of sustainable energy technologies. Firstly, Section 2.1 presents an overview of existing ancillary services. Secondly, due to the paradigm change in the power system, further converter based ancillary services emerge, which are described briefly in Section 2.2. Thirdly, it follows a description of Vehicle-to-Grid suitable ancillary services.

2.1. Existing Synchronous Generator Based Ancillary Services

The conventional control approach relies on the inherent characteristics of synchronous generators [61]. Hereby, large power plants are connected at the transmission level that are controlled by the Transmission System Operator. The following existing ancillary services are summarised and selected based on the review of Oureilidis et al. [61], who described the most common types of ancillary services in the European Union.

2.1.1. Frequency Control

An instantaneous imbalance between generation and consumption directly results in deviations from the nominal system frequency. If the energy demand exceeds the generation, the system frequency declines, while the opposite case induces a frequency incline. Thus, frequency measurements in conventional AC based power system are a direct measure for identifying if generation and consumption have to be aligned. For this purpose, different stages for frequency control exist: Frequency Containment Reserves (FCRs), Frequency Restoration Reserves (FRRs) and Replacement Reserves (RRs) [61].

The three control stages are implemented sequential to cope with the system frequency deviations. Figure 2.1 depicts a simplified schematic of the implemented frequency control sequence. The simplified representation considers the non unity of regulation market requirements across European countries.

The first measure against frequency imbalances is Frequency Containment Reserves or also called Primary Frequency Control. It is intended to compensate the mismatch that leads to imbalances by active power reserves. Usually, the activation of Frequency Containment Reserves takes place within 30 s [61].

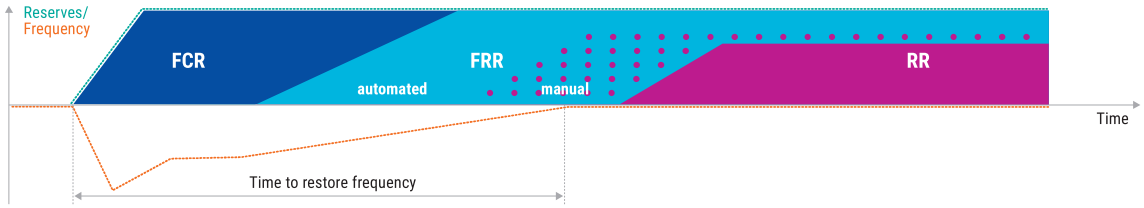

Figure 2.1: Frequency control [24]

Secondly, Frequency Restoration Reserves (Secondary Frequency Control) restore the system frequency to the nominal value. Hereby, the Transmission System Operator activates reserves in the time interval between 30 s and 15 min after the imbalance [61]. One differentiates between automatic Frequency Restoration Reserves (aFRR) and manual Frequency Restoration Reserves (mFRR). Both refer to an either automatically or manually activation of reserves.

Lastly, the Replacement Reserves (Tertiary Frequency Control) are activated restoring and supporting Frequency Restoration Reserves [37]. The manual activation takes place between 15 min (Continental Europe) and hours after the imbalance [61]. Replacement Reserves intend to maintain the system optimum [37].

2.1.2. Voltage Control

Ensuring a stable voltage throughout the whole power system is an objective investigated since decades [41, 93]. Voltage imbalances can occur among others due to tripping generators or power transmission over long distances [94]. The threshold exceedance of voltage levels directly harms system components, whereby concepts such as undervoltage load shedding exist to prevent damage. However, disconnecting loads can be prevented by prior voltage control. Thus, to adjust the voltage level, one controls the leading or lagging reactive power injection. This can be realised by Automatic Voltage Regulators (AVRs) or Static VAR Compensators (SVCs) [61]. Unlike the frequency, voltage is not a system wide synchronised unit. However, similar to frequency control, a three-level hierarchy control based on reactive power provision is present in European power systems [61].

The first measure against the occurrence of voltage deviations is Primary Voltage Control. Based on a local automatic control, which is activated, one adapts reactive power injection physically close to the occurrence of deviation [37]. This first control approach takes place within milliseconds and continues up to one minute [61].

As a second step, Secondary Voltage Control regulates the pilot busses to minimise the deviations at load busses [17]. In contrast to Primary Voltage Control, this subsequently control approach is centralised. Hereby, the activation usually takes place one minute after deviation and can last for several minutes [61].

Lastly, Tertiary Voltage Control intends to be activated relieving reactive power reserves. Hereby the control will be activated manually. After a power flow analysis, optimization of network losses are considered for relieving the reserves. Tertiary Voltage Control activates 10–30 min after the occurrence of voltage deviations [61].

2.1.3. Black-Start Capability

Electricity is a fundamental part of the society relying on a critical infrastructure. Hence, all control mechanism contribute to a stable and secure power system. However, not all blackouts or interference rely on failures within the power system that can be controlled or mitigated. Thus, black-start capabilities are necessary to restore the power system after a black-out takes place.

The cause for every second blackout in the power system are based on weather conditions and falling trees. In their survey, Haes Alhelou et al. [31] analysed not all, but major power system blackouts between 2011 and 2019 around the globe. They list that faulty equipment or human error are the cause for 31.8 % of the blackouts, while weather and falling trees are listed with 50 %. Shifting the scope to the number of affected people, transmission line overload in India affected 620 million people, while the Cyber-attack in Ukraine 230 Million people.

To start the grid after a blackout, appropriate generation units intend to restore the operation after a partial or full shutdown [61]. Hereby, for performing a black-start, the generation units are able to inject energy into the grid without requiring external electrical energy supply. Thus, facilitating the start of other generation units. Not only power plants, but also storage units like pumped storage are able to provide the black-start service to the grid [61].

2.2. Emerging Converter Based Ancillary Services

In their work, Oureilidis et al. [61] reviewed six emerging converter based ancillary services, which are inertial response, active power ramp, frequency response, voltage control, fault contribution and harmonic mitigation. The following section will briefly summarise their description.

Along with the penetration of DC based generation and storage units at the distribution system level, new converter based ancillary services emerge. Not only applicable on photovoltaic systems, but also the integration of electric vehicles with bidirectional charging capabilities require a DC to AC conversion that meets grid requirements. Hence, providing converter based ancillary services can contribute to a secure and stable grid operation, while being a key to reduce the total cost of energy [111]. Accordingly, it is advantageous for the overall analysis to also examine this emerging services.

The demand for Inertial Response inclines with the replacement of synchronous based generation units. The inertia of rotating mass provided by synchronous generator intends to stabilise the system frequency autonomously due to their inherent characteristics. Balancing services such as Frequency Containment Reserves are activated subsequently. Hence, the loss of inertia has to be compensated to avoid frequency response degradation. One opportunity is the implementation of synthetic inertia that enables converter emulating synchronous generators [86].

Volatile generation of renewable energies increases the demand for Active Power Ramping. Their non-constant power output and weather dependency leads to undesired ramping rates, which scale up with the penetration. Oureilidis et al. [61] present an example on how to control those rates. They enhanced a windpower plant with a fast storage system for smoothing the power output.

Frequency response is not only capable based on synchronous generators, but also feasible with converter. Also for balancing services is to recognize, that the replacement of conventional power plants leads to the reduction of system power reserves. Hence, decentralised installed converter are capable to adjust the output power based on the measured frequency.

By injecting or absorbing reactive power, converter are capable of Voltage Control. Hereby, a decentralised distribution of converter facilitates to locally control voltage deviations. At the same time, converter overcome the burden that reactive power cannot be transmitted over long distances. Besides, one expects that the volatile generation of renewable energies has an impact on the voltage profile of the transmission grid. Thus, converter based voltage control can cope to mitigate those issues.

Fault contribution by converters can be realised based on Fault-Clearing or Fault Ride-Through methods. Latter describes the converter capabilities to ride through faults while not disconnecting themselves from the grid. One reason for the demand of Fault Ride-Through is avoiding cascading effects that can lead to the shutdown of several power system units. Besides, Fault-Clearing methods can be realised through varies methods. Oureilidis et al. [61] classified those into three main groups: modification of the existing protective methodologies, reducing undesired behaviour of distributed renewable energy sources during short-circuits and advanced method based on adaptive system and communication technologies.

Lastly, Harmonic Mitigation copes with undesired total harmonic distortion in the power system. Not only non-linear loads in modern grids, but also the penetration of converter based generation units injects harmonics into the grid. Hence, as a further emerging ancillary service, the mitigation of harmonics can be realised through active and passive filtering. Latter relies on inductor and capacitor based filter, while active filter compensates the harmonics during operation.

2.3. Ancillary Services in Relation to Vehicle-to-Grid Technologies

Compared to synchronous generator, electric vehicles differ in technical terms, but are also capable of providing ancillary services. Without excluding other possible services, this section focuses on Peak Load Shaving, Active and Reactive Power Regulation. Further services are listed in the work of [19, 23]. Chapter 4 will recap the services and justify the selection for the conducted sensitivity analysis.

2.3.1. Peak Load Shaving & Load Leveling

The instantaneous balance between generation and load as a system requirement for a stable and secure operation, leads to the demand for peak load shaving and load leveling. The volatile generation of renewable energy sources like windpowerplants or photovoltaic systems are examples that put emphasise on this service. Hereby, electric vehicles are not only capable serving this needs, but especially load leveling also offers the opportunity for vehicles to charge exclusively sustainable energy (i.e. solar based charging [59]).

While load leveling refers to charging the vehicle, peak load shaving requires to discharge the vehicle. Figure 2.2 depicts both approaches in a simplified representation.

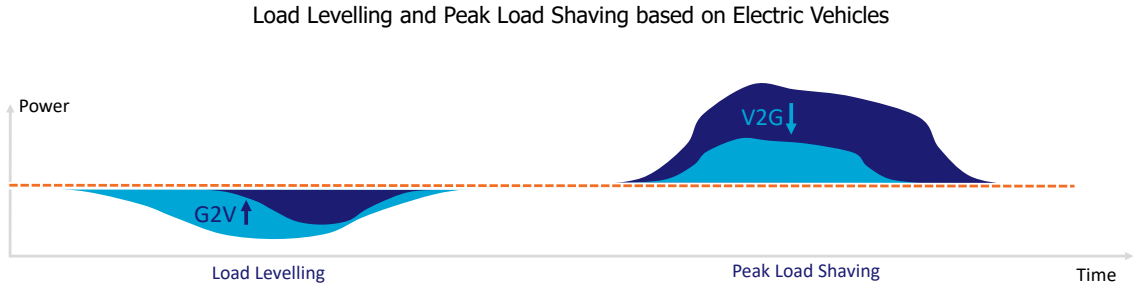

Figure 2.2: Load leveling (Grid-to-Vehicle (G2V)) and Peak Load Shaving (Vehicle-to-Grid (V2G)) based on reference [85].

Focusing on Vehicle-to-Grid, Peak load shaving aims leveling the load by feeding energy into the grid. Hereby bidirectional charging capabilities of an electric vehicle are a requirement for this service.

2.3.2. Active Power Provision for Frequency Control

Active power provision for frequency control holds present market structures. As in the previous section described, bulk generation units at the transmission level are able to provide frequency control on a central approach. Shifting the scope to a major difference by providing the same service through electric vehicles, Figure 2.3 shows example voltage levels for Europe.

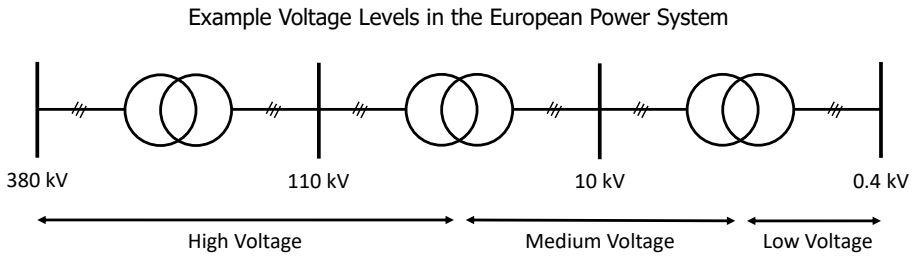

Figure 2.3: Example voltage levels in Europe (adapted from [74]).

On a conventional centralised approach, power plants are connected at high voltage levels [26]. The advantage of frequency is its synchronisation in the power system, whereby it is possible to provide the services in different locations of the grid. Therefore, the decentralised installation of renewable energy sources, storage units and electric vehicles shifts the focus on low voltage levels as well. Hence, the coordination between the Distribution System Operator and Transmission System Operator increases with the penetration [5]. Furthermore, several European countries define a minimum of 1 MW as the minimum power for frequency reserves [61]. Thus, to overcome the limited charging power of vehicles, aggregators are necessary.

2.3.3. Reactive Power Regulation for Voltage Control

Beside the injection of active power, a bidirectional converter topology of vehicles is capable of reactive power provision [105, 108]. Both charging and discharging can lead to local voltage drops across the line as it is visualised in Figure 2.4.

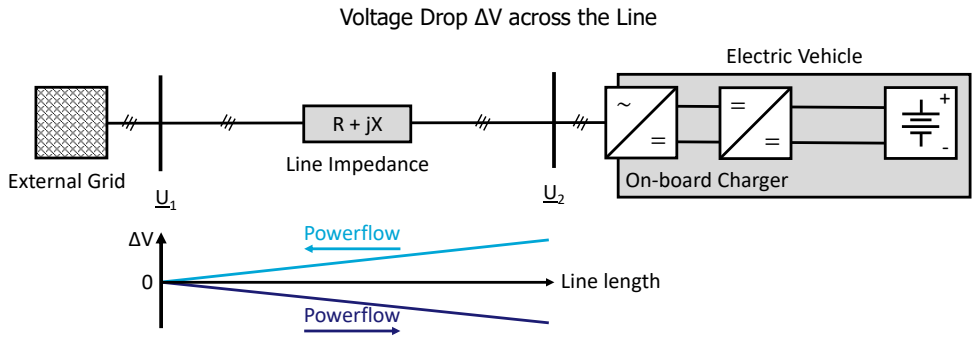

Figure 2.4: Impact of active the active power flow on the voltage magnitude (adapted version of [13]).

As one can see, to maintain the voltage $\underline{U}_1$, the voltage deviation has to be compensated based on the power flow. By injecting less active power, one can lower voltage level deviations to maintain voltage levels at both busses. However, injecting or absorbing reactive power through the on-board charger or charging station mitigates the voltage deviations as well without lowering the active power flow. Besides, electric vehicles have the advantage of controlling voltage deviations locally.

3

Modelling of Electric Vehicles

The previous chapter presents existing and emerging ancillary services as well as those, which are suitable to electric vehicles. In order to analyse the sensitivity of these so-called Vehicle-to-Grid suitable ancillary services, the participation capabilities of an electric vehicle are crucial. Hence, this chapter frames the relevant physical, chemical and electrical processes of the vehicle into a mathematical model to solve the research question in later chapters.

Accordingly, this chapter is organised as follows: firstly, the electric vehicle structure show state-of-the-art interconnections of the battery and supply equipment. Secondly, a closer look into the battery itself and the derived mathematical model is realised. Thirdly, a model for portraying the supply equipment will be presented. Finally, a short preliminary conclusion summarises the main findings for non-technical reader in general terms.

3.1. Structure of an Electric Vehicle

The typical structure of an electric vehicle provide insights on how Original Equipment Manufacturer embed the battery into the vehicle's chassis and how the power electronics are built-in. Accordingly, Figure 3.1 illustrates the chassis itself along with relevant power electronics and the batter pack. Additionally, in Figure 3.2 the battery packaging is visualised based on an open battery pack.

As it can be seen in the first figure, the state-of-the-art electric vehicle embed the battery pack (2) under the driver's position obtaining a low centre of gravity. The front (3) and rear (1) electric motor's

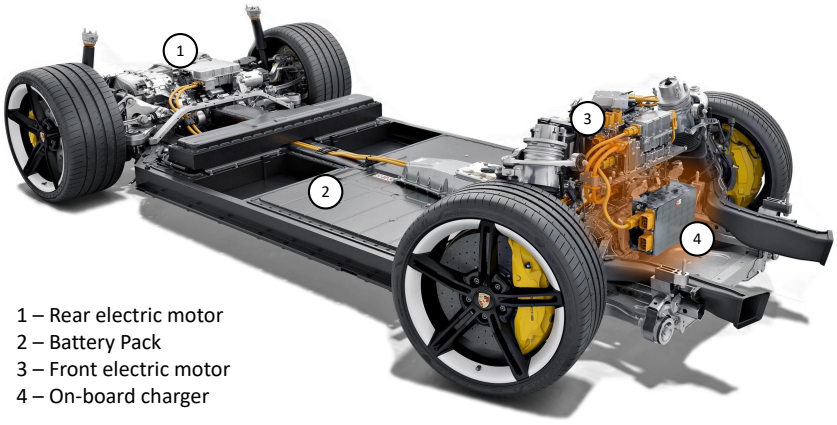

Figure 3.1: Electric vehicle's chassis [22].

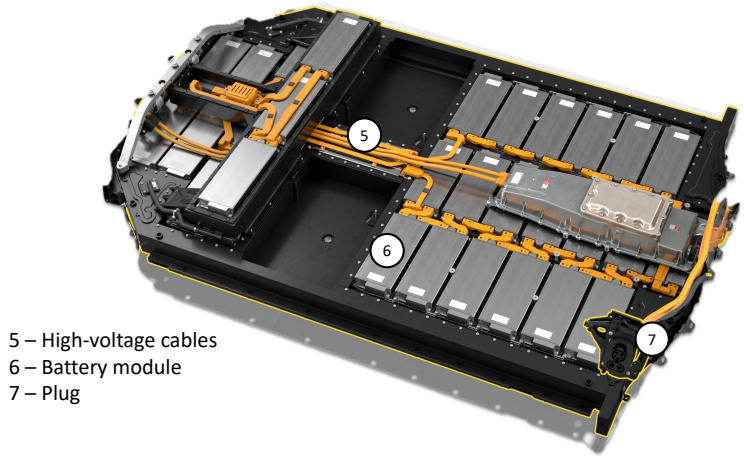

Figure 3.2: Electric vehicle's battery [22].

positions are close to the drive axes. For charging with alternating current, the on-board charger (4), whose proportion is highlighted with an orange shade, is mounted in front of the car as this example presents.

Having a closer look into the battery pack, latter figure shows that one battery pack consists of many battery modules (6). Each battery module interconnects single cells in series obtaining a high board voltage in V and in parallel reaching a high capacity in Ah. Hence, a Li-ion battery can consist of one single or many identical cells [29]. For the interconnection of the modules and the power electronics an orange color indicates high-voltage cables. In order to charge the battery with either direct current or alternating current, standardized plugs (7) are used like CCS1, CCS2, CHAdeMO or others.

3.2. Electric Vehicle's Battery

Compared to combustion based vehicles, where the combustion engine and fuel tank define power and range of a vehicle, both capabilities of an electric vehicle rely mainly on the battery. Currently, Li-ion batteries are used due to their relatively high power and energy density leading to a high to potential for energy storage compared to similar technologies [113]. Accordingly, the working principle of a Li-ion battery will be a central topic within this section, which determines the characteristics of the electric vehicle's battery.

3.2.1. Cell Chemistry of a Li-ion Battery

Deploying a mathematical based electric vehicle model requires a representation of the chemical working principle of a Li-ion battery beforehand. Hence, the schematic of a Li-ion battery is depicted in Figure 3.3 for demonstrating charging and discharging processes.

As the figure outlines, the components of a rechargeable Li-ion battery are an anode, a cathode, a separator, which is highlighted in grey, and an electrolyte. Goodenough[1] defines the working principle as follows: "The chemical reaction between the electrodes has an ionic and an electronic component. The electrolyte transports the ionic component inside a cell and forces the electronic component to traverse an external circuit. In a rechargeable battery, the chemical reaction is reversible" [29]. In an electric vehicle, the external circuit can be either the drivetrain for accelerating the vehicle as a discharging process or an external power supply for the charging process. In this work, the electrical power grid, that represents the ancillary service needs, forms the external circuit. Along with the

[1] John Bannister Goodenough, born July 25, 1922, was awarded with the Nobel Prize in Chemistry together with Michael Stanley Whittingham and Akira Yoshino for their research on lithium-ion batteries.

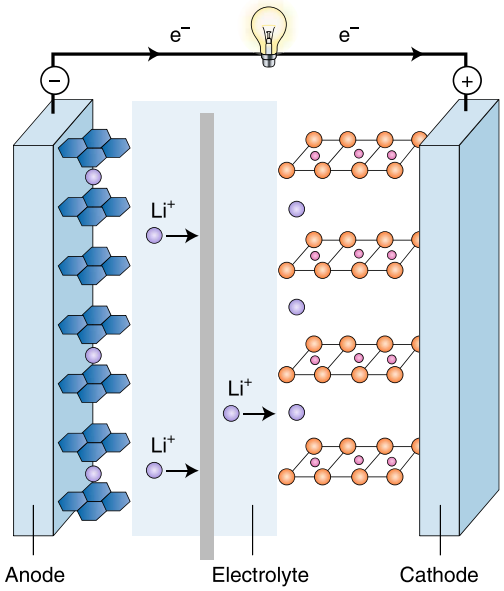

Figure 3.3: Components of a rechargeable Li-ion battery [29].

chemical Equations 3.2.1 & 3.2.5, the charging and discharging process can be further explained.

In a fully charged battery, the anode material is lithiated and passivated with a solid electrolyte interface (SEI). Latter is a layer conducting Li^+, insulating the electronflow and limiting further electrolyte decomposition, which improves the cycle life performance [1]. During discharging, as it was highlighted in Figure 3.3, the delithiation of the anode leads to weight loss due of the anode material loss based on the following oxidation [102]:

$$Li_xC_n \longrightarrow C_n + xLi^+ + xe^- \tag{3.2.1}$$

During delithiation, dissolution of lithium leads to an electron and the ionised Lithium atom. As described above, latter can travel through the electrolyte and separator, while former is driven through an external circuit. The first material used for the anode was graphitic-carbon (LiC_6) [29], which is still applied in state-of-the-art electric vehicles, leading to the following equation [21]:

$$LiC_6 \longrightarrow C_6 + Li^+ + e^- \tag{3.2.2}$$

By discharging the Li-ion battery, the Li-ion flow results in the lithiation of the cathode. Because the electron is driven though the external circuit towards the cathode, the Lithium Ions will react with the cathode material and the electron. Accordingly, the following equation depicts this chemical reduction [102]:

$$x\ Li^+ + x\ e^- + M \longrightarrow Li_xM \tag{3.2.3}$$

Where M represents the lithium alloy of the cathode. Common cathode materials for modern electric vehicles are lithium nickel cobalt aluminium oxide $LiNi_{0.8}Co_{0.15}Al_{0.05}O_2$ (NCA), lithium nickel manganese cobalt oxide $LiNiMnCoO_2$ (NMC) and lithium iron phosphate $LiFePO_4$ (LFP). As an example, Equation 3.2.4 describes the oxidation on a cobalt oxide based cathode:

$$Li^+ + e^- + CoO_2 \longrightarrow LiCoO_2 \tag{3.2.4}$$

The charging and discharging reaction on both electrode materials can be summarised by deriving the corresponding reduction–oxidation. The following chemical equation describes the whole reaction based on a graphitic-carbon anode and a cobalt oxide based cathode:

$$LiC_6 + CoO_2 \underset{\text{charge}}{\overset{\text{discharge}}{\rightleftharpoons}} C_6 + LiCoO_2 \tag{3.2.5}$$

Shifting the scope to the electrolyte, as it was already indicated, its main characteristic is to allow ion travelling. State of the art Li-ion batteries use a mixture of lithium salt and organic solvents [113]. With respect to the SEI layer, the electrolyte composition's properties are crucial for an effective SEI layer formation [1].

Increasing power density in W/kg and energy density in Wh/kg of a Li-ion battery subjects to its complex material properties. Amongst other things, it depends on the voltage potential, density of lithium ions, solid electrolyte interphase (SEI), diffusion coefficient of the electrodes and their conductivity [113]. Here, the cathode material plays a key role for a high energy level by increasing the cathode potential and the capacity of the cathode material [109]. Additionally, Chen et al. [14] explain that the cathode material is the main source of all the active lithium ions. Furthermore, they outline the required reversibly exchange with little structural changes resulting in a long cycle life for the battery material.

In the context of this work, deriving a comprehensive model, which covers all variations of Li-ion battery types, exceeds the scope of the research question. Instead, a selection of a particular battery type has been made. With respect to the state-of-the-art electric vehicle battery technologies and literature review, NMC cell based batteries will be selected. Different electric vehicle studies apply this type of battery in recent publications [11, 12, 97, 98].

3.2.2. State of Charge

In order to measure the level of usable charge remaining in the battery, the state of charge can be taken into account. As a percentage value with respect to the battery's capacity, a battery is fully discharged if the state of charge is 0 % and fully charged at 100 %. Among other things and as it will be explained in the next sections, the state of charge is a parameter for open circuit voltage, charging rate and battery degradation. In order to mathematically describe the state of charge, Equation 3.2.6 will be applied [107]:

$$\mathrm{SoC}(t) = \mathrm{SoC}^0 - \int \frac{I(t) \cdot 100}{\alpha^{\mathrm{U}} \cdot 3600}\,\mathrm{dt} \tag{3.2.6}$$

The state of charge as a function of time t depends on the initial state of charge SoC^0 in %, the usable capacity α^{U} in Ah and the integral over the current I(t). The equation expresses the state of charge in %. Besides, fully discharged or overcharged batteries harm the battery, whereby the real SoC and

the SoC, which is set free for the vehicle's owner differ. Usually, a maximum depth of discharge for the vehicle's battery will be set free for the owner, which is below the maximum of 100 %. Hereby, the battery management system limits the usage of remaining capacity in the battery. In the scope of this work, the full state of charge range from 0 % to 100 % will be investigated.

3.2.3. Open Circuit Voltage

The voltage potential difference between the anode and cathode defines the open circuit voltage V_{oc}. As Section 3.2.1 revealed, a high open circuit voltage increases the power and energy density of a battery. According to the lithiation and delithiation of both electrodes, the open circuit voltage correlates with the state of charge. Consequently, the open circuit voltage can be incorporated as a measure for state of charge and vice versa (see Figure 3.4).

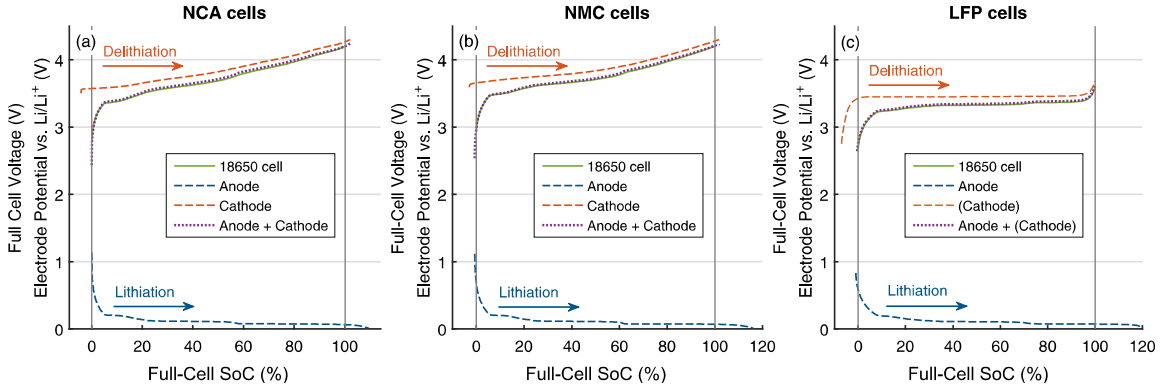

Figure 3.4: Reconstruction of the full-cell voltage of a new cell and the differential voltage spectrum from half-cell data. (a-c) Voltage behavior for low-current charging [38].

The three figures display the open circuit voltage of three different cathode materials as a function of state of charge based on laboratory measurements by Keil et al. [38]. In their work, all three batteries use graphite as the anode material and have a 18650 form. The role of cathode material, resulting in different voltage potentials across the states of charge, becomes obvious. Only a similar voltage behaviour is present throughout all materials for states of charge below 10 %. However, for states of charge above 10 % LFP based cells show an approximately constant voltage with a smaller slope than NCA and NMC cells. Both prior cell's voltages increase steadily after a state of charge of 50 %. Besides, the voltage of LFP cells at high states of charge at around 95 % increases, leading to a peak value.

In order to incorporate a mathematical model of the open circuit voltage into the overall model, an on the state of charge based equation will be selected. In their work, Baccouche et al. [3] developed the following relationship:

$$V_{\text{oc, ev}}\left(\text{SoC}_{\text{ev}}(t)\right) = N_{\text{ev}}^{\text{series}} \cdot \left(p_1 \cdot e^{\alpha_1 \cdot \text{SoC}_{\text{ev}}(t)} + p_2 \cdot e^{\alpha_2 \cdot \text{SoC}_{\text{ev}}(t)} + p_3 \cdot \text{SoC}_{\text{ev}}(t)^2\right) \tag{3.2.7}$$

Where $N_{\text{ev}}^{\text{series}}$ is the number of batteries in series and α_1, α_2 are the dimensionless factors -0.0004523 and -0.1341, respectively. Furthermore, p_1 is given as 3.604, p_1 as -0.2803 and p_1 as $6.871 \cdot 10^{-5}$. These five dimensionless factors subject to the cell temperature and differ if the battery will be either charged or discharged. In order to evaluate these dependencies, Figure 3.5 will be taken into account.

The temperature impact on the open circuit voltage is marginal for states of charges above 10 %. As Figure 3.5a illustrates, the open circuit voltage for lower states of charge can vary up to 0.36 V for a temperature difference of $\Delta T = 40°C$. While for states of charge above 15 % a maximum deviation of

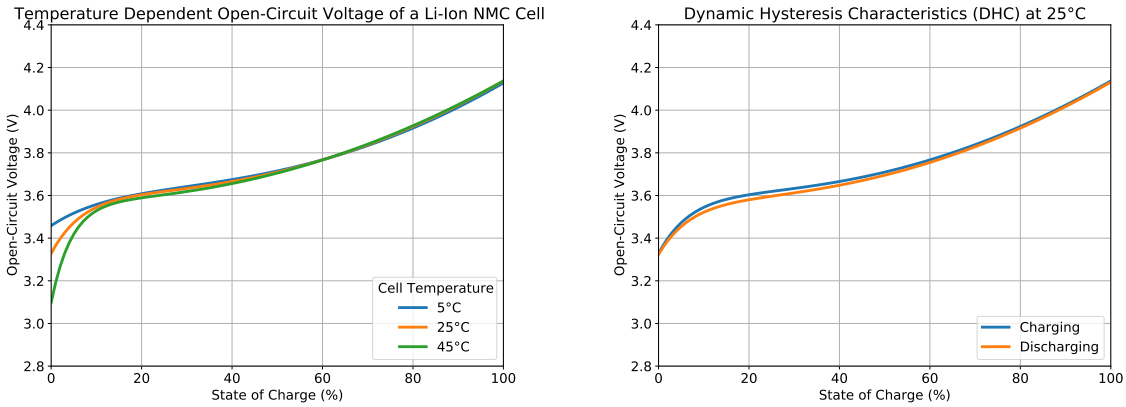

(a) Open circuit voltage at 5°C, 25°C and 45°C.

(b) Open circuit voltage during charging and discharging at 25°C.

Figure 3.5: Open circuit voltage model of Baccouche et al. [3], which depend on (a) temperature and (b) charging & discharging.

less than 0.03 V for the same ΔT is observed.

One may notice the voltage differences during charging and discharging, which is known as the dynamic hysteresis characteristics. As it can be derived from Figure 3.5b, the dynamic hysteresis characteristics has the highest effect on the open circuit voltage at a state of charge of around 15 %. This deviation leads to a voltage difference of 0.025 V at 25°C.

Taking both dependencies into account, the impact of temperature and dynamic hysteresis characteristic on the open circuit voltage will not be considered. Firstly, the effect of different cell temperatures on the open circuit voltage is less than 2 % of the maximum cell's voltage for states of charge above 5 % and less than 0.6 % for states of charge above 15 %. Secondly, the dynamic hysteresis characteristic show a maximum deviation of 0.6 % between the open circuit voltages during charging and discharging. Hence, the introduced dimensionless factors, which are valid for discharging at a temperature of 25°C, are selected along with the mathematical model in Equation 3.2.7.

3.2.4. Charging & Discharging Behaviour

To model the charging and discharging behaviour of a Li-ion battery, a voltage source along with passive components form a simplified circuit. The selection of passive components result in either time-dependent or time-independent circuits. For this purpose, Figure 3.6 depicts two models of a Li-ion cell.

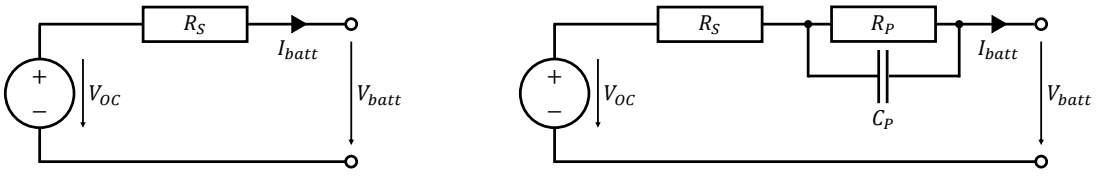

(a) Zero-time-constant model [69]

(b) One-time-constant model [69]

Figure 3.6: Time-independent (a) and time-dependent (b) model of a Li-ion cell [69].

Both, time dependent and time independent battery rely on a voltage source. In the previous section, the open circuit voltage V_{oc} was described as a function of the state of charge. Hence, a voltage source incorporates the open circuit voltage in this model.

A voltage source in combination with a series resistance represent a time-independent model for the Li-ion cell. Figure 3.6a shows the zero-time-constant model of a Li-ion cell, which resistor R_s is in

series to the voltage source. Hence, for charging and discharging behaviour the battery's voltage V_{batt} and current I_{batt} are given as:

$$V_{\text{batt}} = V_{\text{oc}} - R_{\text{s}} \cdot I_{\text{batt}} \tag{3.2.8}$$

$$I_{\text{batt}} = \frac{V_{\text{oc}} - V_{\text{batt}}}{R_{\text{s}}} \tag{3.2.9}$$

However, applying a zero-time-constant model neglects cell dynamics [69]. In order to take these cell dynamics into account, the one-time-constant model in Figure 3.6b enhances the model by a capacitor. The charging and discharging behaviour of a capacitor can be neglected, if the simulation takes place in steady-state conditions.

From a single cell to the overall battery pack of an electric vehicle, the charging and discharging power as well as the C-rate can be derived. Generally, connecting battery cells in series cumulates the voltage, while parallel interconnections adds up the electric charge and current of the package. Hereby, a charging rate that fully charges a battery within an hour is defined as a C-rate of 1. Overall, the power of the vehicle is defined by the following equation:

$$P_{\text{ev}}(t) = N_{\text{batt}}^{\text{series}} \cdot V_{\text{batt}}(t) \cdot N_{\text{batt}}^{\text{parallel}} \cdot I_{\text{batt}}(t) \tag{3.2.10}$$

In order to charge a Li-ion battery different methods exists. Without evaluating charging and discharging approaches, selected methods for electric vehicles are: a) Constant Current - Constant Voltage (CC-CV), b) Constant Power - Constant Voltage (CP-CV), c) Multistage Constant Current - Constant Voltage (MCC-CV), d) Pulse charging, e) Boostcharging with a CC-CV-CC-CV scheme, f) Variable Current Profile [48, 89]. It is obvious, that a control approach and power electronics are implemented which adapt voltage and current for the vehicle, respectively.

Li-ion batteries are almost ideal in terms of charging and discharging losses [106, 112]. In their study, Yang et al. [106] investigated the relationship between coulombic efficiency and battery degradation. They presented a coulombic efficiency of over 99.9% if the normalised capacity is degradated not less than 80%. Hereby, NMC cells as well as LFP cells show an efficiency loss over time, but during the overall lifetime the efficiency never fall below 99.6 %.

3.2.5. Calendar Aging of Li-ion Battery

In the context of Vehicle-to-Grid, discharging capabilities for providing ancillary services subject to the impact on the battery lifetime and its capacity. Beside cycling induced losses, Li-ion batteries aging is a result of capacity fade based on Li-ion and active material loss [47]. "Calendar life performance is a direct representation of irreversible self-discharge capacity loss" [101].

By convention, the end of life conditions of an electric vehicle battery are fulfilled as the maximum battery capacity reaches 80 % of the nominal capacity. It is important to consider that the end of life conditions of an electric vehicle battery are not complementary with the total end of lifetime conditions. Applications with reduced requirements, such as second life battery approaches, are possible. Research conducting on this topic demonstrate that the suitability of 70 %–80 % remaining capacity as a standard automotive battery retirement criterion is not valid [53]. Instead, tracking first life battery ageing data is crucial [52].

Incorporating calendar aging losses into a mathematical model depends on the cell chemistry of the battery. In Section 3.2.3 a differentiation of the open circuit voltage between cathode materials

was already conducted. Corresponding to the selected open circuit voltage model based cathode material, in this section, calendar aging of battery cells based on NMC cathodes are taken into account as well. For this purpose, the model of Wang et al. [101] will be explained, who elaborated a mathematical model based on laboratory measurements. The selected type of battery for their model is a NMC based Li-ion 18650 Cell with a nominal capacity of 1500 mAh. With respect to the already introduced model of Keil et al. [38], both battery models rely on the same type of battery from the same manufacturer, but differ in terms of capacity. Latter use Sanyo UR18650E with a nominal capacity of 20500 mAh, while Wang et al. [101] rely their research on a Sanyo UR18650W battery cell. Hence, it will be assumed that the capacity difference does not affect the degradation model. A capacity fading model for LFP cells can be found in further work [100] or based on the work of Lam et al. [47].

In their work, Wang et al. [101] argue that calendar losses subjects to two parameters, which are time t and temperature T. They derived an equation to incorporate those dependencies:

$$Q_{\text{loss}}^{\text{cal}} = f \cdot e^{\frac{-E_a}{R \cdot T}} \cdot t^{\frac{1}{2}} \tag{3.2.11}$$

Where f represents pre-exponential factor, which is 14876 per day$^{1/2}$, E_a the activation energy of 24.5 in kJ per mol, R the gas constant and T the absolute temperature in Kelvin. In order to express the gradual degradation at time $\hat{t}$, the derivative function can be used [98]:

$$\Delta Q_{\text{loss}}^{\text{cal}}(\hat{t}) = \left.\frac{\delta Q_{\text{loss}}^{\text{cal}}(t)}{\delta t}\right|_{t=\hat{t}} \cdot \Delta t = \frac{1}{2} \cdot f \cdot e^{\frac{-E_a}{R \cdot T}} \cdot t^{-\frac{1}{2}} \cdot \Delta t \tag{3.2.12}$$

In order to visualise the dependencies of these two parameters on the gradually losses, Figure 3.7 depicts both parameter against each other. The z-axis displays the gradually decreasing capacity loss for an hour in percentage of the total capacity. Note that the hourly degradation in the figure depicts the lifetime from 100 days to 1000 days.

On an early stage of a Li-ion battery lifetime, the hourly calendar induced degradation reaches its maximum value. Calendar based capacity loss relies mainly on lithium inventory loss during the

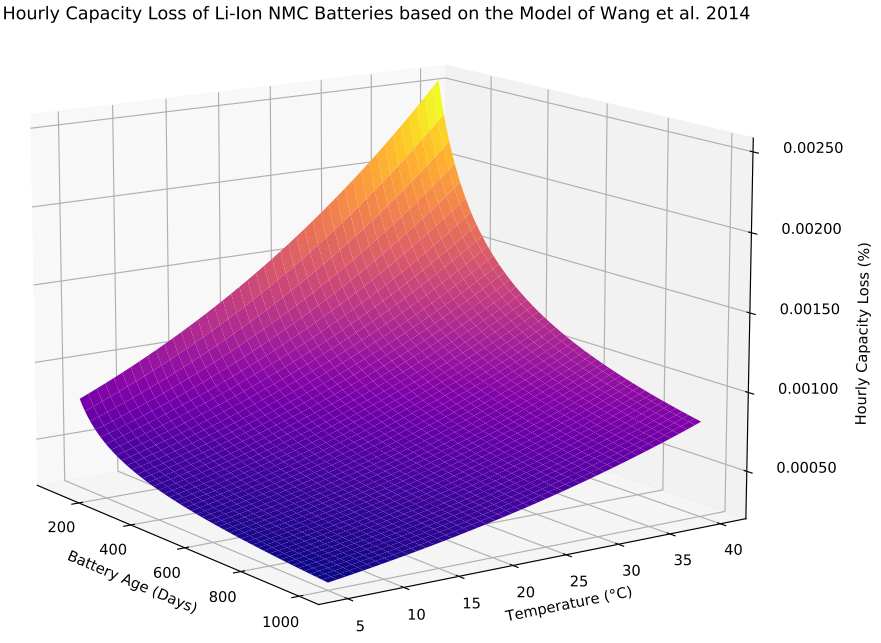

Figure 3.7: Hourly capacity loss based on calendar aging.

formation of the SEI layer at the anode [101]. As the surface plot indicates, these irreversible chemical processes occur predominantly at an early stage of the battery life. It is know, that this process is diffusion limited, leading to a decline of $t^{1/2}$ [101]. During the depicted range of around three years, the hourly degradation declines by the factor of approximately three.

Lower temperatures result in a lower calendar aging over the whole lifetime. The hourly degradation is affected by a temperature dependency due to SEI formation as a thermally activated process [101]. Hence, high temperatures at an earlier stage can degrade the battery approximately ten times more than a cold battery at a later lifetime.

Beside these two parameter, the states of charge of the battery cell have a relevant effect on calendar aging. In their work, Keil et al. [38] conclude that Li-ion cells should not be stored with a high state of charge to increase the battery lifetime. The state of charge dependency is shown in Figure 3.8.

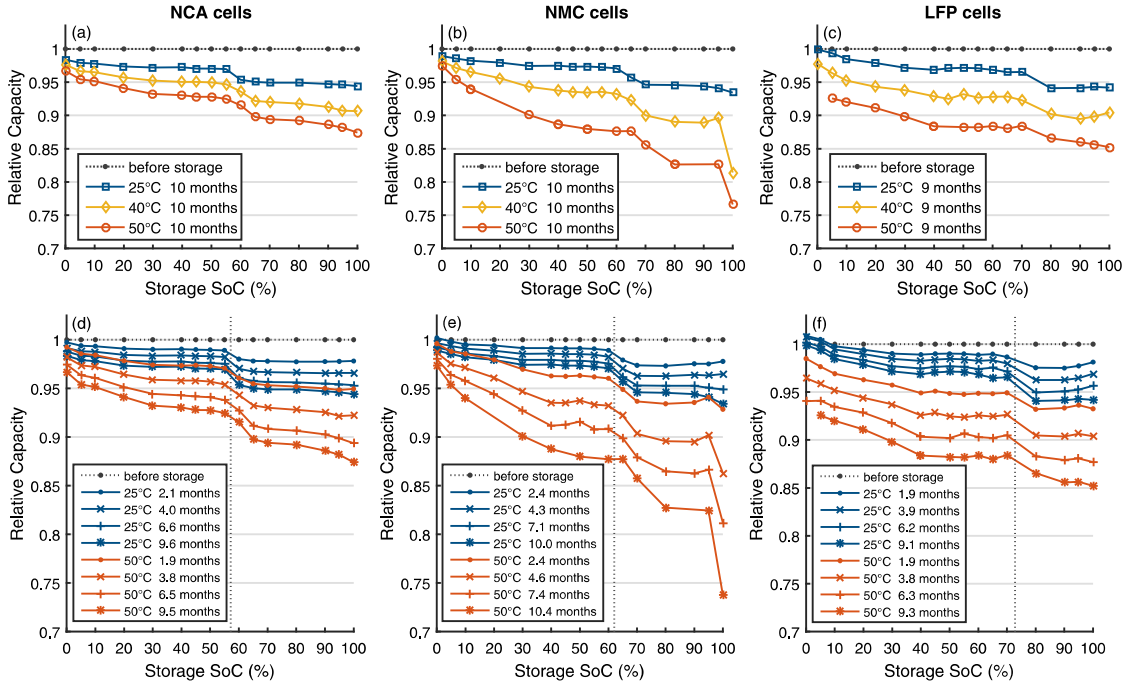

Figure 3.8: Battery degradation after ca. 9-10 months of storage at various SoCs and different temperatures (a-c) & capacity fade for different storage periods (d-f) [38].

The figure not only depicts relevant states of charge and their capacity fade, but also underlines the temperature dependent behaviour of Li-ion batteries. For comparison, LFP and NCA cells are listed beside the NMC cells. One can see that NMC based cells subject to increased degradation in high states of charge above 95 % at high temperatures. Compared to both different cathode materials, the cathode material of a Li-ion cell has a relevant impact on the degradation. Keil et al. [38] summarise in their study that the three different types of commercial lithium-ion cells demonstrate calendar aging does not increase steadily with the state of charge. Instead, they observe plateau regions, which cover intervals of more than 20%–30% of the cell capacity, where capacity fade is largely constant.

Hence, to incorporate the states of charge into the degradation model, a further mathematical model has to be derived. In their work, Calearo et al. [12] enhanced the model of Wang et al. [101] by integrating the identified plateau region of Keil et al. [38]. Their approach demonstrates that the pre-exponential factor f can be expressed as a function of state of charge. Based on Equation 3.2.13, the two models for NMC based cells can be merged.

$$f = Q_{\text{loss}}^{\text{cal}}(t, \text{SoC}) \cdot e^{\frac{E_a}{R \cdot T}} \cdot t^{-\frac{1}{2}} \tag{3.2.13}$$

Where $Q_{\text{loss}}^{\text{cal}}(t, \text{SoC})$ will be equalized with the measurements of Figure 3.8 for a temperature of 25°C. Hence, they described the plateau regions by the following piece-wise defined function.

$$f_{25°C}(\text{SoC}) = \begin{cases} -1.0353 \cdot \text{SoC}^2 + 89.724 \cdot \text{SoC} + 1224.6 & \text{if } 0\% \leq \text{SoC} < 50\% \\ +10.351 \cdot \text{SoC}^2 - 1083.6 \cdot \text{SoC} + 31447 & \text{if } 50\% \leq \text{SoC} < 70\% \\ +2.6384 \cdot \text{SoC}^2 - 409.55 \cdot \text{SoC} + 22035 & \text{if } 70\% \leq \text{SoC} \leq 100\% \end{cases} \tag{3.2.14}$$

Merging these models results in a representation of the state of charge as a further impact on the calendar aging model. Note that the beginning of the section compares both studies based on the selected type of battery. Hereby, the pre-exponential factor based on the approach of Calearo et al. [12] varies with the cell temperature. To compare the resulting model with the conducted measurements of Figure 3.8, Figure 3.9 shows the resulting degradation for the same storage period at 25°C.

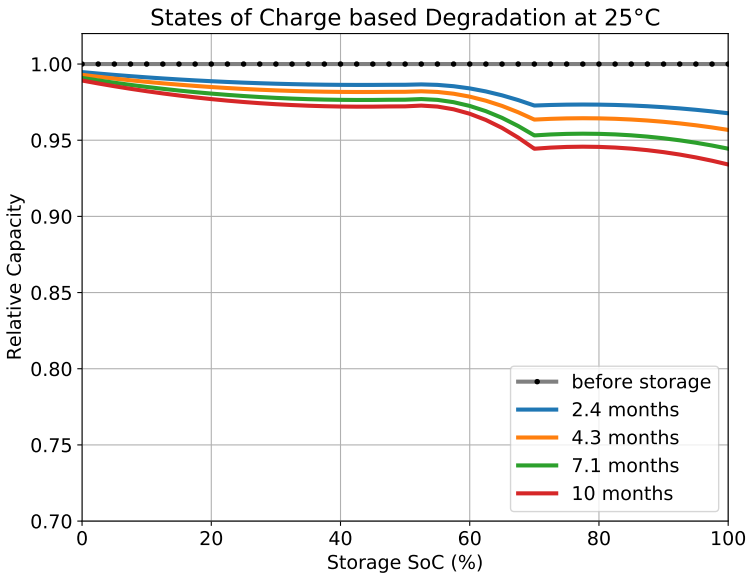

Figure 3.9: Merged degradation model of Calearo et al. [12], Keil et al. [38] and Wang et al. [101]

The proposed model in the figure follows the same behaviour of the calendar aging based measurements. Based on the model, the plateau regions can be depicted, in order to analyse the sensitivity of degradation in later sections. A mathematical representation of the deviation between the overall model and specific measurements will not be carried out in the scope of this work. The reason is that the main purpose of the model is the identification of sensitivities rather than predict or approximating an overall lifetime.

3.2.6. Cycling Induced Capacity Fade

Beside calendar aging, cycling induced fading affect capacity losses of an electric vehicle as well. It is apparent, that cycling induced losses occur during the charging and discharging periods. The degradation depends on the charging rate as well as the cell's temperature and the total throughput [101].

The implemented model of Wang et al. [101] not only covers calendar aging, but also cycle induced aging. Based on their laboratory measurements, they subtracted the calendar losses from the overall losses leading to the cycling induced losses as an additive approach. They fitted the model for cycling losses by the following equation:

$$Q_{\text{loss}}^{\text{cycle}} = B_1 \cdot e^{B_2 \cdot I_{\text{rate}}} \cdot A_{\text{h}} \tag{3.2.15}$$

Apparently, the losses depend on the charging rate I_{rate} in an exponential relationship. The charging rate is expressed through the C-rate and the total throughput A_{h} based on ampere hours. To recap, the C-rate is an indicator for the amount of charging or discharging current in relation to the total capacity. Whereas, the total throughput A_{h} is the I_{batt} multiplied with the timeinterval Δt:

$$A_h(\Delta t) = I_{\text{batt}} \cdot \Delta t \tag{3.2.16}$$

Furthermore, the cycling induced losses are temperature dependent as well, whereby they incorporate this dependency by a non-linear function as the parameter B_1 and B_2 show:

$$B_1 = a \cdot T^2 + b \cdot T + c \tag{3.2.17}$$

$$B_2 = d \cdot T + e \tag{3.2.18}$$

The parameter a, b, c, d and e are defined in Table 3.1. It has to be noticed, that rounding those coefficients is not recommended.

Table 3.1: Coefficients for the model of Wang et al. [101].

Coefficient	Value	Unit
a	$+8.61242532 \cdot 10^{-6}$	1/Ah-K^2
b	$-5.12524472 \cdot 10^{-3}$	1/Ah-K
c	$+7.62915691 \cdot 10^{-1}$	1/Ah
d	$-6.7 \cdot 10^{-3}$	1/K-(C-rate)
e	$+2.35$	1/(C-rate)

As it was done in the previous section, different charging rates and temperature variations that are affecting the battery degradation and can be incorporated by describing the degradation through the derivative function of Equation 3.2.15. For this purpose, Equation 3.2.19 describes the degradation at time $\hat{t}$ [98].

$$\Delta Q_{\text{loss}}^{\text{cycle}}(\hat{t}) = \left.\frac{\delta Q_{\text{loss}}^{\text{cycle}}(t)}{\delta t}\right|_{t=\hat{t}} \cdot \Delta t = B_1 \cdot e^{B_2 \cdot I_{\text{rate}}} \cdot I_{\text{rate}} \cdot \Delta t \tag{3.2.19}$$

Accordingly, a representation of the model is realised through Figure 3.10, which visualises the resulting degradation for different cell temperatures and charging rates.

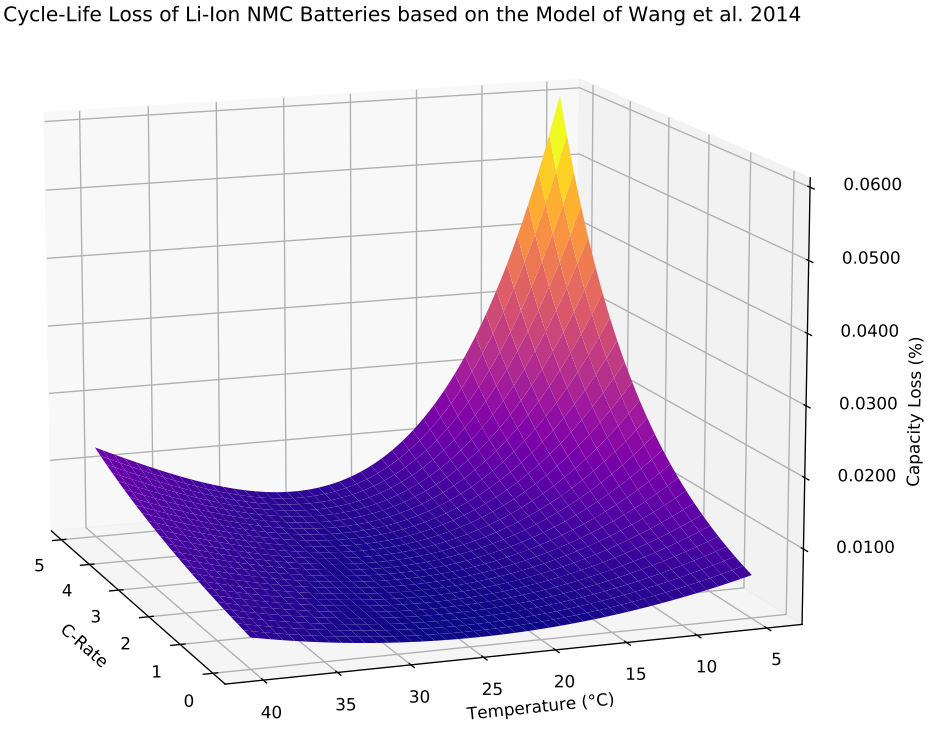

Figure 3.10: Cycling induced losses against temperature and C-rate.

As the figure depicts, high charging rates at lower temperature result in the highest degradation. To prevent those conditions, battery management systems are able to prevent high C-rates at low temperatures. Nevertheless, high C-rates at ideal cell temperature conditions harm the battery less than low C-rates at undesirable temperature conditions. Ideally, charging and discharging processes should take place at around 25 °C for this type of battery.

3.3. Electric Vehicle and its Supply Equipment

Beside the battery itself, an electric vehicle supply equipment is necessary in order to transfer energy from the grid to the battery and vice versa. With unidirectional alternating current and direct current based charging methods, the roll-out of two technologies already takes place. In the scope of this work, the induced losses by the supply equipment form an important factor for deriving the results of bidirectional charging capabilities.

3.3.1. Grid-Connected Charging Approaches

A simplified representation of alternating current and direct current based charging is given in Figure 3.11a and Figure 3.11b, respectively. For completeness, in Figure 3.11c, inductive charging is depicted as well.

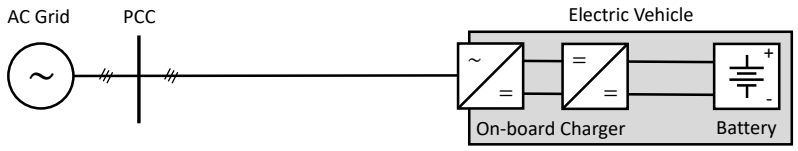

(a) AC charging.

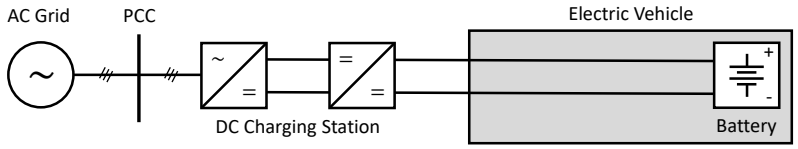

(b) DC charging.

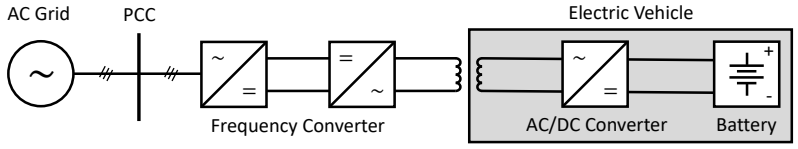

(c) Inductive charging.

Figure 3.11: Simplified model for Alternating Current (a) and Direct Current (b) charging with PCC as the point of common coupling and the relevant power electronics without considering relevant controller (i.e. batter management system). In (c) a simplified representation of inductive charging is illustrated.

Firstly, present AC charging requires a so-called on-board charger (OBC) that provides charging capabilities for AC based sockets in combination with a wallbox or mobile charger. As Figure 3.11a outlines, the on-board charger rectifies the alternating current and the DC/DC converter adapts the voltage according to the battery's voltage level. One may notice that neither a mobile charger nor a wallbox is depicted in the simplified model. Both can be neglected as their operation mainly intends to monitor safety related parameter such as fault currents or the communication between the vehicle and grid. However, neither an AC wallbox nor mobile charging stations influence the current or voltage directly through power electronic circuits. Instead, power electronics of the electric vehicle receive setpoints to adjust the charging power (i.e. from a wallbox or home energy manager).

Secondly, state-of-the-art DC charging is realised based on an external charging station, which rectifies the alternating current of the power system. Similar to the on-board charger, it adapts the DC voltage through a DC/DC converter outside the vehicle afterwards. Referring to the right-hand side of the simplified representation in Figure 3.11b, the vehicle's battery is directly connected with the DC charging station. DC charging stations are beneficial for a higher charging power, because the increased demand for installation space due to higher power ratings does not affect the vehicle.

Thirdly, inductive charging is in the interest of electric vehicle charging strategies, because it does not require plugging in the vehicle. Not only unidirectional charging, but from a technical point of view, it is possible to provide Vehicle-to-Grid services based on inductive charging [16]. However, this electric vehicle charging technology is at an early stage and will not be considered in the scope of this work. Nevertheless, inductive charging has the benefit to access a full battery of a parked vehicle, while the other methods have to create an incentive for the user to plug in the vehicle, if the batters is already charged.

Both AC and DC based charging in combination with an AC Grid require a rectifier and a DC/DC converter for unidirectional charging. The main difference of both methods is, if the alternating current will be rectified by the charging station (i.e. DC wallbox) or within the electric vehicle itself (i.e. on-board charger). For bidirectional charging, both methods require a bidirectional converter topology. A review of converter topologies is given in reference [77].

Required filters, safety equipment, costs and regulatory aspects will not be covered in the scope of this work and are therefore neglected. For simplicity, this work argues that from a power electronics point of view, AC-charging and DC-Charging in combination with an AC grid can be both represented by an AC/DC and DC/DC converter topology. Hence, the intended model covers both charging approaches.

3.3.2. Converter Efficiency

Converting alternating current to direct current and vice versa subjects to the efficiency and maximum power rating of the converter. For unidirectional charging processes, the on-board charger and dc charging station have been introduced in the previous section. It was argued that a bidirectional converter topology is inevitable for vehicle to grid approaches.

Generally, the efficiency η is defined as the ratio between the input power and output power as Equation 3.3.1 shows. Due to conservation of energy, the input power cannot exceed the output power, whereby η is in the range between 0 and 1, which can be transferred to a percentage value.

$$\eta = \frac{P_{\text{out}}}{P_{\text{in}}} \tag{3.3.1}$$

In order to incorporate converter based parameter like power, voltage and current level, the model of Chivelet et al. [15] will be applied. Generally, the model has been used for research on photovoltaic system inverter modelling [20, 66]. In their work, Chivelet et al. mathematically describe the efficiency based on Equation 3.3.2.

$$\eta_{\text{inv}} = \frac{2 \cdot R_{\text{S}} \cdot P_{\text{AC}}}{V_{\text{DC}}^2} \cdot \frac{1}{1 - \sqrt{1 - \frac{4 \cdot R_{\text{S}}}{V_{\text{DC}}^2} \cdot \left(P_{\text{AC}} + \frac{V_{\text{AC}}^2}{R_{\text{P}}}\right)}} \tag{3.3.2}$$

P_{AC}, V_{AC} represent alternating current based apparent power and voltage, respectively. The direct current based voltage is given by V_{DC} of the vehicle's battery. In order to describe resistive losses, a series resistance R_{S} and a parallel resistance R_{P} are used. Former represents coupling losses between DC and AC side of the converter like commutation losses [20]. Latter covers the operation losses of converter, which impact is higher in the low power regions of the converter and decreases for higher power ranges as their relatively impact declines [20]. An approximation of the losses is possible by Equations 3.3.3 and 3.3.4.

$$R_{\text{S}} \approx \frac{P_{\text{DC}} - P_{\text{AC}}}{I_{\text{DC}}^2} \tag{3.3.3}$$

$$\frac{1}{R_P} \approx \frac{P_{DC} - P_{AC}}{V_{AC}^2} \tag{3.3.4}$$

Davila-Gomez et al. [20] argue that ”most suitable set of values P_{DC}, P_{AC} and V_{DC} for calculating R_P are those nearest to the zone of slope change in efficiency curve”.

A representation of different possible converter types based on the introduced model of Chivelet et al. [15] is given in Figure 3.12.

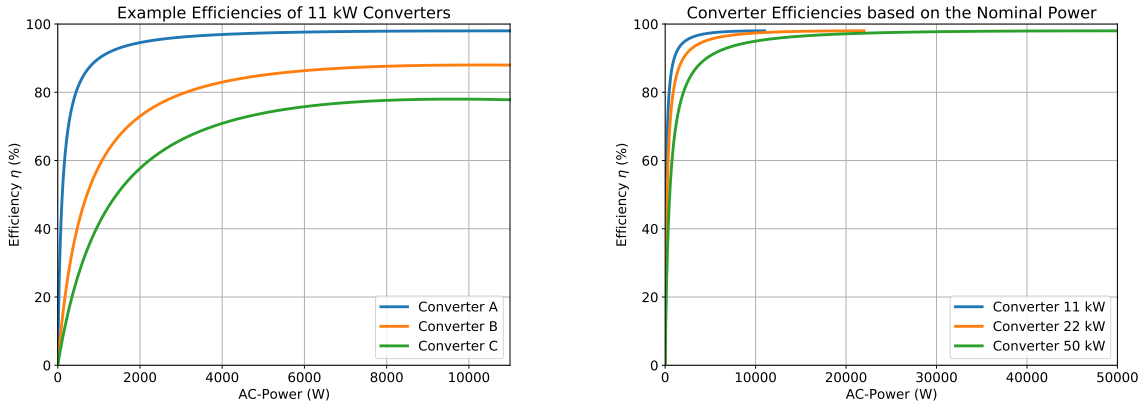

(a) Different efficiency characteristics for 11 kW converters.

(b) Efficiency characteristics for 11 kW, 22 kW and 50 kW converter.

Figure 3.12: Example converter characteristics that can be covered based on the model of Chivelet et al. [15].

On the left hand side, Figure 3.12a show three converter with different efficiency curves based on a variation of the mismatch between the AC and DC active power. Thus, converter A has the lowest mismatch resulting in higher efficiencies to an almost ideal power conversion ($\eta_{A,max}$ = 98 %). With converter B and C, an incline of the power mismatch show the impact on the overall efficiency curve ($\eta_{B,max}$ = 88 % and $\eta_{C,max}$ = 78 %). The operation losses in the lower power zone become apparent in all three cases.

Increasing the nominal power lead to a more inefficient power conversion in the low power region of the converter. Figure 3.12b depicts three converter with the same efficiency characteristics of converter A. By adapting the nominal AC power of the converter, the nominal efficiency can still be reached, but enlarges the less efficient range.

3.3.3. Thermal Losses

Beside conversion losses, thermal losses occur, due to the internal resistance of the battery and wires. To recap from Section 3.2.4, the simplest equivalent circuit of a battery consists of a voltage source and series connected resistor. This resistance depends on temperature, state of charge, cycles, current and internal electrochemical conditions [42].

Determining the total resistance that leads to heat dissipation depends on the interconnection of a battery pack and wires. Equation 3.3.5 determines the total resistance of a battery pack, while Equation 3.3.6 shows the resulting heat dissipation in W.

$$R_{batt} = R_s \cdot \frac{N_{ev}^{series}}{N_{ev}^{parallel}} \tag{3.3.5}$$

$$P_{\text{loss}} = I^2 \cdot \left(R_{\text{batt}} + R_{\text{wire}}\right) \tag{3.3.6}$$

It is apparent that high currents in combination with a high internal resistance lead to higher losses. Hence, a high battery pack voltage reduces the current flowing though the battery, whereby heat dissipation can be mitigated. Simultaneously, this approach allows to reduce the cross section of wires.

In general, the internal resistance and interconnection of cells varies for each electric vehicle. In their paper Kieldsen et al. [42] determine an internal resistance of 380 mΩ by conducting measurements on a Li-ion based electric vehicle. Besides, Muenzel et al. [55] identified the ohmic resistance for various 18650 cells that varies from 47 mΩ to 400 mΩ before and after cycling.

For reference and without considering wire resistances, the internal resistance of an example electric vehicle can be carried out. Referring to the same manufacturer and cell chemistry, that has already been used in the scope of this work, an internal resistance of less than 100 mΩ is given. As an example, 60 parallel rows with each 100 in series connected cells depicts a board voltage of roughly 400 V and 50 kWh. Hence, according to Equation 3.3.5, a total resistance of 166.67 mΩ can be determined.

As a first approximation, the thermal losses during charging indicate the impact of heat dissipation in the vehicle. For instance, charging with 11 kW and 100 kW leads according to Ohm's law and an on-board voltage of 400 V to a current of 27.5 A and 250 A, respectively. By using an internal resistance of 166.67 mΩ and Equation 3.3.6, thermal losses of either 0.126 kW or 10.416 kW would occur.

3.3.4. Electric Vehicle Thermal Management

Previous sections emphasised the temperature dependency of the cell's temperature with respect to cycling induced capacity loss and calendar aging. The thermal management of an electric vehicle is both, complex and vehicle dependent, but also use case dependent. In their review, Xia et al. [104] underline the complexity by referring to multiple mechanism, which are coupled to electricity, electrochemistry, heat transfer that varies with time, temperature, state of charge and other aspects.

The thermal losses during charging and discharging, that lead to a rising cell temperature, depends on the charging current and internal resistance. The previous section revealed that the thermal power losses follow a linear trend with respect to the internal resistance, but a quadratic increase in terms of charging current. Thus, interconnections, which can lead to a higher on-board voltage and lower current can decrease thermal losses. However, both internal resistance and interconnections are vehicle-dependant leading to different thermal management requirements.

Another dependency for the thermal management is the shape of the battery cell. State-of-the-art battery technologies mainly occur in either prismatic, cylinder or pouch cells. Their form and size result in different heat generation, heat transport and heat dissipation characteristics [104]. Assuming a thermal model would not only require the selection of a shape, but also the packaging approach. Among others, the selection of shape affects the heat distribution on all connected cells in a vehicle's battery [72].

Both above mentioned aspects result in various requirements for the thermal management control approach. Several cooling strategies exist, like passive cooling, liquid based cooling or air based cooling [104]. It is apparent that the demand for cooling strategies increases with higher charging currents, but subjects to efficiencies and costs. Besides, Kim et al. [43] compare existing battery thermal management system and conclude that an effective approach can combine various advantages of those strategies based on the purpose of the electric vehicle.

Another important aspect is the use case dependency that leads to various thermal operation conditions for the battery. Seasonal effects and different global locations are a driver for different challenges of the thermal management in order to cope with ambient temperature and weather conditions. The demand for cooling and pre-heating an electric vehicle differs if, in example, the operation takes place on a winter day in Norway or during a hot summer day in Spain. Other aspects are driving patterns that affect not only the availability of the vehicle, but also the operation condition. Ideally, the vehicle is already in optimal conditions for charging and discharging after a journey, but deviations from this conditions may have to be compensated by the thermal management (esp. for higher charging rates). Thus, it is not possible to draw definitive conclusions [34, 103]

Overall, in the scope of this work, it is argued that enabling the thermal management by high charging currents should be avoided. As it will be later seen, increasing the charging power instead of scaling up the fleet size can rise other issues. Hence, the thermal management will be neglected, because charging rates that enable the thermal management would increase further energy demand that decreases the efficiency and increases costs.

3.3.5. Standby Losses

While the efficiency model of the converter only covers the standby losses of the converter, further standby consumptions have to be incorporated. It has to be noticed that both, electric vehicles and internal combustion engines in idle conditions draw electrical energy to provide services like remote control. While the energy demand of wireless access points for car keys are not relevant for charging or discharging, monitoring systems should be taken into account.

In the scope of this work, the relevant components for charging and monitoring are depicted in Figure 3.13.

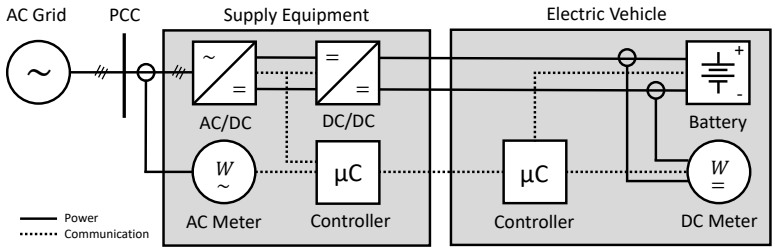

Figure 3.13: System components which are involved for the charging and discharging process. Both µC represent all required microcontroller.

The example shows DC based charging, but the following argumentation is valid for all charging approaches. Both, the supply equipment and the vehicle itself require a microcontroller (µC) that enables the communication process between the supply equipment and the vehicle. Especially for intelligent charging and with respect to the infrastructure, the maximum charging power will be communicated. Not only for the control algorithm, but also for safety monitoring, the currents and voltages have to be measured. For the overall process, will be assumed that 100 W additional power through these components is required.

3.4. Preliminary Conclusion

This chapter presented a mathematical model that incorporates the physical, chemical and electrical properties relevant for a charging process of an electric vehicle. On the one hand, Section 3.2 described the battery itself in terms of state of charge, charging behaviour, on-board voltage and degradation. Whereas on the other hand, Section 3.3 focused on the electric vehicle and the supply equipment. Based on both models, a preliminary conclusion can be drawn.

State-of-the-art plug-in electric vehicle rely on a Li-ion based cell chemistry, which properties subject among others on the cathode and anode material. Hence, a single model that covers all types of batteries is not identified in literature. This work selected lithium nickel manganese cobalt oxide based cells (NMC) as the battery under investigation. All mathematical equation, which are applied, rely on two studies, which approximated the degradation based on laboratory measurements. The different laboratory measurements are compared.

The on-board voltage varies with the state of charge of the battery, while temperature and charging/discharging characteristics can be neglected. Generally, based on the voltage of the battery one can derive the state of charge of the battery. It was outlined that the temperature dependency of the open-circuit voltage mainly affects states of charge below 10 %. In the context of discharging the vehicle's battery, those states are likely to be not in the interest of Vehicle-to-Grid research. Hence, they are neglected. Additionally, the so-called dynamic hysteresis characteristics describes the voltage difference between charging and discharging. Those affects are described as relatively small compared to overall context.

Discharging current can be modeled time independent and Li-ion batteries are almost ideal. Capacitive effects can lead to time-dependent charging curves, but steady state conditions will be evaluated in the scope of this work. Besides, compared to other battery technologies, Li-ion batteries induce almost no losses during charging or discharging (efficiency over 99.6 %).

Calendar aging is one mechanism that leads to capacity losses of the battery. Hereby, the model includes that different temperatures, battery ages and states of charge lead to non-linear aging effect. In general, high calendar aging occurs on an early stage of the battery life, at high states of charge and at high temperatures.

Beside calendar aging, cycle life losses are the second mechanism that leads to capacity fade of a Li-ion battery. While low temperatures are likely to minimise calendar-life losses, low temperatures and high charging rates result in the highest cycle-life loss. In ideal conditions, the battery operates at minimum degradation at around 25°C. It is argued that a battery management system prevents that high charging rates can be drawn from the vehicle's battery during temperatures which deviate from those conditions.

Beside the vehicle's battery, a model for the supply equipment and the electric vehicle itself has to be derived. In the context of both, mainly three losses affect the operation of the charging and charging process: conversion efficiency, thermal as well as standby losses.

Bidirectional charging capabilities for Vehicle-to-Grid based ancillary services require the conversion of the battery's DC voltage to the AC grid. Hence, the bidirectional conversion subject to the power electronics efficiency. For this purpose a non-linear model includes a variation of power conversion efficiencies by adapting the nominal power and nominal efficiency.

One of the losses that occurs during charging are the thermal losses, which depend on the internal resistance of the battery and interconnections. Those losses follow a linear relationship to the resistance, but increase quadratic with the current. With the focus on battery degradation, this work assumes that certain charging currents would not require the activation of the thermal management system.

The second power losses cover the standby losses of the controller and measurement units. Due to lack of data that is valid for all electric vehicle models, a fixed consumption of 100 W is assumed.

To recap, Table 3.2 summarises the parameter under investigation along with their dependencies for the vehicle's battery. Whereas, Table 3.3 lists those dependencies, that are relevant for the supply equipment. While the sensitivity of some parameters are already identified as neglectable, the sensitivity analysis in Chapter 6 will go more into depths.

Table 3.2: Electric vehicle parameter for Vehicle-to-Grid

Parameter	Coefficient	Unit	Section	Dependencies
State of Charge	SoC	%	3.2.2	Usable Capacity Current
Open Circuit Voltage	V_{oc}	Volt	3.2.3	State of Charge Series connected Batteries Temperature Dynamic Hysteresis Characteristics
Discharging Current	i_{batt}	Ampere	3.2.4	Series Resistance Open Circuit Voltage Parallel connected Batteries
Calendar Aging	$Q_{\text{loss}}^{\text{cal}}$	%	3.2.5	Temperature Battery Age State of Charge
Cycling Losses	$Q_{\text{loss}}^{\text{cycle}}$	%	3.2.6	C-rate Temperature Ah-Throughput

Table 3.3: Electric vehicle supply equipment parameter for Vehicle-to-Grid

Parameter	Coefficient	Unit	Section	Dependencies
Converter Efficiency	η	%	3.3.2	Power AC Power DC Voltage AC Voltage DC Series Resistance Parallel Resistance
Thermal Losses	P_{loss}	Watt	3.3.3	Line Resistance Connector Resistance Series connected Batteries Parallel connected Batteries
Standby Losses	P_{standby}	Watt	3.3.5	Controller Power Consumption

4

Modelling of Ancillary Services

Derived from the described ancillary services in Chapter 2, a model representation is proposed suitable for conducting a sensitivity analysis. Firstly, Section 4.1 justifies the selection of ancillary services for the scope of this work. Secondly, it follows a description of a suitable power system topology representation. Thirdly, to determine limits and capacities of power system's components, a statistical distribution grid analysis is introduced. Lastly, the selected power system analysis tool will be presented.

4.1. Selected Ancillary Services

Four ancillary services are selected for conducting a sensitivity analysis: peak load shaving, active power provision for frequency regulation, active power ramping and reactive power provision for voltage stabilisation. The selection will be justified without excluding or evaluating other ancillary services that are discussed Chapter 2. A selection has to be carried out to not exceed the scope of this work.

Peak load shaving is one service under investigation, because of the increasing decentralised penetration of volatile sustainable energy sources. The roll-out of electric vehicles in combination with domestic charging can support these energy sources locally when their power provision are scarce. Compared to load leveling, for peak load shaving bidirectional charging capabilities inevitable. Thus, not only the demand of the grid, but also the required technical enhanced charging capabilities leads to the selection.

Active power provision for frequency regulation is selected as it holds present market structures. While synchronous generator serve in a conventional power system the demand for frequency control, the replacement of these generation units shifts the focus to alternatives. As required for peak load shaving, the active power provision goes along with bidirectional charging capabilities. Consequently, a sensitivity analysis with respect to the technical capabilities as well as the market participation potential will be conducted.

Active power ramping as an ancillary service will be investigated because the energy transition strives toward an increased share of renewable energies. As a driver for several ancillary services, the energy transition leads to identifying opportunities to balance the volatile generation of sustainable energy technologies. As the third active power based service, active power ramping is considered by emerging converter based ancillary services. Within this work, the capabilities of electric vehicles to serve this services as well will be covered.

Reactive power provision for voltage control is in the interest due to local voltage deviations. As it was outlined, transmitting reactive power over long distances is limited. Thus, compensating local voltage deviations subjects to limit reactive power reserves capable for compensation. Therefore, an increased share of not only converter, but also electric vehicles could provide reactive power locally.

4.2. Power System Topology Representation

For conducting a sensitivity analysis, the selection of a suitable power system representation has to be made. It is obvious, that not each bus in the power system has the same demand for ancillary services. While some buses require voltage stabilisation, other buses may not require any services. Not only the power system component itself, but also the grid topology determines those needs.

This work relies on grid topologies on the distribution level representing the needs of ancillary service along with the integration of electric vehicles. The selected ancillary services rely mainly on the demand for voltage stabilisation, frequency stabilisation, reduction of component loading and active ramping support. Hence, two grid topologies will be presented in this section. In later chapters, those will be taken as reference to evaluate both, a first approximation of the grid sensitivity and the overall sensitivity of Vehicle-to-Grid.

A simplified distribution grid with a single bus that connects the electric vehicle fleet as well as the total demand highlights the component loading. In particular, line loading and transformer loading are in the interest, if the power flow aims an upward direction to parallel or upstream networks. Figure 4.1 illustrates the distribution grid along with the electric vehicle, which is represented through a battery and power electronics (as explained in Section 3.3.1).

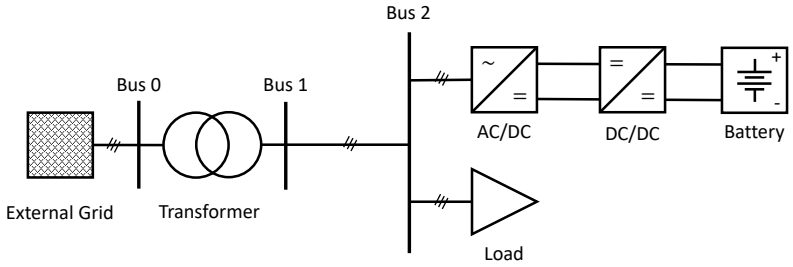

Figure 4.1: Simplified low voltage grid used for transformer and line loading.

As one can see, the distribution grid is connected to the external grid via a transformer. The vehicle fleet or a single vehicle shares the same bus (Bus 2) as the load. Hereby, the load will represent the total demand of the distribution grid. The low voltage side of the transformer (Bus 1) is interconnected with Bus 2 through a line. This interconnection will form the focus of the line loading. The simplified model grid topologies has the advantage that one can easily extract the resulting component loading based on the active power demand of the load and active power provision of the vehicles.

Voltage instabilities can occur if the voltage drops across the line, which leads to exceeding the voltage threshold. In order to create those unstable voltage conditions, a line topology is selected. Figure 4.2 shows the network under investigation.

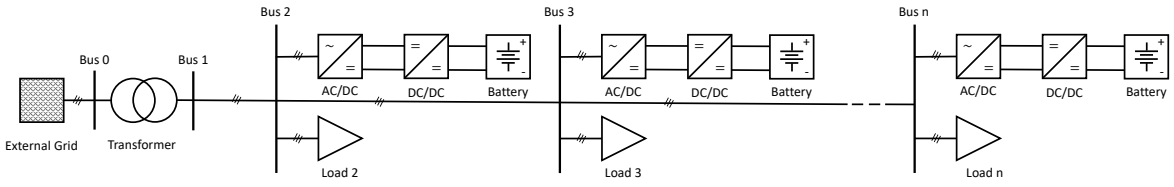

Figure 4.2: Simplified and radial low voltage grid used for voltage drops.

Again, the figure represents a distribution grid, but the number of busses is increased to n-busses.

On each bus, an electric vehicle will be connected along with a load. Hence, an even and uneven distribution of both, generation and load across the line can be realised. Further topologies represented in Europe are open ring and meshed power systems [40].

4.3. Limits and Capacities of Power Systems

As introduced, ancillary services aim to intervene supportive in order to maintain a secure and reliable grid operation. Nevertheless, by providing those services, the power system limits and capacities have to be considered. Saldaña et al. [70] advise that a power system analysis in terms of strength, sensitivity of parameter and disturbance determines the service for the grid. Accordingly and as the previous section indicated, not all buses require the same type of supporting services. For instance, network areas can be overloaded due to their maximum capacities or rely on different state-of-the-art technologies. Thus, this section aims to present the grid sensitivity by investigating the power system components.

A statistical representation of the power system facilitates to conduct a sensitivity analysis. In their work, Kerber et al. [40] present a statistical distribution grid analysis and a reference network generation. They rely their research on 87 distribution grids in South Germany (Bavaria). Based on this network data, they developed a strategy for classifying low voltage grids. It has to be considered that the data originates from the year 2008. Nevertheless, the average expected power system component lifetime is 38 years for conductors, 30 years for cables, 35 years for transformers, and 30 years for circuit-breakers [110]. Thus, this work assumes no significant statistical deviations for state-of-the-art grid topologies in this region. Accordingly, their statistical analysis will form the grid representation of this work.

The nominal transformer power rating differ per installation location. Kerber et al. [40] classify the low voltage grids in city, village and suburb. By identifying the apparent power of a transformer per class, one obtains the relative frequency of transformer ratings. Figure 4.3 depicts the apparent power against the relative frequency per class.

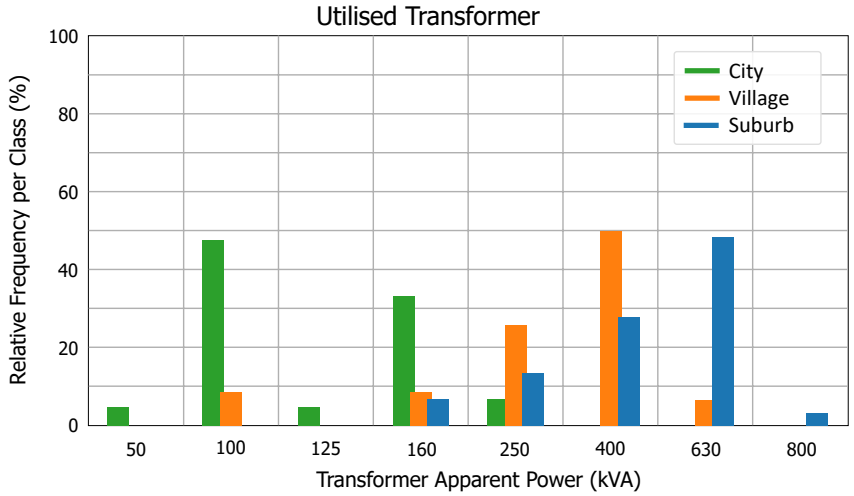

Figure 4.3: Utilised transformer per class (translated & adapted version of Kerber et al. [40]).

Statistically, the utilised transformer in suburbs and villages rely on a higher nominal rating than those installed in cities. Around 45 % to 50 % of the city's transformer subject to a nominal apparent power of 100 kVA. Compared to that, around 50 % of the transformer in villages and suburbs are rated with an apparent power of 400 kVA and 630 kVA, respectively. Needless to say, the network topologies per class can differ, whereby one can not derive a general conclusion about the network capacities.

Hence, the apparent power per consumer enhances the statistical representation of the power system capacities.

By shifting the scope to the transformer rating per consumer, one can approximate the network capacities for cities, villages and suburbs. Figure 4.4 depicts the Weibull-distribution of the transformer rating per consumer. Following the same classification approach as before, on average and for 50 % of the consumer in cities, one assigns 5 kVA of the transformer apparent power per consumer. In comparison, this value varies for suburbs (around 11 kVA) and villages (7.5 kVA). Taking 11 kVA as a reference, on average, more than 90 % of the consumer rely on less assigned apparent power. Thus, not only the nominal sizing of transformers, but also the apparent power per consumer varies for different locations.

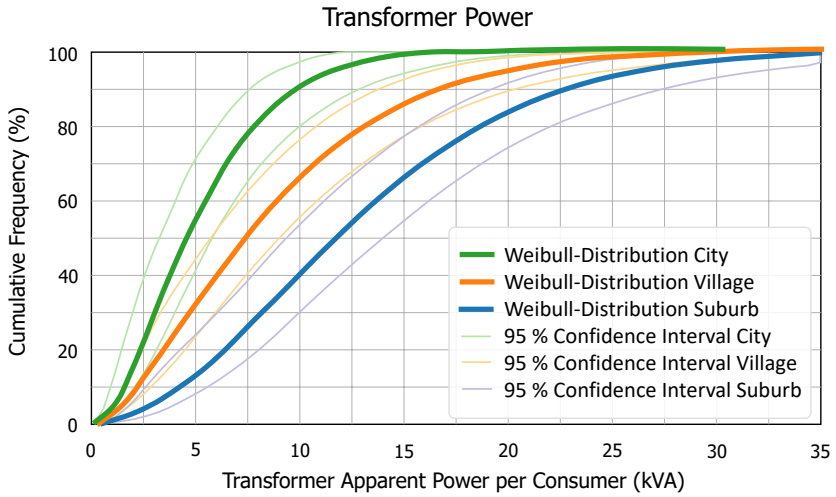

Figure 4.4: Transformer power per consumer (translated & adapted version of Kerber et al. [40]).

With respect to cable sizing and the total line length, a general classification is not representative. Kerber et al. [40] argue that the total line length show no statistical patterns that can be mapped to the described classifications. Similar, they identified that almost all utilised cables are 150 mm^2 aluminium cable. Other selected cable cross-sections are 185 mm^2 or 70 mm^2 cables based on copper.

Above that, the nominal rating of the transformer and apparent power per consumer subjects to different requirements. Especially for cities, the lowest network component sizing are present, which can be traced back to its requirements. Kerber et al. [40] argue that a higher number of consumers and the resulting lower share of peak values determines the sizing. Additionally, the actual component loading and accessible apparent power per consumer depends on the use case.

4.4. Selected Power System Analysis Tool

In order to simulate Vehicle-to-Grid based ancillary services, the simulation approach for the power system needs to be defined. Compared to the introduced model for electric vehicles and their supply equipment, the power system model is not described yet. Unlike the already presented models, several simulation tools exist, which facilitates that no model for the power system components have to be derived. Among others, in the context of power system simulations GridLAB-D, OpenModelica, PowerFactory as well as pandapower are in the scope of research [63, 88]. Hence, based on those simulation tools, a suitable model as well as the solver can be selected.

From a model perspective, the proposed power system representation has to include electrical models of lines, transformer, busses and the external grid. Based on the presented power system topologies, it is mandatory to have the equivalent circuit models to conduct the sensitivity analysis. All listed

tools portray those models, as those are basic components of a power system. Thus, from the model perspective, no analysis tool is excluded due to the model requirements.

In this work, the analysis tool selection is mainly driven by parametrization possibilities, interfacing opportunity, automation and steady-state conditions. The power system analysis tool within the conducted sensitivity analysis is pandapower [88]. Pandapower aims the automation of analysis, which facilitates the parametrization of components. Furthermore, one can directly access the model library in a python environment. Because transients are not in scope of this work, steady state conditions will be determined based on their pandapower power flow solver. Their numerical solver applies the Newton-Raphson method.

5

Sensitivity Based Analysis Approach

As the model for the electric vehicle, its supply equipment and the power system has been outlined, the sensitivity analysis can be conducted. With respect to the research question, it is required to define the sensitivity parameter to solve how sensitive are bidirectional charging capabilities for Vehicle-to-Grid based ancillary services against vehicle characteristics. Thus, this chapter introduces the proposed analysis approach, by listing the sensitivity parameter first and describing the framework for the analysis afterwards.

5.1. Sensitivity Parameter & Quantification

For this analysis, the sensitivity parameter have to be revealed along with the identification of their affiliation and ranges. Figure 5.1 recaps the bidirectional power flow capabilities of a vehicle, that has been introduced in Chapter 1.

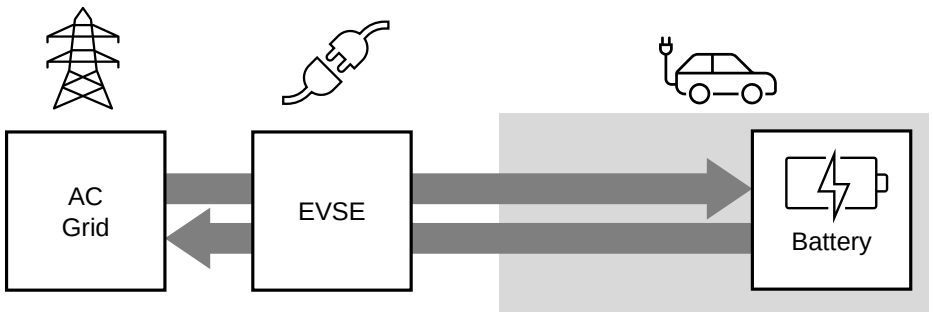

Figure 5.1: Vehicle-to-Grid as a system consisting of the AC grid,
the electric vehicle supply equipment (EVSE), the electric vehicle (EV) and its battery.

The figure depicts the AC grid, the electric vehicle supply equipment and electric vehicle as three subsystems. Accordingly, one can map the mathematical model from previous chapters to the three subsystems of Vehicle-to-Grid. Based on these model descriptions, one can list the model parameter and affiliate their dependencies.

By covering all parameter of the Vehicle-to-Grid model, one obtains 13 parameter, which depend on 34 dependencies. Table 5.1 summarises all sensitivity parameter along with their dependencies, affiliations and ranges. As one can see five parameter are assigned to the electric vehicle itself, three to the supply equipment and five to the grid. Furthermore, the number of dependencies for each parameter vary. While one can see as well that an intersection of dependencies is present, the sensitivity of these parameters not necessarily affect the system equally. Thus, in this work, those

Table 5.1: Sensitivity parameter and their dependencies under investigation.
(Dependencies, which range is denoted as ”-”, are a result of the model’s dependencies.)

Parameter	Affiliation	Unit	Dependencies	Range
State of Charge	EV	%	Usable Capacity Current	max. 250 Ah 0-125 A
Open Circuit Voltage	EV	Volt	State of Charge Series connected Batteries Temperature Dynamic Hysteresis Characteristics	0-100 % - 5-45 °C -
Discharging Current	EV	Ampere	Series Resistance Open Circuit Voltage Parallel connected Batteries	100 mΩ 400-800V -
Calendar Aging	EV	%	Temperature Battery Age State of Charge	5-40 °C 0-1000 days 0-100 %
Cycling Losses	EV	%	Temperature C-rate Ah-Throughput	5-40 °C max. 5-C 0-125 Ah
Converter Efficiency	EVSE	%	Power AC Power DC Voltage AC Voltage DC Series Resistance Parallel Resistance	0-50 kW 0-50 kW 230V/380V 400-800V - -
Thermal Losses	EVSE	Watt	Line Resistance Connector Resistance Series connected Batteries Parallel connected Batteries	100 mΩ - - -
Standby Losses	EVSE	Watt	Controller Power Consumption	100 W
Transformer Loading	Grid	%	Power Flow Apparent Power Rating	0-400 kVA 400 kVA
Line Loading	Grid	%	Power Flow Cross-section	0-400 kVA 150 mm^2
Generation	Grid	W	Active Power Ramping	0-100 %
Load	Grid	W	Active Power Demand	0-400 kW
Bus Voltages	Grid	V	Power Flow Reactive Power Provision	0-400 kVA $\cos(\phi) = 0.95$

dependencies will be carried out separately.

Along with the sensitivity parameter, indicators for the analysis are inevitable in order quantify the sensitivity. The listed sensitivity parameter will be measured against efficiency, degradation, power system loading, ancillary service provision, vehicle fleet, prices and market potential. Their change in accordance to the parameter will form the quantification of this analysis.

To conclude, for the sensitivity analysis it is not only mandatory to cover all dependencies, but also to define the quantification of the system. Especially the amount of dependencies leads to a variety of states, that Vehicle-to-Grid can take on. Thus and in the overall context, even if not all dependencies will be described in the following analysis, the analysis intends to be comprehensive. Thereby, the next chapters will emphasise primarily these parameters and dependencies that reveal anomalies in the context of the defined indicators.

5.2. Sensitivity Analysis Framework

As all three model have been outlined separately, the framework for the sensitivity analysis needs to be defined. In this section, the framework will be described based on different categories derived from comparable framework classifications in literature [75]. Thus, time resolution, elements & modelling, accessibility and usability are in the scope of this description.

The general structure of the framework relies on an input and output based Vehicle-to-Grid portfolio. Figure 5.2 depicts the general framework. As it can be seen, the Vehicle-to-Gird model portfolio consists of the presented models from the previous chapters. The uncertain parameter at the input are those, which are revealed in Table 5.1 of the previous section along with their dependencies. Based on the input parameter of the model portfolio, one can derive the sensitivity of Vehicle-to-Grid as well as implications between the models. These implications will be explained in the next section.

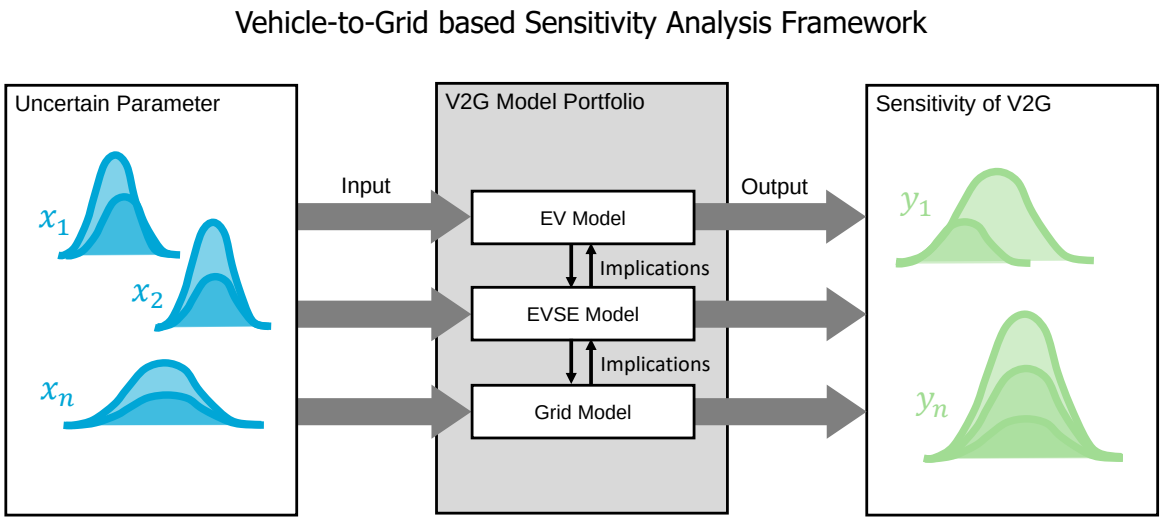

Figure 5.2: Framework of the sensitivity analysis.

The analysis will be conducted in steady-state conditions. The sensitivity of states and conditions will be investigated primarily, whereby transients are not part of the analysis. Furthermore, the time resolution of all presented models will not be linked or synchronised. Instead, implications between the models will be given.

The elements and models are accessible on a white box approach. While the electric vehicle and its supply equipment are expressed by the presented equations, the power system model uses a stand-alone power system analysis tool (pandapower). Nevertheless, all models are accessible, which is required for identifying the parameter, that are analysed.

Lastly, from a usability perspective, the framework is embedded into a Python based environment. The automation and parameterization opportunities of pandapower are accessible with python scripts [88]. Therefore, the model for the electric vehicle and electric vehicle supply equipment will rely on Python as well. Thus, one can analyse the sensitivity results within the same environment.

5.3. Model Implications

According to the analysis framework, the implications within the model portfolio require further explanation. Thus, Figure 5.3 illustrates the implications. As one can recognise on the top of the figure, the electric vehicle, its supply equipment and the AC grid are illustrated as described in the first section of this Chapter. Below following, the two implications are pointed out, which are referred to as first implication and second implication.

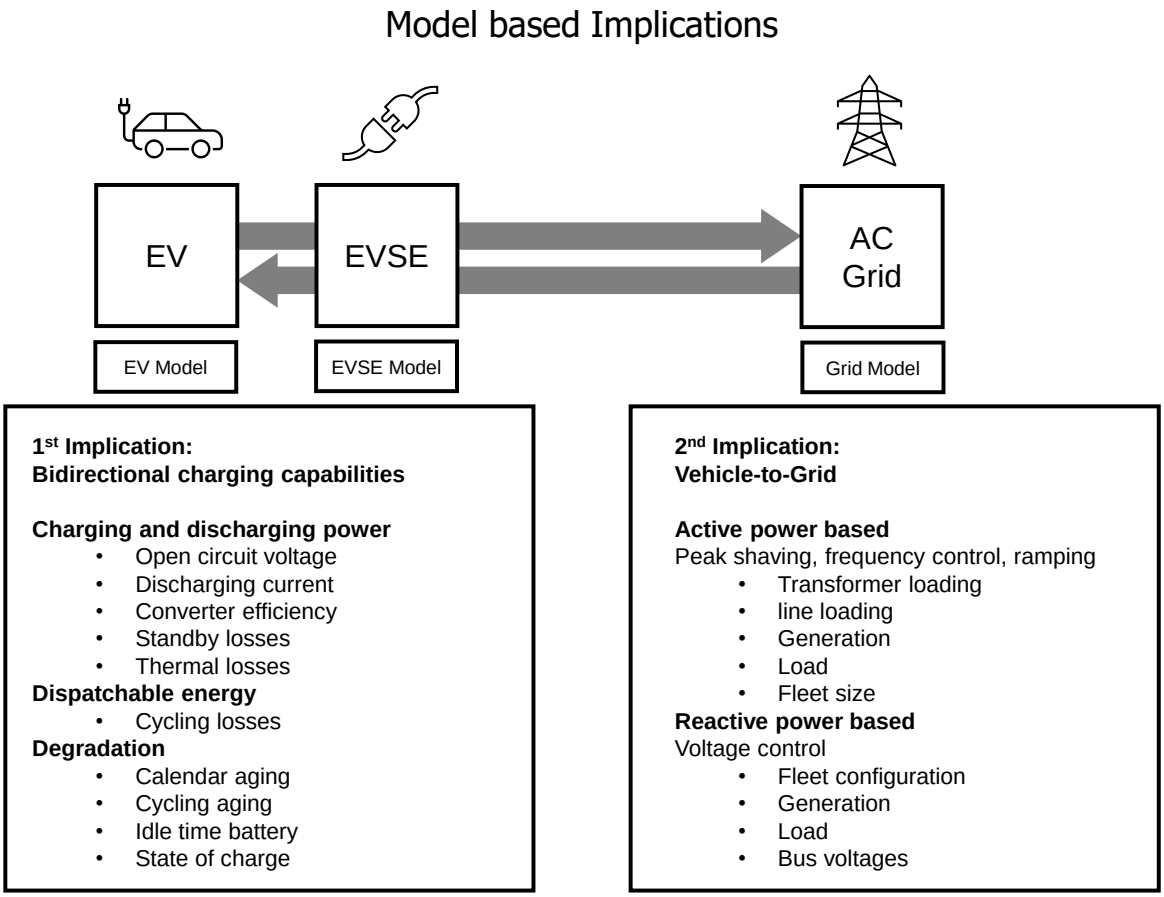

Figure 5.3: Model based implications.

As the first part of the research question, the bidirectional charging capabilities are investigated. Hereby, the electric vehicle and its supply equipment provide these capabilities. Thus, the implications between the electric vehicle and the supply equipment will be carried out. One can sort the parameter from Table 5.1 into three categories, which are namely: charging and discharging power, dispatchable energy and degradation. By merging both parameter and their dependencies, one obtains the first implications and sensitivities, which will be presented in Section 6.1.

Secondly, followed by the first implications, Vehicle-to-Grid suitable ancillary services are under investigation as the second implication. The implications from the bidirectional charging capabilities will be merged to the ancillary services to obtain the second implications. Hereby, one can divide the parameter from Table 5.1 into active power and reactive power based. While latter mainly represents voltage control in this work, active power based ancillary services are peak shaving, frequency control and ramping. One may note, that the fleet size and its configuration are not listed in the table,

because the table mainly focuses on a single vehicle. However, for the services, the fleet size will be investigated as well. Section 6.2 covers the second implication.

Overall, the sensitivity analysis includes the sensitivity of both, the model and the implications. Thus, the electric vehicle, the supply equipment as well as the AC grid can reveal sensitivities either induced by themselves or by merging with another subsystems. Furthermore, both will be applied on the costs and resulting Dutch market potentials, which are analysed in Section 6.3.3.

6

Sensitivity Analysis of Vehicle-to-Grid

How sensitive are bidirectional charging capabilities for Vehicle-to-Grid based ancillary services against vehicle characteristics? To solve the research question in the next chapter, this chapter reveals the sensitivity of bidirectional charging capabilities in Section 6.1 based on the mathematical model presented in Chapter 3, first. Secondly, the sensitivity results of a single electric vehicle provide relevant implications for selected ancillary services that are outlined in Section 6.2.

6.1. Electric Vehicle Bidirectional Charging Sensitivity

In the context of bidirectional charging capabilities, three parameter are primarily in the interest for Vehicle-to-Grid suitable ancillary services, namely (dis)charging power, dispatchable energy and degradation. The following section will present their sensitivity to obtain an insight on how the vehicle could participate in different ancillary services later on.

6.1.1. Sensitivity of Electric Vehicle Charging & Discharging Power

Adapting the charging power in order to either charge or discharge the battery subjects to a non-linear behaviour in terms of efficiency and losses. The Figures 6.1b & 6.1a depict the converter losses, standby consumption, resistive losses and the resulting cumulative losses against charging power. It has to be mentioned that the nominal efficiency of the converter is 98 %.

To begin with absolute losses depicted in Figure 6.1b, one can see converter and resistive losses are dependent of the charging power, while standby losses are independent. Latter losses occur due to

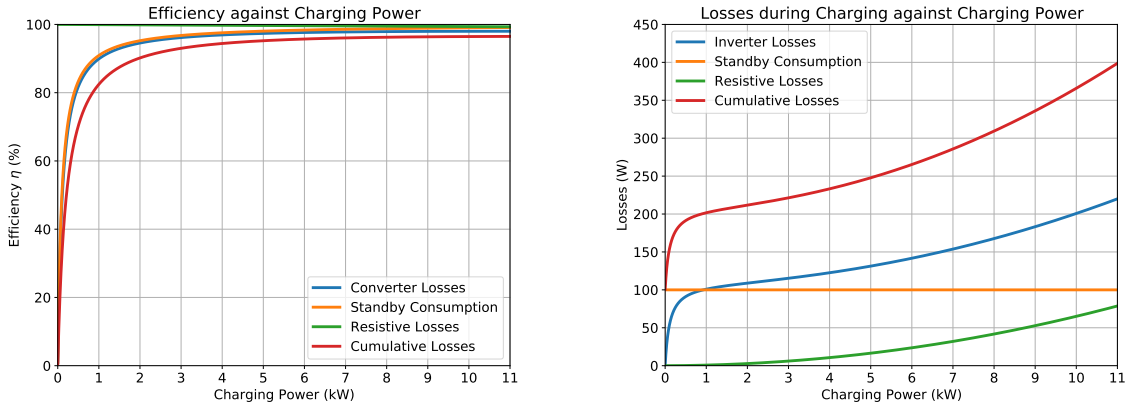

(a) Efficiency.

(b) Absolute losses.

Figure 6.1: The impact of different losses (a) in terms of efficiency and (b) represented in absolute values.

the communication and monitoring of the charging process (see Section 3.3.5). In the scope of this work, the standby losses are assumed to be 100 W. In contrast, both converter and resistive losses depend on charging power in a non-linear context (see Sections 3.3.2 & 3.3.3). The overall resistance is assumed as 100 mΩ.

By cumulating all losses, the overall losses against charging power follow a non-linear slope with an offset loss. In the power regions from 0 W to 1 kW, the cumulative losses approximately doubles to a value of 200 W. This effect relies mainly on the operation losses of the converter and the standby losses of the vehicle. Whereas, applying charging rates above 1 kW, the initial slope of converter losses declines. However, in those conditions, resistive losses increase. Due to the quadratic impact of current on the resistive losses, one obtains less than 100 W of losses for a charging power of 11 kW and 100 mΩ. These losses mainly result in heat dissipation. Thereby, it has to be mentioned that for the displayed power range, the thermal management is theoretically assumed as not enabled. Hence, it has to be taken into account for higher charging rates (see Section 3.3.4).

As the absolute values of losses mainly increase with power, the efficiency allows to evaluate the overall performance by taking the ratio between output and input power into account. For this purpose, Figure 6.1a plots the efficiency against charging power. Complementary to the different results that are presented along with Figure 6.1b, low power ranges below 1 kW are more inefficient than higher charging rates for the represented system design. However, for charging or discharging with a power above 1 kW an efficiency of over 80 % and up to 97 % is reachable by using a high efficient converter.

In the context of bidirectional charging capabilities, an overall cycle has to cover both, the charging and discharging process. It is obvious, that bidirectional charging capabilities require the investigation of a full cycle, because feeding the grid with energy, requires charging of the battery beforehand. Hence, Equation 6.1.1 defines the overall cycle efficiency.

$$\eta_{\text{cycle}} = \eta_{\text{charging}} \cdot \eta_{\text{discharging}} \tag{6.1.1}$$

The non-linear behaviour of efficiencies for either charging or discharging process can significantly decrease the overall efficiency. In order to show the impact of charging efficiency and discharging efficiency on the overall cycle efficiency, Figure 6.2a and Figure 6.2b summarise the relevant operation points. While the configuration in Figure 6.2a relies on a high efficient converter topology, Figure 6.2b

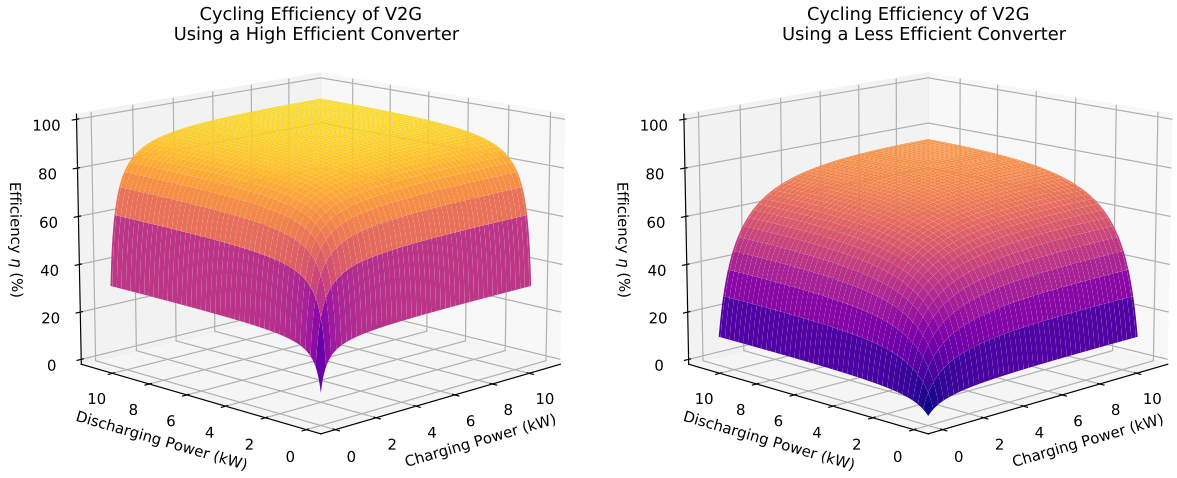

(a) High efficiency converter with η_{max} of 98 %.

(b) Less efficient converter with η_{max} of 88 %.

Figure 6.2: Combined charging and discharging efficiency.

uses a less efficient converter (see Converter A and B in Section 3.3.2) to demonstrate the significance of the converter selection. To recap, the maximum efficiency of Converter A is 98 % and 88% for Converter B. Both figures depict a range from 100 W to 11 kW.

To begin with Converter A in Figure 6.2a, the overall efficiency of one cycle varies between 10 % and 93 %. As expected based on the previous figures, applying a charging power in the low efficient areas (below 1 kW) decreases the overall efficiency. If the vehicle not only charges with 100 W, but also discharges with 100 W, the overall efficiency is around 10 % for the described topology. Whereas, high overall efficiencies can only be reached if both processes operate in high efficient ranges of the converter. By applying charging rates above 1 kW, efficiencies of over 68 % can already be obtained. For power ranges of 1 kW to 11 kW, those values form a relatively constant plateau region with efficiencies up to 93 %. If either one process operates at a low charging power of 100 W, a maximum efficiency of around 26 % can be reached.

Selecting a less efficient converter topology can reduce the overall efficiency to a minimum of less than 5 % and a maximum of 75 %. Even if the maximum efficiency of Converter B is 88%, by taking the previous mentioned losses into account and operating the converter in not ideal conditions can lead to an efficiency of less than 5 %. As observed for Converter A, charging rates below 1 kW for both processes are the most inefficient operational conditions. However, by reducing the nominal efficiency of the converter, it is still possible to obtain efficiencies of 75 % for the full cycle, if those conditions are avoided.

6.1.2. Sensitivity of Electric Vehicle as an Energy Storage

Along with power based capabilities for bidirectional power flows, the duration of supplied power correlates with the sensitivity of dispatchable energy. Hence, besides determining the operational power, the dispatchable energy is crucial for the duration of supply and vice versa.

Apparently, but not trivial, dispatching energy from the vehicle's battery leads to lowering the state of charge that affects the user. Hence, dispatching energy will again shift the focus on a multidisciplinary scope that has to cope with the user behaviour. Especially, the duration of supply and maximum dispatchable energy emphasises the role of the user that will determine how the user participates in the market. In the scope of this section and work, the sensitivity will focus on the technical sensitivity.

Discharging the battery increases the stress on the battery, but lower C-rates have a lower degradation. To evaluate the sensitivity of dispatchable energy, the battery degradation provides an indicator for the vehicle's capabilities as an energy storage. For this purpose, Figures 6.3a & 6.3b compare two battery packages with 50 kWh and 100 kWh.

Both figures show the capacity loss in percent against the total throughput in MWh for different C-rates. To recap, the C-rate is relative to the battery's capacity, whereby 1-C corresponds can be converted to 50 kW for the former battery and 100 kW for latter. Both packages use the same type of cell (Li-ion with NMC cathode, as defined in Chapter 3).

The total throughput for a batterypack increases with a larger capacity, but calendar aging is constant. Section 3.2.5 revealed the calendar aging for a single battery cell. By increasing the number of cells in a battery pack, calendar aging of the battery pack will follow the same trend as single cell. However, by increasing the number of cells, more energy can be stored and dispatched from the battery with the same degradation as both figures reveal. Hence, for the same total throughput calendar aging of both packages is equal, but less cycling induced degradation occurs for the larger battery pack.

Discharging both battery packages with the same charging power results in different cycling induced degradations. While the total throughput in Figures 6.3a & 6.3b follows a linear trend, the C-rate has an exponential slope. This exponential slope mainly promotes two aspects of increasing the battery capacity. Firstly, discharging a 100 kWh battery package with 300 kW (3-C) leads to a higher

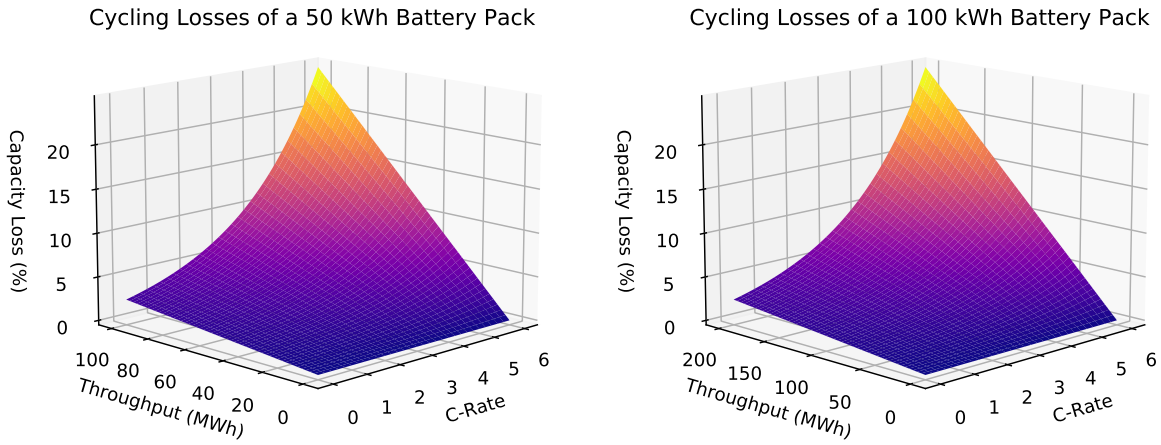

(a) 50 kWh.

(b) 100 kWh

Figure 6.3: Cycling losses of a (a) 50 kWh and (b) 100 kWh against the total throughput and C-rate.

degradation than using a domestic charger with 11 kW (0.11-C). Hence, a lower discharging time goes along with a higher cycling induced degradation due to high C-rates. Secondly, doubling the amount of capacity leads to halving the cycling induced degradation for the same total throughput. Consequently, approaching the vehicle's battery as an energy storage, requires the selection of a suitable charging power according to the battery capacity.

Overall, by increasing battery capacity three major effects result: longer range, C-rate can be decreased without lowering the charging power and more total throughput can be obtained. Hence, it is desirable to increase the battery capacity of the battery for Vehicle-to-Grid applications in technical terms. However, it is important to consider that size, weight and costs limit higher battery capacities.

6.1.3. Sensitivity of Electric Vehicle Degradation

The sensitivity analysis of dispatched energy assessed the degradation as a result of the discharging process, which is a common practice in Vehicle-to-Grid research. However, putting emphasis on the degradation, the identification of favourable conditions in terms of degradation reduction can be revealed.

To recap, the overall degradation is the result of calendar and cycling induced losses. Hereby, Section 3.2.5 outlined that high states of charge lead to a higher calendar induced aging of the battery. It was highlighted, that instead of applying a linear behaviour between state of charge and calendar aging, plateau region were observed. With respect to cycling induced losses, low C-Rares lead to a lower degradation.

Discharging the battery to reduce high states of charge results in a lower calendar aging and can lead to an overall degradation reduction. First and foremost, discharging the battery increases the degradation, because of cycling induced losses. However, the lower state of charge results in lower degradation per time than the initial state of charge. To evaluate if discharging can lead into an overall degradation reduction, the degradation per time for a higher state of charge can be compared to the lower state of charge and its degradation. Hence, the difference between both degradations increases with the time as well and can be determined. The additional stress by discharging the battery to a lower state of charge is incorporated by the following equation:

$$\left.\frac{\delta Q_{\text{loss}}^{\text{cal}}(t, \text{SoC}_{\text{high}})}{\delta t}\right|_{t=\hat{t}} \cdot \Delta t \overset{!}{\geq} \left.\frac{\delta Q_{\text{loss}}^{\text{cal}}(t, \text{SoC}_{\text{low}})}{\delta t}\right|_{t=\hat{t}} \cdot \Delta t + \Delta Q_{\text{loss}}^{\text{cycle}}(\hat{t}) \tag{6.1.2}$$

$$t_{\text{pass}} = \Delta t \overset{!}{\geq} \left.\frac{Q_{\text{loss}}^{\text{cycle}}(t) \cdot \delta t}{\delta Q_{\text{loss}}^{\text{cal}}(t, \text{SoC}_{\text{high}}) - \delta Q_{\text{loss}}^{\text{cal}}(t, \text{SoC}_{\text{low}})}\right|_{t=\hat{t}} \tag{6.1.3}$$

Consequently, t_{pass} represents the time in hours that has to pass until the lower state of charge leads to an overall lower degradation. In this context, Figure 6.4 depict the plateau regions for four battery ages along with the time required to pass.

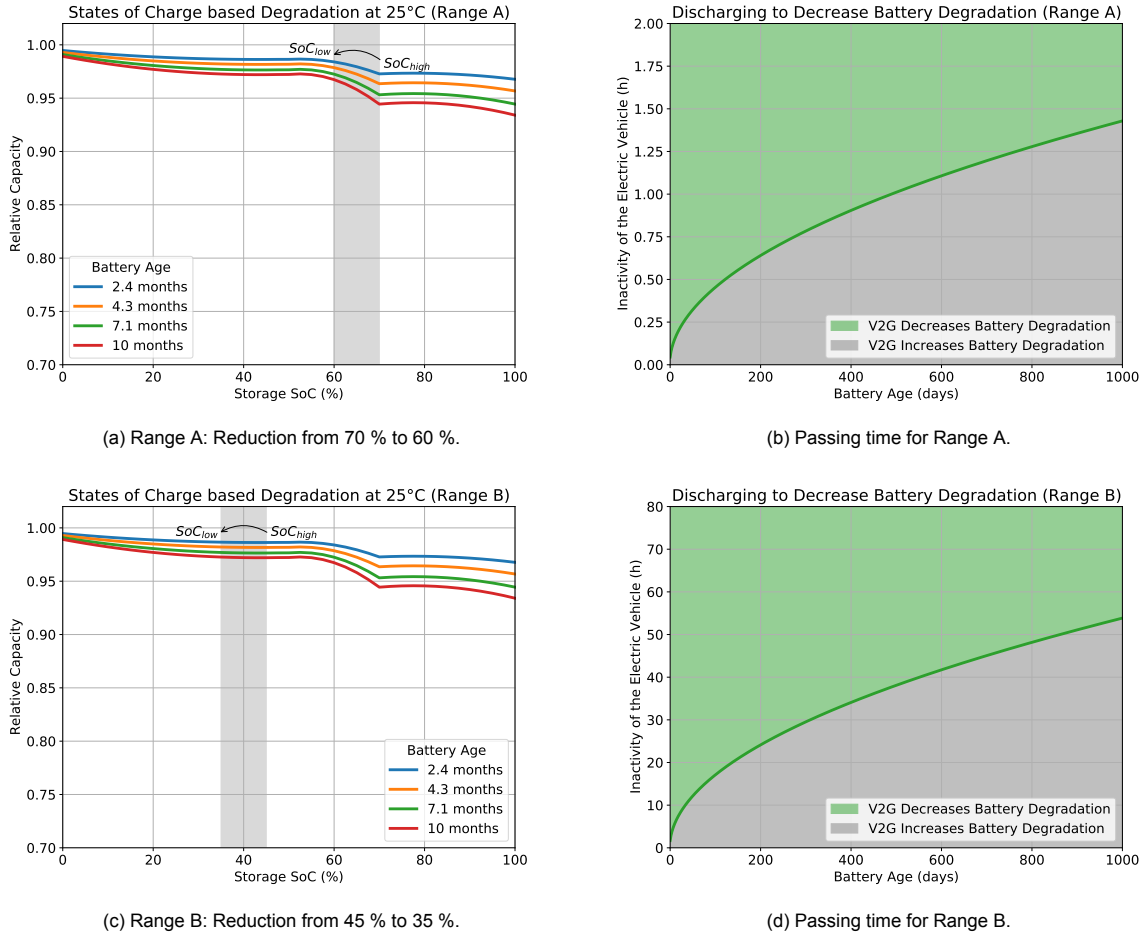

(a) Range A: Reduction from 70 % to 60 %.

(b) Passing time for Range A.

(c) Range B: Reduction from 45 % to 35 %.

(d) Passing time for Range B.

Figure 6.4: State of charge reduction approach for two different state of charge ranges in (a) and (c) while (b) and (d) show the resulting passing time for both ranges.

Both figures on the left hand side highlight two different state of charge reductions with the incentive to lower calendar induced degradation through discharging. Former figure focuses on the range, where a state of charge reduction leads to the shift from one plateau to another. Besides, latter figure applies a state of charge reduction without resulting in a lower plateau region state. Figures 6.4b & 6.4d plot the minimum passing time t_{pass} until the overall degradation begins to decline. Along the x-axis the age of the battery in days increases, while the y-axis indicates t_{pass} for different C-rates. Before comparing different C-rates, only 1C will be in the focus for the first investigations.

The longer the reduced state of charge lasts, the higher the potential that degradation can be reduced in both cases. Both, Figures 6.4b & 6.4d indicate that the lower state of charge can decrease the overall degradation of the battery. By comparing the figures, it is apparent that the slope of both curves is independent from the state of charge. Hence, the state of charge reductions only differ in the time t_{pass} that has to pass. In general the more time passes, the more degradation can be potentially reduced.

The plateau regions for calendar aging create an incentive to discharge the battery at selected states of charge. All Li-ion batteries that are mentioned in the scope of the work (NMC, NCA & LFP), have the characteristics of plateau regions for calendar aging (see Figure 3.8 in Section 3.2.5). The example of NMC based Li-ion cells in Figure 6.4 revealed that shifting the state of charge to a lower plateau can lead to a lower degradation. The time t_{pass} until the degradation can be lowered was around twenty times lower for an favourable state of charge reduction.

The older a battery is, the longer a low state of charge has to last until a degradation reduction takes place. Due to irreversible chemical reactions, calendar degradation at an early stage of the battery's lifetime is higher than at a later stage. Hence, the lower degradation of older batteries lead to a lower incentive to discharge the battery for obtaining an overall lower degradation.

6.2. Sensitivity of Vehicle-to-Grid based Ancillary Services

In continuation of the sensitivity analysis based on electric vehicle characteristics, the grid perspective forms the scope of the following section. Hereby, Section 2.3 already outlined that among others, peak shaving, active power provision for frequency control, active power ramping as well as reactive power for voltage control is in the interest of Vehicle-to-Grid research. Hence, all four ancillary service form the scope of this section's sensitivity analysis.

6.2.1. Sensitivity of Peak Shaving

While demand response promotes the incentive of adapting the charging power at different times, Vehicle-to-Grid approaches enhance the vehicle capabilities by peak shaving through discharging the battery. The previous section emphasised effects on the vehicle, whereas this section reveals the sensitivity of peak shaving on the distribution level.

The component loading of the distribution network will indicate a measure for limitations. Peak shaving may not only be a service in the distribution network, but also for upstream or parallel networks, which are physically connected. This requires to take the transformer into account. Hence, the distribution network from Chapter 4, which is depicted in Figure 4.1, illustrates the grid under investigation.

Where the transformer in this work is rated to 400 kVA, and the lines are NAYY 4x150 SE with a length of 50 m. The voltage level at the primary side of the transformer is 10 kV and 400 V at the secondary side. Furthermore, the load on bus 2 represents the power demand of the distribution network. In this case it is neglected if the loads are placed on different busses with different physical locations. Instead, the power demand of the distribution network is measured on the same bus where the electric vehicles are connected. One electric vehicle is represented by the battery, a DC/DC converter and the DC/AC converter. The previous sections revealed that an increased charging power lead to a higher degradation and the activation of the thermal management system. Hence, in this section, 10 kW per Vehicle is applied and scaled up.

With respect to the research question, the sensitivity will be evaluated primarily. It is apparent, that the working conditions of all components will determine the results accordingly. Thus, the sensitivity of peak shaving can be extracted from the network by simulating a variety of working conditions.

As a result, Vehicle-to-Grid based peak shaving can provided in order to satisfy three different demands of the grid, which are reduction of component loading, increasing the maximum power provision of the distribution network and providing active power to upstream or parallel networks.

For the identification of these services, Figure 6.5 outlines the transformer and line loading, respectively. In both figures, the x-axis depicts the demand of the load up to an active power of 400 kW. The y-axis scales up the amount of vehicles, that provide an ancillary service with 10 kW discharging power each. Based on both loading plots, the identification of the three operation conditions are:

Firstly, peak shaving provides the capability to reduce transformer and line loading. Taking zero vehicles as reference, along the x-axis the increased demand of the load leads to a loading up to 120 % for the selected transformer. As expected, the same behaviour is observed for the selected line, but the loading is around two times higher due to the specific line selection. Accordingly, increasing the number of electric vehicles (compare y-axis) reduces the loading of both components. Shifting the scope to the diagonal dark blue region reveals the minimum of the network loading. Obviously, the minimum loading occurs when the demand of the load intersects with the power provided by the vehicles.

Secondly, peak shaving can increase the maximum rated power capabilities of the distribution network. It was already highlighted, that without the electric vehicle fleet, the transformer limits the network power capabilities to 400 kVA. Within the distribution network, the lines limit the power capabilities

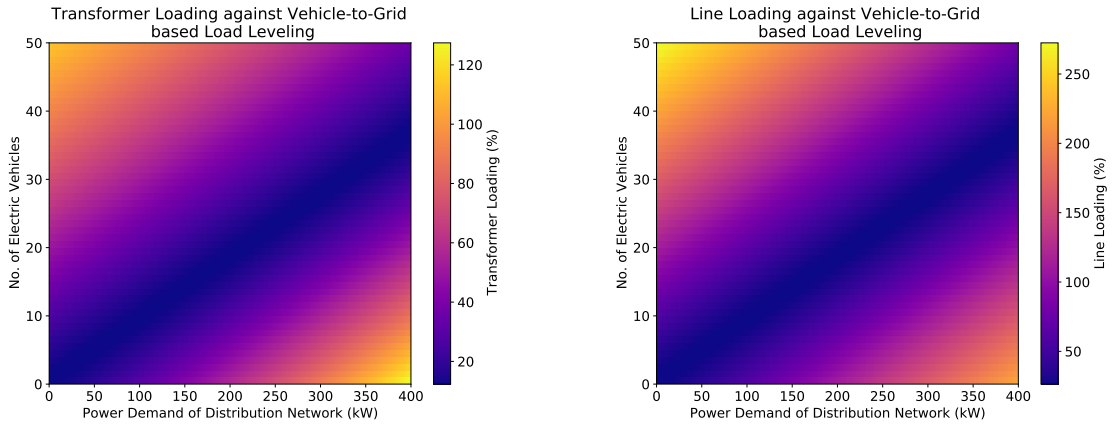

(a) Transformer loading.

(b) Line loading.

Figure 6.5: Vehicle-to-Grid based active power provision with 11 kW from each electric vehicle. The x-axis depicts the power demand of the distribution network on the low voltage side of the transformer. The transformer loading (a) and line loading (b) are a reference for the stress on the example network.

further. Focusing on the transformer as the coupling between distribution grid and the external grid, electric vehicles have the capability to supply a power demand that would exceed the nominal rating of the transformer. Hence, beside feeding the load through the upstream network, electric vehicle are an additional power source.

Thirdly, providing peak shaving services for upstream or parallel networks is physically limited. In both figures the operation points above the diagonal blue line represent the cases, where the provided power of the vehicles exceeds the demand of the load. Hereby, the direction of the powerflow is reversed. Instead of supplying the load from the external grid, the electric vehicles feed power to the external grid. As both figures show, the upstreaming power flow is physical limited by the transformer and lines. Hence and similar to the opposite case, the amount of vehicles providing power to the upstream or parallel networks is limited by the transformer and lines. This rises the issue that increasing the nominal power rating of each vehicle within a fleet would not be unlimited by the network.

Overall, the integration of electric vehicles for peak shaving in a fleet configuration is mainly limited by the network capabilities. However, this section outlined, that Vehicle to Grid has the capabilities to shave peaks beyond the maximum power rating of the network. Additionally, the network loading can be varied by adapting the number of electric vehicles. For this reason, it has to be noticed that peak shaving in parallel or upstream networks can stress the network components additionally, leading to upper powerflow limitations.

6.2.2. Active Power for Frequency Regulation

In order to provide Vehicle-to-Grid based frequency regulation, the vehicle fleet at the distribution level injects active power to level imbalances at the transmission grid. This section reveals the sensitivity of active power provision in terms of limitations, efficiency, response type and dispatched energy. A differentiation between Frequency Containment Reserves (FCRs), Frequency Restoration Reserves (FRRs) and Replacement Reserves (RRs) will not be made in this section. Instead, the sensitivity of the response to the demand of frequency regulation will form the scope of this section.

Similar to peak shaving services for parallel or upstream networks, the active power provision to the transmission system is physically limited. In the previous section, the sensitivity analysis in Figure 6.5 revealed how the transformer and lines affect an upstream power flow. Hence, the maximum power provision of the electric vehicle fleet on the distribution level subjects to the components of the power system, too.

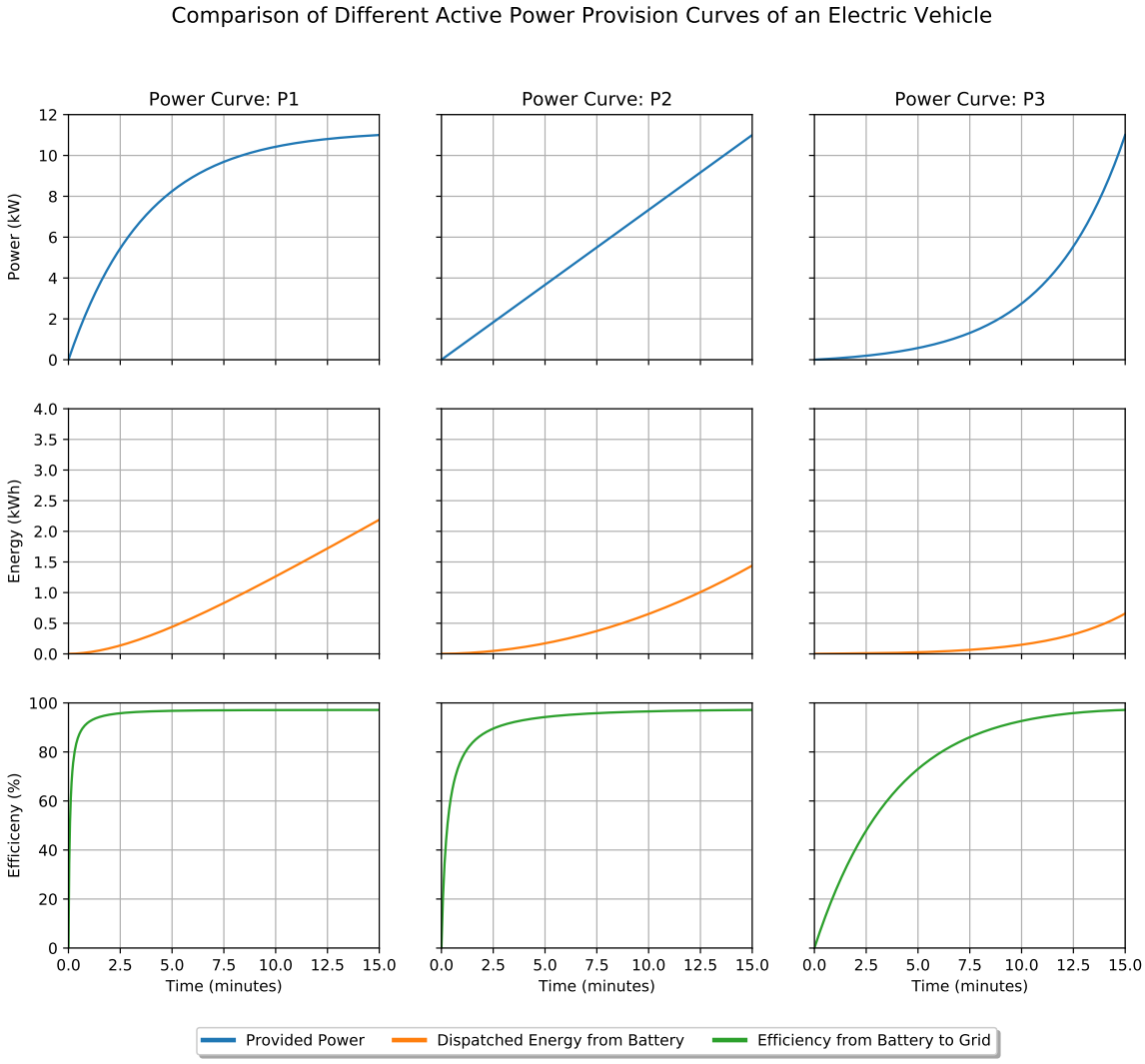

Figure 6.6: Response types.

The response of a single electric vehicle can be measured in terms of active power provision, efficiency and dispatched energy. To evaluate the active power provision three power curves will be investigated. Accordingly, the first row of Figure 6.6 shows three power curves under investigation.

The depicted curves have a peak value of 11 kW, but differ in their slope until they reach 11 kW. Power curve P1 follows a steep slope in the beginning, while type R2 depicts a linear slope and R3 an has a steep slow in the end. For all three curves, the resulting dispatched energy from the vehicle is shown along with the efficiency. The power curves not represent the active power demand for frequency control directly. Instead, the figure shows how different power curves would affect the sensitivity of both values. The linear power curve (P2) is a reference for a ramp and its sensitivity is given by power curves P1 and P3. One may note that the common x-axis lists a time frame of 15 minutes to demonstrate an exemplary service time.

All three power curves intend to reach the same nominal power of the converter, but resulting in different dispatched energy. By following a linear power curve (P2) towards 11 kW, the dispatched energy would be less than 1.5 kWh for a time period of 15 minutes. Taking a 50 kWh battery pack as a reference, less than 3 % of state of charge will be dispatched for providing this service. By demanding a higher slope in the beginning (P1), one has to withdraw more than 4 % state of charge for the same period. In contrast, the strong slope in the end of the service provided by P3 requires less energy (<1 %).

By providing an active power curve, which dispatches less energy, the average efficiency declines. Due to the low efficiency in the low power ranges of the converter, the average efficiency tends to be higher at the nominal converter power. For comparison, the average efficiency of P1, P2 and P3 are 95 %, 92 % and 75 %, respectively. Overall and because active power is demanded, one can accept a lower efficiency because the total energy demand is still lower.

Additionally, the active power provision of electric vehicles for frequency control can rely on response times of a few seconds and balancing market structures are present. In their work, Bilh et al. [4] analysed that one access point is able to handle 1000 EVs without violating a four seconds latency. Thus, an aggregator would be able to control the power curves of the whole fleet. With respect to present market structures, Section 6.3.3 will recap frequency control from an economical point of view.

6.2.3. Active Power Ramping

The weather depend power output of solar and wind based power plants result in a demand for active power ramping to compensate those fluctuations. Here, electric vehicle may form one opportunity to support the grid by providing either a flexible power output or input. On the one hand, if the power output increases, but the power demand of the grid is unchanged those fluctuations can be compensated through flexible charging the vehicle. On the other hand, if the output declines and the demand cannot be met, discharging is a further opportunity for compensation. The same principle applies to a constant power output and a changing power demand. In the focus of this work, the active power ramping demand of renewable energies will be considered. One may note, that active power ramping subjects to the same physics as presented in the balancing market. However, compared to the balancing market, an aggregator can already schedule electric vehicles in their portfolio beforehand in order to avoid activating balancing market mechanism later on.

In order to evaluate the sensitivity of the demand for active power ramping, the power output changes of different renewable energy sources can be considered. As an example, the Transmission System Operator TenneT determines the forecast for the expected output of renewable energies in the Dutch region. The intraday forecast data [25] for 2020 will be used. Figure 6.7 shows the sorted generation changes per 15 minutes along with their occurrence during the year in %. The three bar plots below the top figure depict the share of positive and negative generation changes. Note that instead of focusing on the demand, reasons for the power output change, which are not based on weather changes (like maintenance etc.), only the generation changes are important for this analysis. Furthermore, the actual generation is not important, because only the ramping rates are in the scope of this active power ramping approach.

How many electric vehicles are necessary to compensate the ramping rates of electric vehicles depends on the installed capacity. In the Netherlands, the installed capacity of solar, wind onshore and offshore were 5710 MW, 3973 MW and 1709 MW, respectively (2020) [25]. Hence, the total share on the total installed capacity was 29.11 % (total grand capacity: 39132 MW) [25]. Beyond the depicted range of the figure, the highest variation of ramping rates vary between 1190.0 MW and -584.0 MW per 15 minutes. Those fluctuations are present for onshore windpowerplants. To compensate both peak values, 119 thousand and around 59 thousand vehicles with a (dis)charging power of 10 kW would be required for compensating the active power ramping of those fluctuations.

As expected, no constant power outputs of renewable energy sources are present, but the share of a constant power output per year and energy source varies. It is obvious, that no generation output for several hours per year are present due to weather and geographical conditions. For instance, the night time leads to no generation for solar based power plants. Hence the power output ist constantly zero, resulting in the highest share of no ramping rates. Nevertheless, the positive ramping rates in the Netherlands for solar, wind onshore and offshore were 26.94 %, 48.56 % and 43.75 %, respectively. The deviations between the share of either positive or negative ramping rates vary from 0.3 % for wind offshore to around 2 % for solar. On the one hand, onshore windpower plants

show the highest share of ramping rates beside 0 MW per 15 minutes. On the other hand, solar require more vehicles to cover the same share per year. Ten thousand vehicles with each 10 kW of provided power would be able to compensate 80 % of the ramping rates. With the same amount of vehicles, one can compensate the fluctuations of onshore and offshore windpowerplants by around 98 %.

Regardless if compensating the ramping rates is needed, it is important to consider if the ramping can be provided decentralised. In example, translating the above results into terms of grid capacity, a simplified approach is to replace the number of vehicles into the number of transformer available. As an example, by assuming 400 kVA per transformer at the distribution level, it is required to have 250 transformer available, if the ramping rates should be compensated either in parallel or upstream networks. However, if the ramping rates can be compensated decentralised on the same network level, transformer limits may not be relevant (see Section 2.1).

For further analysis, the absolute values will be replaced by relative numbers. Putting those values into units of MW for each installed capacity of energy source, the share of renewable energies can be neglected. Instead, the weather dependency for the Dutch region becomes more apparent. Furthermore, the impact of physical distance between the electric vehicle and renewable energy source declines. The reason for that is, that transformer limits do not have to be assumed for further interpretations. Figure 6.8 highlights the ramping rates for each MW of installed capacity along with the amount of vehicles per MW of installed capacity to meet those fluctuations.

Taking approximately the same range into account to compensate around 80 % of solar based

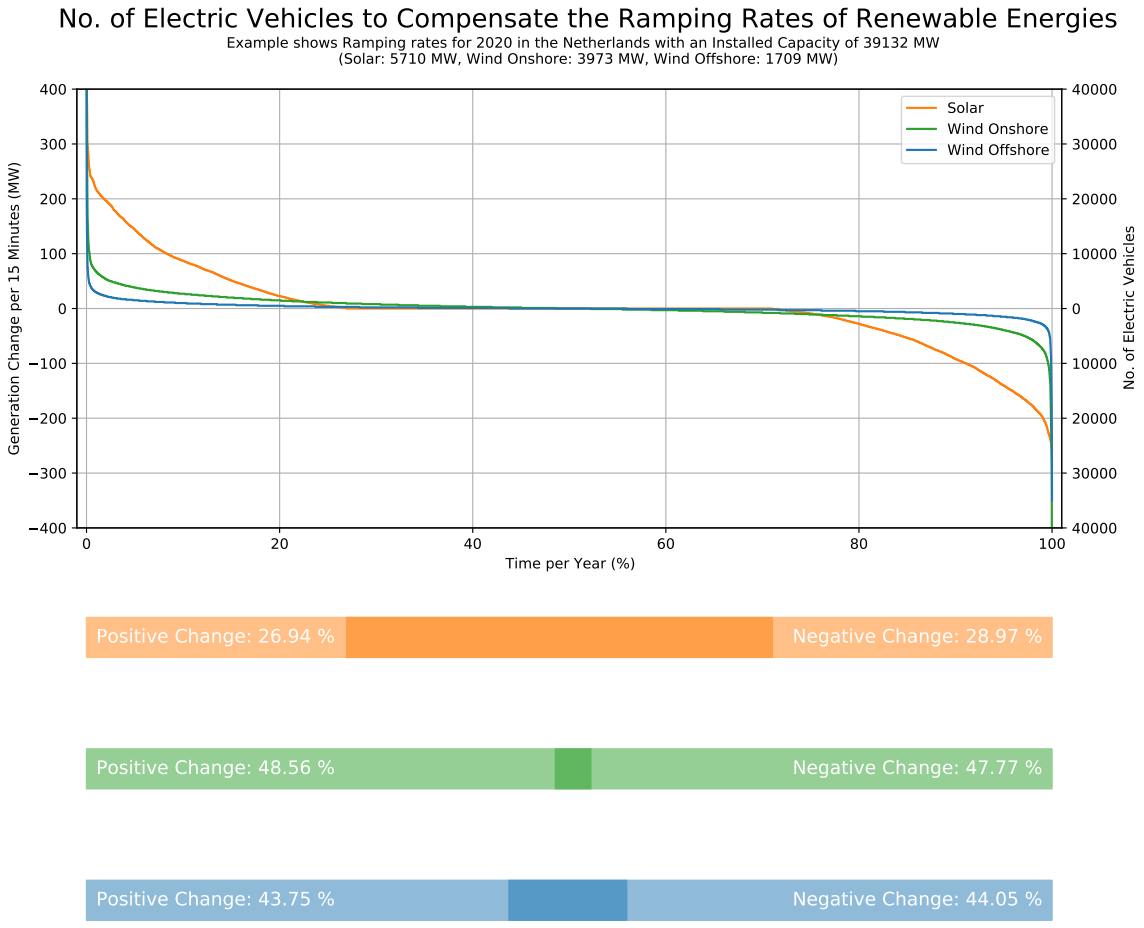

Figure 6.7: Active power ramping of renewable energies in the Netherlands.

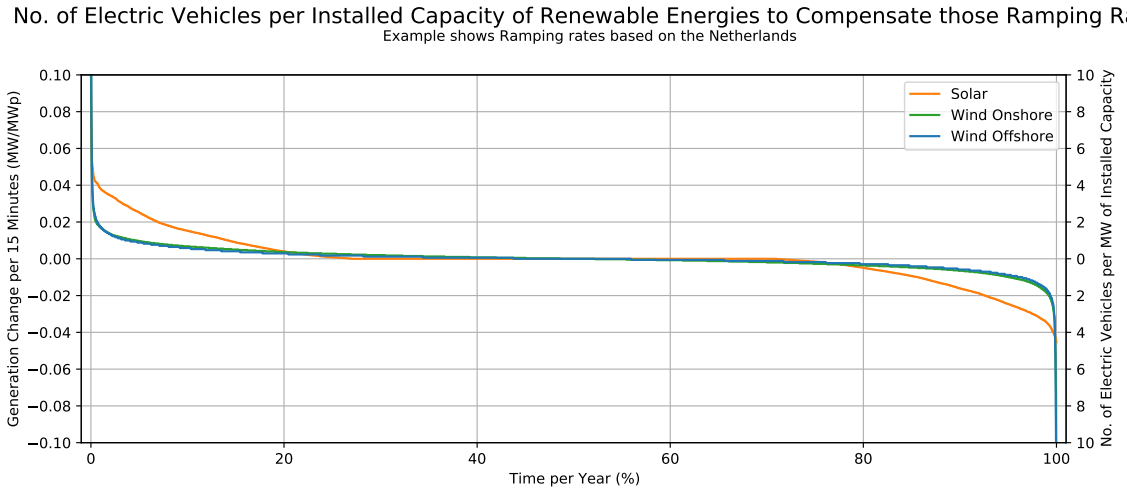

Figure 6.8: Active power ramping per MW of installed capacity.

ramping rates and 98 % of windpowerplant based ramping rates, two electric vehicles per MW of installed capacity would be necessary. As the figure depicts, the generation changes per MW of installed capacity require for the above mentioned range around 20 kW per 15 minutes per installed capacity. Hence, this case requires two electric vehicles with an active power provision of 10 kW each. In example, a windpark in the Netherlands with an installed capacity of 20 MW, who intends to be able to compensate 98 % of the 15 minute rampings would require 40 electric vehicles. Besides, the maximum amount of vehicles, which is beyond the scope of this figure, presents the demand of more than 31 vehicles per MW of installed capacity. This case occurs for positive ramping demand of offshore windpowerplants.

6.2.4. Reactive Power for Voltage Regulation

Beside active power injection, the provision of reactive power is a further electric vehicle based ancillary services. In Chapter 2, the concept of reactive power provision to control the voltage level was explained. An increased share of electric vehicles rises issues in terms of energy losses, voltage deviations, and transformer overloading [99]. This case focuses on an increased energy demand at the distribution level that causes a voltage drop across the lines.

Bidirectional charging capabilities with reactive power provision enable to operate the electric vehicle in four control modes. To provide insights how the adaption of reactive and power set points determine those modes, Figure 6.9 depicts the 4-quadrant operating scheme.

Both figures declare active power P on the x axis, where a positive value corresponds to the charging process, while negative values imply discharging. Furthermore, positive reactive power values on the y axis result in providing capacitive reactive power and positive values express inductive reactive power. As illustrated in (a), a fixed cos(ϕ) of 0.9 is applied, while (b) shows an adaption of the reactive power from $-Q_{\text{ref}}$ or Q_{ref} to Q^*. By providing reactive power, the active power may have to be reduced in order to consider the maximum apparent power of the converter.

Based on the four operational modes, the grid operator can rely on different control modes in order to guarantee voltage stability. In the scope of this work six configurations are investigated:

1. Uncontrolled power demand of 11 kW on each bus as a reference for uncoordinated charging.
2. Controlled power demand by active power reduction to 8.8 kW on each bus.
3. Controlled power demand by active power reduction to 8.8 kW and cos(ϕ)=0.95 on each bus

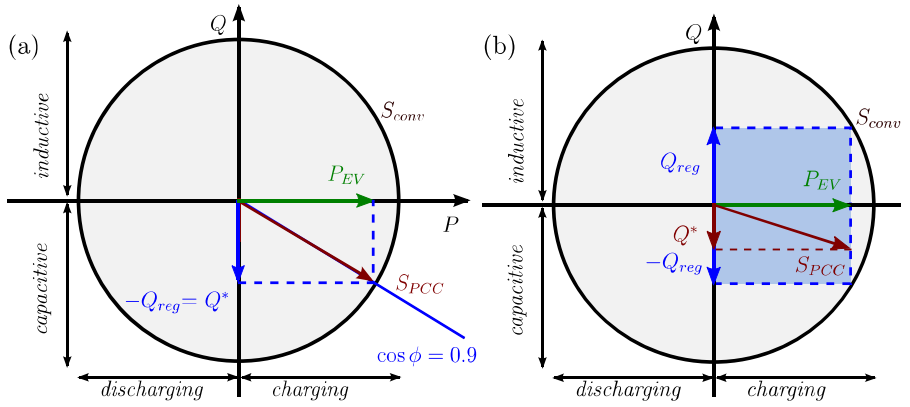

Figure 6.9: 4-Quadrant EV converter operating scheme while charging for (a) constant power factor concept, and (b) proposed voltage enhanced support with dynamic power factor [46].

4. Controlled power demand by active power reduction to 10.45 kW and cos(ϕ)=0.95 on each bus
5. Uncontrolled power demand of 11 kW on each bus, except the last vehicle, which provides -10.45 kW and cos(ϕ)=0.95 (V2G)
6. Uncontrolled power demand of 11 kW on each bus, except the last vehicle, which provides -11 kW and cos(ϕ)=1 (V2G)

For validating these concepts, the distribution grid with the radial topology from Chapter 4 is taken as a reference. The same transformer and line characteristics from the previous section are selected. Figure 4.2 of Chapter 4 visualises the line topology. The multiple bus network for the simulation consists of 20 busse with a line length of 50 meter to each other.

By applying a load flow analysis, the resulting bus voltages and component loadings can be extracted and compared. The outcome of all six configurations are summarised in Figure 6.10 and Table 6.1. With respect to voltage control as the main incentive, the first focus lays down on the voltage drop across the lines in Figure 6.10. It has to be mentioned that the reference bus is set higher than the nominal voltage, because of the expected voltage drop. The figure marks the voltage threshold of ±10 % in grey.

Uncontrolled charging with 11 kW at each bus results in a voltage drop that falls below the minimum voltage threshold. As mentioned at the beginning of this section, increasing the share of electric vehicles at the distribution level rises concerns regarding voltage deviations. Configuration 1 as the only completely uncontrolled stresses the network, whereby the busvoltages after Bus 13 are too low. Hence, mitigating the impact of electric vehicles on the distribution level emphasises the need for controlled charging.

Reducing either active power or providing reactive power together with an active power reduction maintain the voltage levels. Both, Configuration 2 & 3 reduce the active power demand, leading to a decreased current flow and therefore to a lower voltage drop. Hence, by adapting the charging power of all vehicles, the voltage level can already be satisfied, without andy bidirectional charging capabilities. If those power demands are controllable in terms of reactive power provision, Configuration 3 shows how the voltage level can be shifted closer to the nominal voltage.

By providing reactive power at each bus, it is possible to increase the charging power on each bus without falling below the voltage threshold. Configuration 2 demonstrated how a reduction of the active power as one option of the grid operator improves the voltage quality. However, taking Configuration 3 into account, one can see how reactive power facilitates to increase the charging power to 10.45 without exceeding the voltage limit. In this case 5 % of the nominal converter power has to be reduced

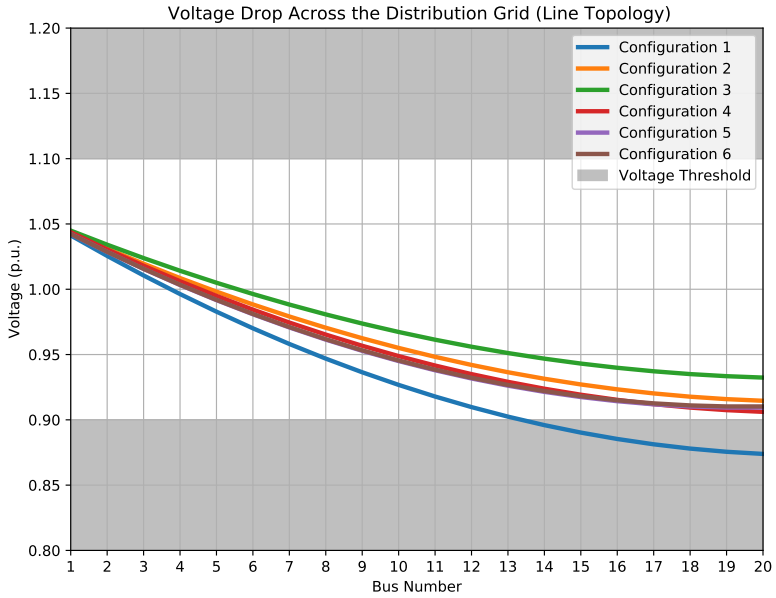

Figure 6.10: Resulting voltage drop across the grid nodes.

instead of 20 % as Configuration 2 demonstrated.

In an overloaded situation with uncontrolled charging vehicles or loads, enabling Vehicle-to-Grid can maintain voltage stability as well. For this purpose, Configuration 5 represents the case, where 19 uncontrolled loads or vehicles with each 11 kW are present at those busses. However, Bus 20 injects active power of 11 kW in order to meet the voltage level. Based on the figure, the services of the single vehicle has approximately the same impact as reducing the power consumption at all busses with and without reactive power (Configuration 2 & 4).

Vehicle-to-Grid services with reactive and active power provision can reduce voltage deviations. Based on the example Configuration 6, rather than injecting the maximum active power it is feasible to inject reactive power as well. By comparing both Vehicle-to-Grid approaches (5 & 6), one can argue that the effects on the voltage deviations are approximately equal. Thereby, reactive power injection in combination with bidirectional charging capabilities can reduce the impact of an uncontrolled vehicle fleet.

Shifting the focus from the voltage level to the components, the transformer loading can be an indicator to evaluate the stress on the network for all configurations. The transformer loading and configuration are depicted in Table 6.1.

As all configuration indicate, the transformer loading is due to the sizing of the network not crucial

Table 6.1: Summary of the configurations together with the resulting transformer loading.

Configuration	V2G	P_{conv} (kW)	$\cos(\phi)$	$P_{conv,\,n}$ (kW)	$\cos(\phi)_n$	Transformer Loading (%)
1	✗	11.00	1	11.00	1	28.16
2	✗	8.80	1	8.80	1	21.90
3	✗	8.80	0.95	8.80	0.95	22.76
4	✗	10.45	0.95	10.45	0.95	27.51
5	✓	11.00	1	-10.45	0.95	24.90
6	✓	11.00	1	-11.00	1	24.82

in this case. However, one can see that uncontrolled charging has the maximum stress on the transformer. Just reducing the active power demand at all busses reduces the loading by over 6 %. Even if the voltage level for Configuration 4 does not exceed the threshold, the transformer loading can only be reduced by less than 1 %.

Derived from these results, the grid operator has a variety of opportunities to avoid voltage imbalances. Except a full uncontrolled and uncoordinated charging configuration, all five configuration meet the voltage level at all busses. For the selection of a suitable operation, it is important to consider the control opportunities at all busses. However, one can argue that even if all vehicles are uncontrollable, Vehicle-to-Grid services at the end of line are possible to reduce voltage deviations.

6.3. Sensitivity of Vehicle-to-Grid based Costs & Market Potentials

The main interest of the thesis is to identify the sensitivity of bidirectional charging capabilities for Vehicle-to-Grid based ancillary services against vehicle characteristics. While vehicle characteristics not only rely on technical capabilities, the sensitivity of financial aspects enhances the scope of Vehicle-to-Grid services. As the introduction outlined, instead of a use case driven approach, the applied methodology in this thesis intends to reveal favourable and avoidable conditions. Hence, this section summarises the sensitivity of degradation costs and discharging costs. As a reference, the costs will be measured against the dutch energy market in order show how the sensitivity affects the market potential.

6.3.1. Sensitivity of Electric Vehicle Battery Replacement Cost & Degradation

Pricing the value of the battery pack of the electric vehicle itself is a measure for the degradation costs. In the previous sections, battery degradation was measured in percentage loss of capacity. Hence, one can map the gradual degradation to the costs for the battery owner.

Before determining a price for the battery pack, it is crucial to outline how these prices differ. Figure 6.11 shows the price of a battery pack per kWh of capacity from 2018 and projected to 2030. Lutsey et al. [51] rely their prices on technical studies and automaker statements. All prices are noted in $ per kWh of capacity.

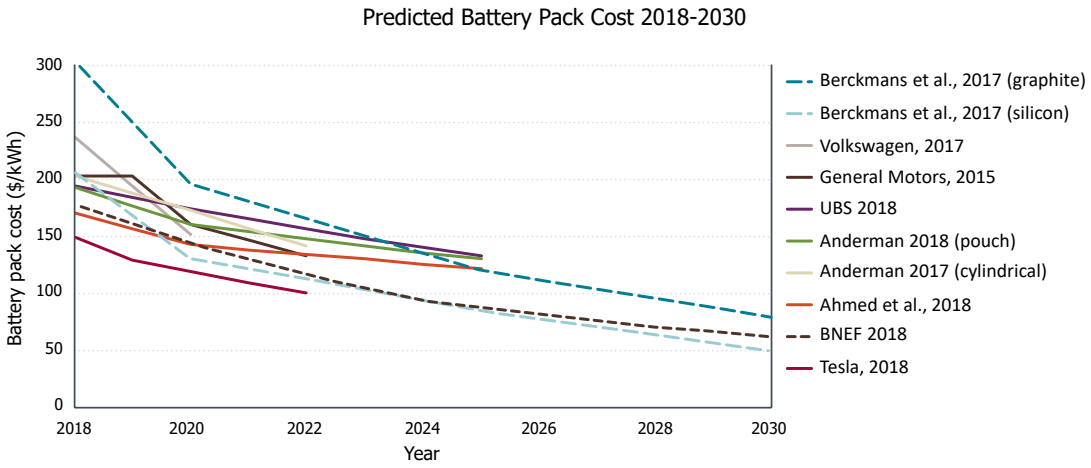

Figure 6.11: Electric vehicle battery pack costs from technical studies and automaker statements [51].

The depicted studies expect that from 2018 to 2030 the prices per kWh decline. While for 2018, the battery pack costs vary between 150 $/kWh and 300 $/kWh, all studies expect that the price fall to 150 $/kWh and below within the next years. For 2030, Berckmans et al. expect that for silicon based Li-ion cells, one obtains prices of around 50 $/kWh and around 80 $/kWh for graphite based Li-ion cells.

In order to determine the battery degradation costs, the conditions, where a battery has to be replaced are crucial. As it was already outlined, by convenience the end of life conditions are achieved, when the battery capacity reaches 80 % of the initial capacity. Again it has to be noticed that those conditions are not undisputed (see Section 3.2.5). However, in the scope of this work a state of health of 80 % will be applied as the replacement condition, too.

For determining the price of degradation, one can price the gradual loss, which is induced by additional cycling. Reducing the capacity from the initial state of health to the end of life conditions results in a range for degradation. With a SoH_{init} of 100 % and SoH_{repl} of 80 %, 20 % degradation can be excepted before the replacement takes place. Here, driving pattern and user behaviour determine the share of

calendar aging and cycling induced losses that affect the degradation.

The degradation costs of the battery not only determine the discharging costs completely, but also the replacement fee are proportionate costs. For a representation of the full replacement costs, Equation 6.3.1 depicts both costs.

$$\text{Degradation Costs} = \underbrace{\frac{Q_{\text{loss}}^{\text{cycle}} \cdot C_{\text{batt}}}{\text{SoH}_{\text{init}} - \text{SoH}_{\text{repl}}}}_{\text{Cycling Induced Costs}} + \lambda \cdot \text{Replacement Fee} \tag{6.3.1}$$

The cycling induced costs expresses the gradual costs of loss in relation to the minimum state of health, as it was explained in the previous paragraph. Additionally, the replacement conditions for each battery may be reached at an earlier or later stage depending on the Vehicle-to-Grid discharging strategy. Hence, λ determines the responsible share of Vehicle-to-Grid on the replacement fee. In this work, it is argued that both, replacement fee and λ depend on the vehicle and user behaviour. Thus, the sensitivity analysis focuses on the cycling induced costs.

Discharging based degradation costs are sensitive against temperature and C-rate. Figure 6.12 shows the sensitivity for a 150 € battery pack considering only degradation. The degradation costs are depicted in € per kWh of dispatched energy. In a higher resolution, Figure 6.13 shows the same plot for two selected temperature ranges.

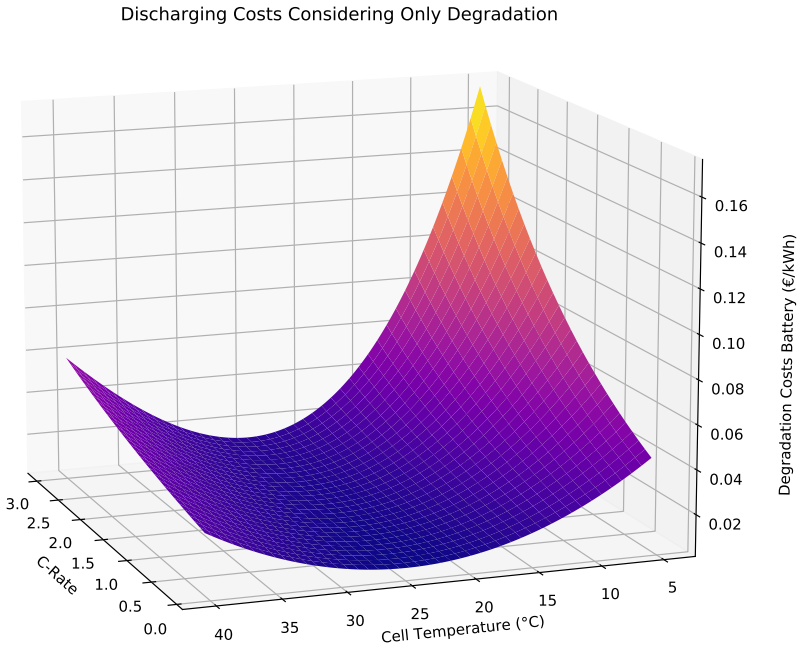

Figure 6.12: Vehicle degradation costs based on 150 € per kWh of capacity.

Prices for the degradation costs can be lower than 0.01 €/kWh or exceed 0.10 €/kWh depending on the operation conditions. As the figure shows, the temperature dependency leads to concave shape with a minimum around 25 °C for all C-rates. Deviations from ideal cell temperatures can increase the costs ten times. High C-rates at low temperatures exceed 0.10 €/kWh, whereas all C-rates below 1-C induces costs less than 0.07 €/kWh. Optimal cell conditions and a C-rate of 0.5-C fall below prices of 0.01 €/kWh.

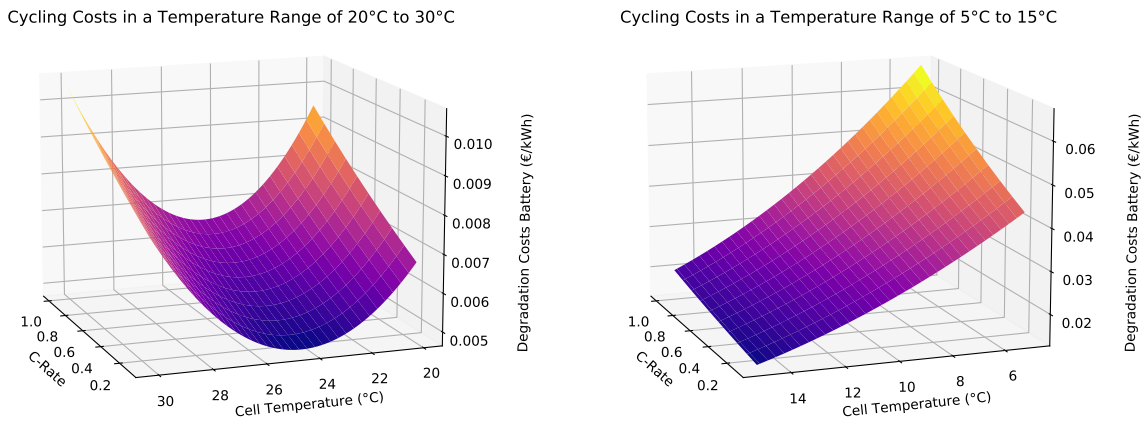

(a) 20°C to 30°C.

(b) 5°C to 15°C.

Figure 6.13: Discharging costs considering only degradation for a selected temperature range.

Applying a discharging strategy that intends to reduce battery degradation can lead to positive financial benefit of discharging. Section 6.1.3 revealed that high states of charge offer the opportunity to reduce degradation through discharging. This approach emphasised that high states of charge lead to a higher calendar aging and discharging allows lowering calendar aging. The reduced state of charge as the new operation condition of the battery has to last long enough until the degradation declines. Generally, idle times of the vehicle provide the opportunity to meet those temporal conditions. Hence, discharging can reduce the total degradation leading to no additional costs and a financial benefit through the lifetime expansion of the battery can be expected.

Lastly, calendar aging as an unavoidable degradation process neither has a benefit for the user nor offers the opportunity to generate a financial income. As calendar aging is a process of time, the gradual decline of degradation takes place without any usage of the vehicle, leading to a loss of opportunity for using the battery in any applications. Hence, if the vehicle's battery is completely unused, degradation still takes place. With the focus on opportunity costs one can obtain a financial benefit by discharging the battery, but not if capacity fade through calendar aging takes place.

6.3.2. Sensitivity of Discharging Costs

Beside the degradation of the battery itself, the charged energy determines the minimum price for the dispatchable energy. As a first assessment, the levelized cost of energy for renewable energy sources will be taken into account. The next section covers market prices that includes day-ahead markets, negative prices and income through ancillary services. Meanwhile, this section focuses on the levelized costs in order to cover cases where market participation is not necessarily the primary intention (i.e Vehicle-to-Home).

The decarbonisation of the transport sector relies on charging energy from renewable sources, like hydropower, solar, wind and bioenergy. Figure 6.14 depicts the price development of those technologies from 2000 to 2019. The prices are based on the 2019 $ and taken from the International Renewable Energy Agency [35].

The levelized cost of energy for hydropower, solar, wind and bioenergy falls worldwide below 0.15 $/kWh. As the figure shows, hydropower represents the lowest levelized cost of energy for all renewable sources in 2019. One may see that the levelized costs of energy for hydropower and bioenergy are compared to the other sources relatively constant over the last decade. Besides, onshore windenergy as well as photovoltaic decline constantly over the last years. It is noticeable, that within the last decade the levelized cost of energy for photovoltaic can be reduced more than seven times. Offshore wind energy experienced an incline of costs after 2006, but constantly declines since

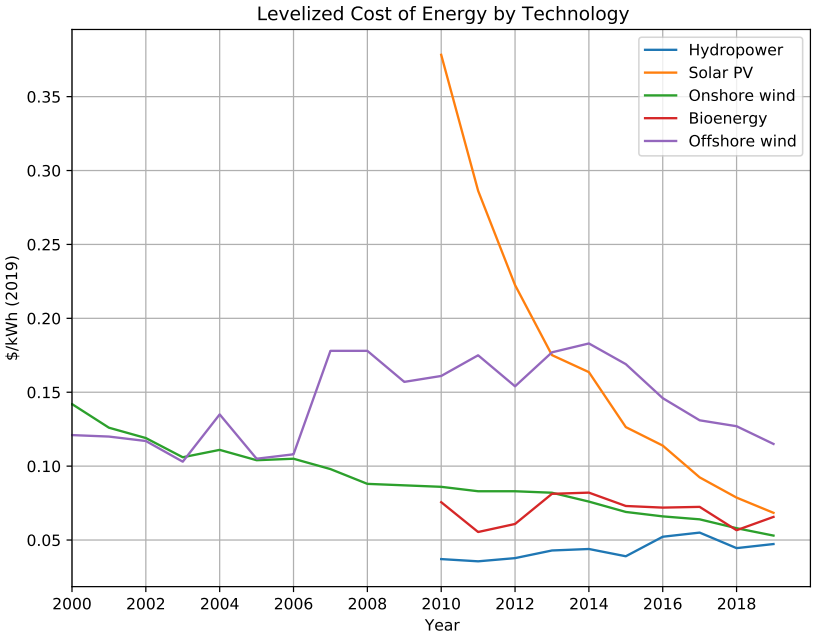

Figure 6.14: Worldwide levelized cost of energy for different renewable energy sources [35].

2014, whereby it reaches the same value as before.

Beside the levelized cost of energy, which are relevant renewable energy source owners, the European electricity prices for households have to be taken into account as well. The domestic prices per kWh vary between 0.0396 €/kWh and 0.3006 €/kWh including tax and levies within the European Union according to the European Statistical Office [60]. They list that the highest costs in the European Union are present in Germany (0.3006 €/kWh), Denmark (0.2819 €/kWh) and Belgium (0.2702 €/kWh).

In order to demonstrate how the energy price and Vehicle-to-Grid design affect the price sensitivity, two cases are listed. Firstly, one case relies on a high efficient converter (98 %) with 11 kW and charging costs of 0.1 €/kWh under ideal cell conditions. Secondly, a converter with a higher nominal power of 50 kW will be applied, which has a nominal efficiency of 78 %. Additionally, the second case subjects to charging costs of 0.3 €/kWh and a cell temperature of 5°C. Figures 6.15 & 6.16 summarise the results of both cases for different charging discharging power. Both cases rely on the same type of battery as well as a nominal battery capacity of 50 kWh.

The first case demonstrates conditions for Vehicle-to-Grid that can leading to total discharging costs between 0.12 €/kWh to 0.21 €/kWh. Figure 6.15 illustrates that if both, charging and discharging takes place at charging power values closer to the nominal power, one can achieve the lowest discharging costs. Compared to the initial charging prices, additional 0.02 €/kWh would have to compensate degradation and energy losses. Hence, an increase of 20 % takes place. Meanwhile, if one applies a lower charging or discharging power, the prices rise up to 0.22 €/kWh. For instance, if the vehicle charges with 1 kW and discharges with the same value, discharging costs of 0.15-0.16 €/kWh are present. Especially low power values can occur if one designs Vehicle-to-Home applications for domestic loads, which can be below 1 kW. Hence, not only in terms of efficiency, but also in terms of costs, this has to be considered for Vehicle-to-Home system designing.

Shifting the scope to a costly design that does not rely on optimal conditions for Vehicle-to-Grid, the discharging costs can exceed 15 €/kWh. As it was seen, especially a low power range tend to increase the price due to the lower efficiency. In Figure 6.16, Case B depicts charging and discharging power values up to 50 kW. The lowest price under the described conditions is 0.64 €/kWh, which occurs at a charging and discharging power of around 34 kW. These costs are more than five times higher

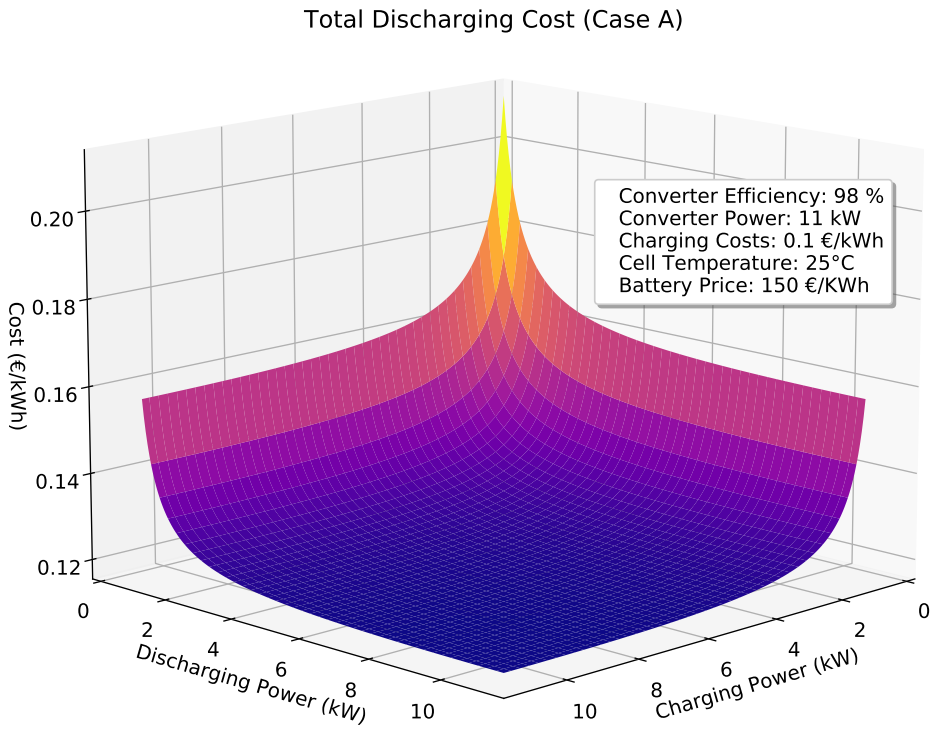

Figure 6.15: Vehicle-to-Grid configuration Case A (500 W to 11 kW).

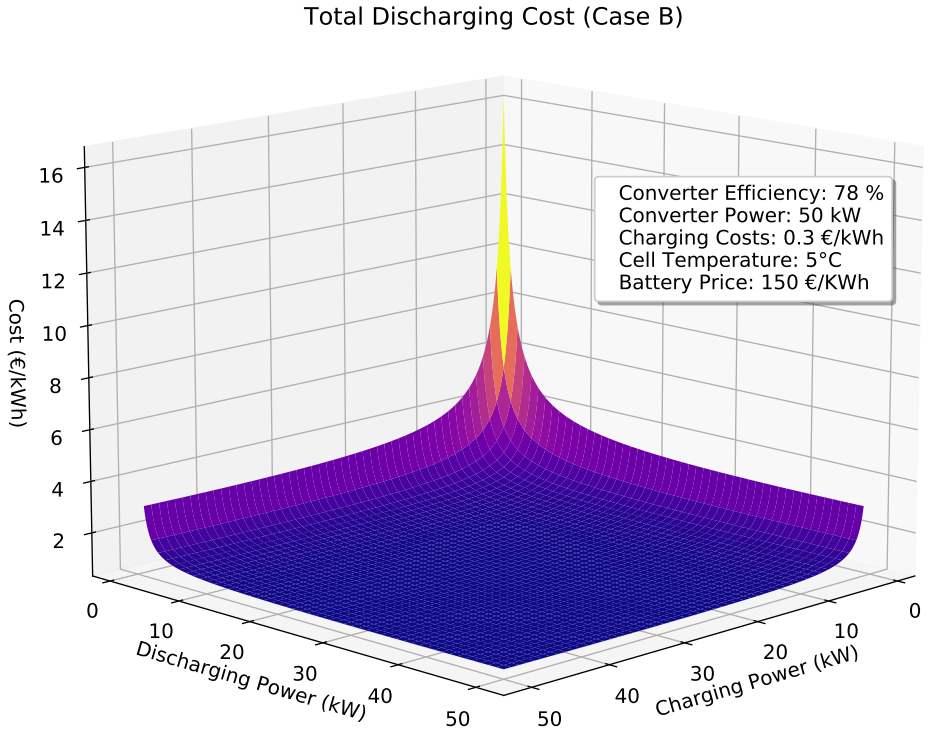

Figure 6.16: Vehicle-to-Grid configuration Case B (1 kW to 50 kW).

than the lowest costs, which occurs in the first case. However, the lowest price are not present at the maximum power of the converter, because of the resistive losses. Besides, one has to consider that charging and discharging can enable the thermal management, which is not considered in the scope of this work. However, it is advised that if one applies higher charging power values (i.e. for 50 kW) the thermal management should not be neglected, which can decline the efficiency leading to higher energy costs. Furthermore, by comparing the low power areas (1 kW), one can determine discharging costs of more than 15 €/kWh. Hence, the discharging prices is sensitive against the converter design and charging prices.

Taking the charging price sensitivity into account, a higher battery pack price per kWh has only a minor effect on the discharging costs for Case A. By increasing the price from 150 $/kWh to 250 $/kWh, 1 kWh of discharged energy is only increased by less than 0.01 € for the optimal condition. Compared to that, the optimal conditions for Case B rises to around 0.08 € per kWh for the same battery price increase. The reason for the minor impact of degradation on the discharging costs subjects to the favourable cell conditions and low C-rates for Case A.

6.3.3. Dutch Day-ahead Market Prices

The sensitivity analysis of costs revealed that discharging costs are crucial for determining the financial value of Vehicle-to-Grid. In order to obtain an indicator for the sensitivity of costs, one can apply the Dutch day-ahead market as a reference. Against the approach of this work, which intends to avoid use cases in order to reduce uncertainties, the following and next sections only act as an example. This allows to map the sensitivity of costs against the market potential in terms of participation opportunities. Thus, it is not intended to solve the question how economical the participation could be.

The day-ahead market provides the opportunity to rely the charging strategy on flexible electricity prices. The electricity prices for Dutch households in the second half of 2020 was 0.1361 €/kWh on average including tax and levies [60]. Without tax and levies, the price per kWh of electricity was 0.1124 €/kWh. To compare these prices to the day-ahead market, Figure 6.17a shows the price distribution of the day-ahead market for 2020.

Translating the domestic electricity prices into units of MWh, one can see that the day-ahead market falls below 112.40 €/MWh more than 99 % of the time per year. One has to notice that the day-ahead market prices do not cover the grid fees that the households have to pay. However, the flexible prices lead to possible bidding strategies for ev aggregators [30].

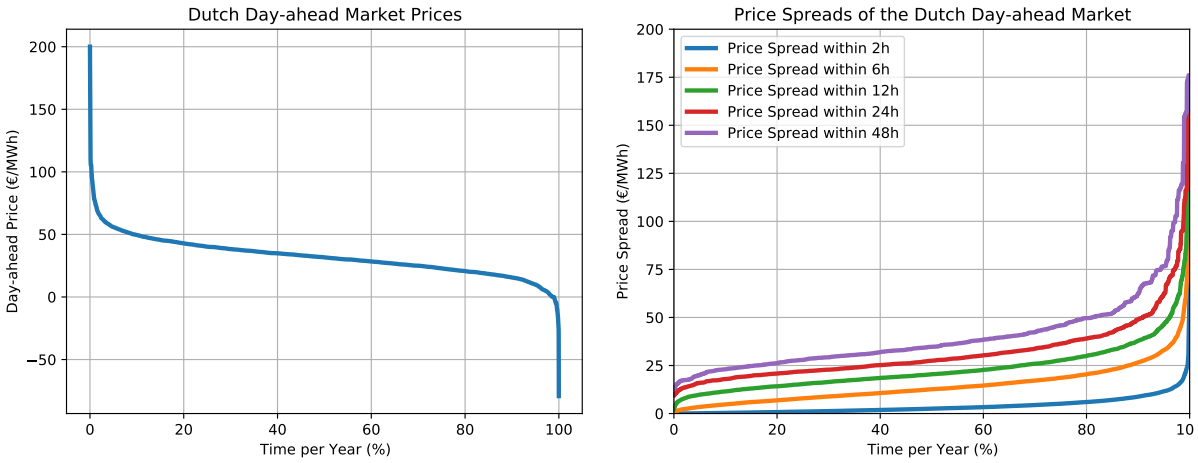

(a) Sorted prices.

(b) Price changes within different time periods.

Figure 6.17: Dutch day-ahead Market for 2020.

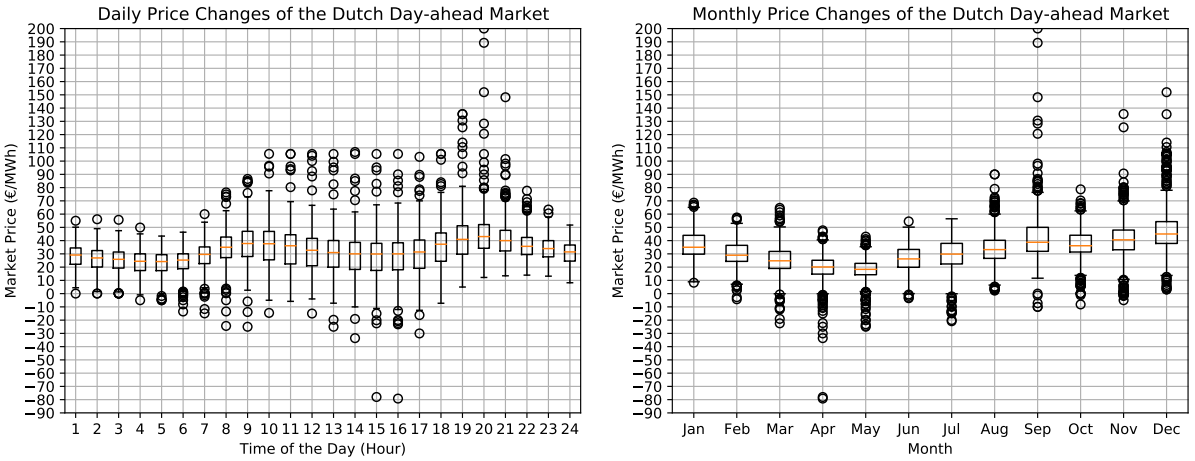

(a) Daily price changes.

(b) Monthly price changes.

Figure 6.18: Seasonal changes in the Dutch day-ahead market for 2020.

While charging primarily gives preference to negative and low prices, discharging aims high electricity prices. Apparently, both conditions occur during the year with a maximum of 200.04 €/MWh and minimum of -79.19 €/MWh leading to a price spread of almost 280 €/MWh. Nevertheless, around 80 % of the year, the prices vary between 15 €/MWh and 50 €/MWh. Thus, it is import how likely it is that the price changes within a certain time period. This implies if one can apply a flexible charging and/or discharging strategy.

The longer the timer period under investigation lasts, the more opportunities to identify a higher price spread within the period exist. Figure 6.17b emphasises five different time periods, that begin with two hours and end with two days. Focusing first on the two hour time interval, for around 80 % of the time within the year one can expect price changes of less than 6 €/MWh. However, if the time period is enhanced to six hours, one exceeds the price spread of 6 €/MWh already in more than 80 % of the time. It has to be noticed, that for all time periods, it not necessarily implies that the highest spread occurs directly between the beginning and end of the time period. By increasing the time period further to 48 hours, one can expect price changes up to 176.03 €/MWh. Throughout the whole year, the maximum price spread within 48hours is always at least 12.61 €/MWh.

To identify if specific times of the year are likely to be linked to a specific market price or a widely price spread, a price distribution per time of the day can be used. Hence, in Figure 6.18a, one can extract the day-ahead market prices for 2020 based on the time of the day. Based on the data, the average price for 2020 was 32.23 €/MWh. The maximum deviation from this average value is the average price of over 40 €/MWh at 8 PM. At the same time the highest peaks occur, which maximum was already determined as 200.04 €/MWh. Negative electricity prices occur mainly in the morning and afternoon. Generally, the price spread between 10 PM and 6 AM are more narrow compared to the daytime.

Shifting the scope from the day to seasonal price spreads, the monthly deviations act as a reference. Along with Figure 6.18b, one can see that rather than having seasonal effects, monthly deviations are present. These price deviations depend on various factors, like weather conditions, holidays etc. Hence, in the scope of this work, it is argued that one cannot derive a general causality for this effect.

6.3.4. Dutch Balancing Market Prices

The balancing market is in the interest of Vehicle-to-Grid research, due to higher prices per MWh. To recap from Chapter 2, one differentiates between upward and downward regulation. On the one hand, upward regulation intends providing power to the grid. This can either be realised through injecting active power or by reducing the active power demand. On the other hand, downward regulation forms the opposite case. Hence, one either reduces the power injection or increases the power demand. With respect to Vehicle-to-Grid, the focus of this work will rely on upward regulation. Downward regulation would be possible, if the vehicle already injects active power into the grid and reduces its output. However, by applying upward regulation, the vehicle is able to inject power as soon as one demands frequency control without those preconditions.

The prices for Frequency Containment Reserves and Frequency Restoration Reserves differ in terms of magnitudes and occurrences of prices above 0 €/MWh. For assessment, Figure 6.19 depicts prices for Frequency Containment Reserves (FCR) and Frequency Restoration Reserves (aFRR & mFRR) against the number of occurrences within a year. The selected time under investigation includes the period from 21.04.2020 till 20.04.2021.

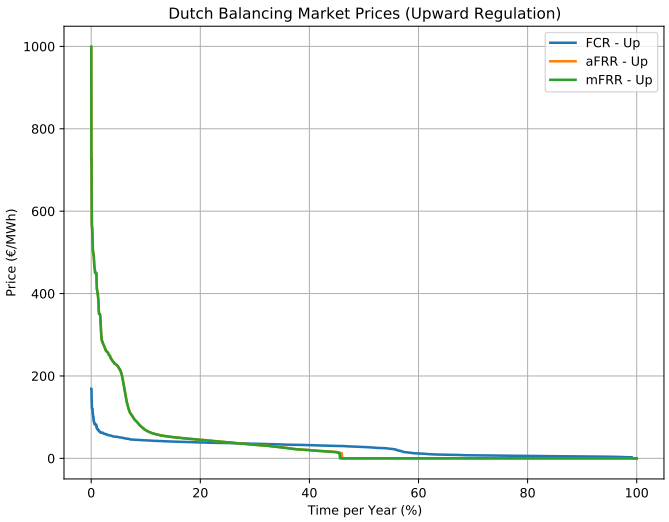

Figure 6.19: Dutch balancing market prices (upward regulation).

As it can be clearly seen, the highest prices for frequency control are present for Frequency Restoration Reserves. Prices up to 999 € are reached within the time period, which is almost five times higher than the highest day-ahead market price. Nevertheless, by evaluating the time per year, where the prices are positive, more than 54 % of the time prices for Frequency Restoration Reserves are 0 €/MWh. It has to be noticed that occurrences of prices above 0 €/MWh for automatic activated reserve and manually activated reserve only differ by less than 0.5 %.

The highest price for Frequency Containment Reserves are less than the maximum prices for Frequency Restoration Reserves, but prices above 0 € occur more often. One receives prices above 2.50 €/MWh for around 99 % of the time by providing Frequency Containment Reserves. For less than 6 % of the time per year, prices exceed 50 €/MWh in 2020-2021. Meanwhile, only for 27 % of the time the Frequency Containment Reserves are smaller than those for frequency Restoration reserves. However, the periods, where former prices are higher, never exceed 37 €/MWh

Compared to the day-ahead market, where the time per day show different price spreads, Frequency Restoration Reserves show not the same behaviour. Following the same approach as for the day-ahead market, an identification of prices, which can be mapped to a specific hour was conducted. However, the boxplot show no tendency, which can be extracted for further conclusions.

Both, prices for Frequency Containment Reserves and Frequency Restoration Reserves in upward regulation for the depicted time period were positive. Generally, it has to be noticed that negative prices not only in the day-ahead market exist, but also in the balancing market. During the depicted range negative prices only occurred for downward regulation. In this case, instead of receiving money from the Transmission System Operator, the Balancing Responsible Parties have to pay [10].

6.3.5. Sensitivity of the Market Potentials in the Dutch Energy Market

The sensitivity and changes of both, the vehicle's costs and the market prices have been analysed separately. By combining the results, one can outline how these sensitivities affect the market potentials of Vehicle-to-Grid. As it was seen for the Dutch energy market, an aggregator can rely on flexible prices by participating in the day-ahead or balancing markets . Hence, both markets form the scope of this section.

Because the market participation subjects to uncertainties like driving pattern, the market potential

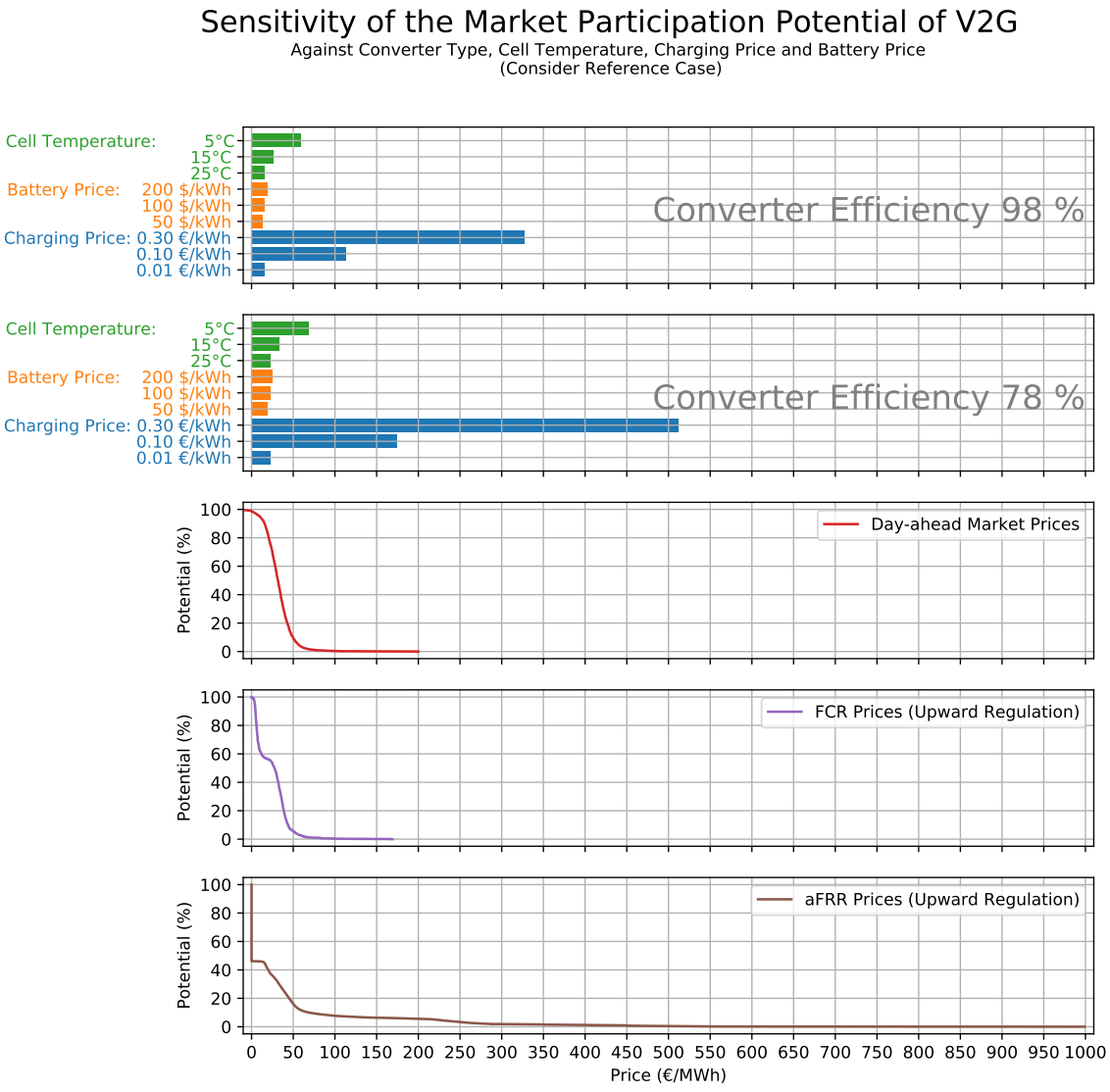

Figure 6.20: Sensitivity of the market participation potential of Vehicle-to-Grid.

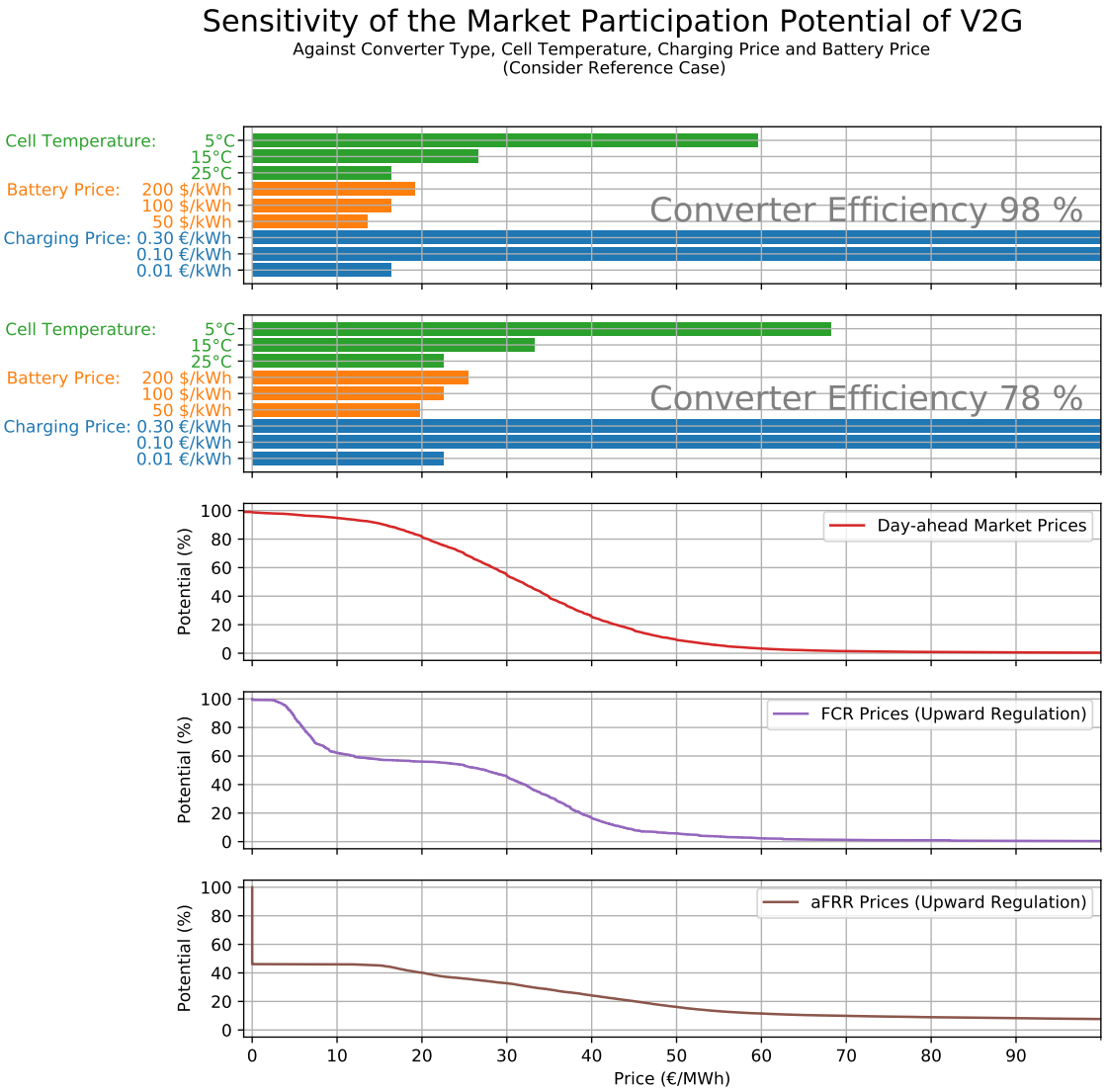

Figure 6.21: Sensitivity of the market participation potential of Vehicle-to-Grid (selected range).

will be measured as the maximum possible participation time per year. In this work, this participation time is defined as the time, where the costs (excluding fees and taxes), are lower than the prices, which one obtains in the market. As it is stated, the maximum participation time cannot be reached if the driving pattern does not match to the hours, which are economical. However, the participation time can indicate how both sensitives lead to different market potentials for Vehicle-to-Grid. For this purpose, Figure 6.20 summarises the most relevant sensitives, which were identified in the previous chapters. In Figure 6.21 a closer frame of Figure 6.20 is represented.

The main objective of the figure is to map the sensitivities of costs to the sensitivities of financial income. Because all five plots are aligned vertically to each other, one can compare all prices against each other. The two upper plots show the sensitivity of different Vehicle-to-Grid cases and their costs. The three last plots show the prices for the day-ahead market, Frequency Containment Reserves, Frequency Restoration Reserves respectively. For each Vehicle-to-Grid case, one can determine how often (in percentage of the year) prices exceed those costs. As an example, taking the first bar into account, a converter efficiency 98 % and cell temperature of 5 °C lead to a price of almost 60 € per MWh. By vertically mapping this costs to both markets, one can see that all markets have prices that exceed those costs in less than 20 % of the time per year. For comparison, by adapting the cell

temperature to ideal conditions (in this case 25 °C), the costs fall below 20 €/MWh. Hence, the market potential increases to over 80 % for the day-ahead market, almost 60 % for Frequency Containment Reserves and to over 40 % for the Frequency Restoration Reserve services. Note that the maximum potential for latter in 2020 was around 46 % due to the amount of hours with 0 €/MWh.

Before analysing the figure completely, one has to understand that only one parameter will be changed for each case. All parameter are taken from the reference case, which is defined in Table 6.2. The degradation of a full cycle is considered. This reference case should cover favourable conditions, such as ideal cell temperatures and low charging prices. By adapting one parameter, the sensitivity of this parameter will result in a different market potential.

Table 6.2: Summary of the reference case.

Parameter	Values
Battery Size	50 kWh
Cell Temperature	25 °C
Battery Price	100 $/kWh
Charging Price	0.01 €/kWh
Converter Power	11 kW

Shifting the scope back to the figures, the sensitivity of cell temperature, battery price, charging price and converter efficiency will be analysed. Here, two different converter for each sub-barplot differ in terms of nominal efficiency. All parameter on the y-axis are analysed for both converter. This approach allows to evaluate how a lower converter efficiency affects the whole case, because the lower efficiency draws more power from the battery to provide the same service.

Firstly, the participation potentials on all markets are highly sensitive against the charging price. The depicted charging prices vary from one euro cent to 30 euro cent per kWh. To recap, the worldwide leveled cost of electricity for renewable energy in 2019 varied between four and twelve cent per kWh (compare Figure 6.14). Prices of 30 cent per kWh can occur at public charging stations. However, if those prices are used for charging, the potential to participate in the day-ahead market and balancing market for Frequency Containment Reserves declines to 0 %. Only the balancing market for Frequency Restoration Reserves is able to compensate these costs for around 2% of the time per year by using a high efficient converter. Using a converter with an efficiency of 78 %, one obtains only at 0.3 % of the time higher prices. In contrast to that, if the charging process relies on a charging price of one cent per kWh, it is possible to reach for almost 90 % of the time a price, which exceeds the costs (day-ahead market). Again, these prices are without fees and tax.

Secondly, the cell temperature's impact on the battery degradation increases the costs for bidirectional charging capabilities. As all three cell temperatures outline, deviations from the ideal cell temperature of around 25 °C lead to increased costs per kWh. Hence, the participation potential for all markets varies with the cell temperature as well. In example, operating the vehicle at 25 °C results in a maximum potential of almost 90 % and 45 % for the day-ahead market and the (aFRR) balancing market, respectively. Hereby, one may note that a share of 46 % of the year are identified as the maximum possible participation time for providing Frequency Restoration Reserve services. Lower cell temperatures are beneficial to reduce calendar aging, but during charging and discharging higher cycling induced capacity losses are present. Hence, for a cell temperate of 5 °C, the potential for both markets decline to less than 5 % and to around 10 %, respectively.

Thirdly, compared to the previous parameter, the battery price has the lowest impact on the Vehicle-to-Grid sensitivity in terms of costs for favourable conditions. In favourable conditions, the degradation was identified as low compared to other conditions, like high charging rates at lower or higher temperatures. Hence, operating the vehicle in favourable conditions is crucial to avoid a high sensitivity of the battery costs. Nevertheless, the battery price per kWh has noticeable sensitivity and becomes important for lower temperatures. As expected, lower battery prices reduces the total costs for Vehicle-to-Grid. In

terms of market potential, by reducing the price from 100 $/kWh to 50 $/kWh, one reaches a potential of 92 % for the day-ahead market and almost the full potential of 46 % for the (aFRR) balancing market.

Fourthly, a lower converter efficiency increases both, the stress on the battery as well as the energy demand to compensate the losses. By accepting a lower efficiency, which can occur for production cost reduction, more energy is drawn from the battery. The increased energy demand, which compensates the losses, result in more energy that has to be paid. Even if 0.01 €/kWh are determined as the charging price, one has reduces the potential from almost 90 % to 75 % in the day-ahead market. Similar to that, the lower efficiency results in a potential reduction from around 44 % to around 37 % for Frequency Restoration Reserve services.

7

Evaluation & Discussion

Before drawing a conclusion as well as answering the research question, this chapter conducts a reflection of the work. Both, the applied methodology and the model are discussed. Hereby, the methodology is evaluated based on the limitations and strength for solving the research question. Furthermore, a critical reflection on the model forms the second part of this chapter.

7.1. Evaluation of the Methodology

The methodology of this work relies on the approach to reduce the impact of all uncertainties which are beyond physical limitations. By analysing the physical sensitivity primarily, it is intended to extract favourable and avoidable conditions of Vehicle-to-Grid. Within this section, resulting limitations and strength of this methodology are revealed.

On the one hand, limitations are the simplified economic analysis as a measure for the sensitivity and the primary focus on the component layer. Firstly, to measure the sensitivity of Vehicle-to-Grid, an indicator was necessary to define. Thus, a monetary value can be applied in order to reveal the potential of Vehicle-to-Grid in the Dutch balancing and day-ahead market. However, the costs and revenues are not comprehensive, because aspects like penetration, fees and levies are not covered. Secondly, even if the results lead to the opportunity to demonstrate how sensitive Vehicle-to-Grid is, it is not possible to answer how profitable it is in general. This relies on the focus made in this work, which intends to solve the technical sensitivity. Even if the research question does not define to solve this issue, a general statement would help for the rollout of this technology. However, based on the work conducted, it is likely that a general statement regarding the profitability of Vehicle-to-Grid would not cover the full complexity of the topic.

On the other hand, circumventing the usage of specific use cases broadens the view on Vehicle-to-Grid use cases in general. As stated, one can not simply answer if Vehicle-to-Grid is applicable for all electric vehicle users, because it subjects to their use case. This leads to the advantage of this work, which intends to identify favourable and avoidable conditions regardless of use cases. Hence, instead of assuming use case related dependencies beforehand and interpreting the results afterwards, one can avoid certain conditions based on this work. For instance, this methodology revealed that assuming a charging prices is highly sensitive for the amount of times, where a participation in the day-ahead market or balancing market is possible. Additionally, without relying the work on specific or general use cases, Vehicle-to-Grid niche use cases are not excluded. Those niche use cases can occur in changing conditions due to the energy transition, the development of autonomous driving and different market penetrations.

Overall, the methodology primarily focuses on the technology itself leading to the outlined decisive advantages. With respect to the conclusion in the next chapter, the methodology can be applied on all different layers as well. Thus, by merging the sensitivity analysis of the user behaviour layer, business layer and regulation layer, it is possible to identify a suitable use case or business model.

7.2. Evaluation of the Model

The model in this work represents the electric vehicle's battery, the electric vehicle supply equipment and two grid topologies. Hereby, the evaluations will cover each part separately.

The battery model in this work is mainly driven by the aspect that Vehicle-to-Grid approaches have to consider degradation as a factor of cost. Hence, the current model covers calendar aging and cycling induced aging for a specific NMC based Li-ion cells only. Thus, it is likely that other types of cell and cells from different manufacturer can vary in terms of degradation. The model covers the battery's state of charge, temperature, charging rate, total throughput and battery age. Both, calendar aging and cycling aging are applied as an additive approach, even if some papers argue that interactions between both aging mechanism exist [67, 68]. However, Keil et al. [38] argue that separating the aging mechanism is not possible in practical aging studies and therefore superposition will be applied. It is not expected that those interactions change the outcome of this work significantly. Comparable research that relies on the same degradation model evaluated the model against a state-of-the-art vehicle. They conclude that the model predicts similar degradation results over a lifetime of five years [87].

Beside the battery model, the electric vehicle supply equipment requires a representation to model important aspects, such a non-linear losses. The scope of this work presents three efficiencies to cover different converter topologies and possible manufactures. One may argue that a nominal efficiency of 78 % for the lowest efficient converter is well below state-of-the-art power electronics. However, Kieldsen et al. [42] identified losses of 15 % up to 40 % on selected electric vehicles. They argued that the value is far above state-of-the-art power electronics and assumed that Original Equipment Manufacturer prioritise the minimisation of costs leading to a lower efficiency. Additionally, efficiency measurements conducted on an adapted electric vehicle confirm that power electronics units are the predominantly losses for charging and discharging [2]. In their paper, Ranaweera et al. [2] conclude the power electronics units losses are highest of all components in either electric vehicles or building. Additionally, they argue that the percentage losses are less at mid and high current charging, which underlines the observations of the introduced model in this work. However, their measurements show a mismatch between charging and discharging efficiency. In the scope of this work, charging and discharging efficiencies are equal and it is argued that the mismatch subjects to the design of the converter topology. As an example, Lo et al. [49] applied a topology on their bidirectional grid-connected converter, which presents a higher discharging efficiency than charging efficiency. Besides, the thermal management is not part of the model. It is obvious that the activation of the thermal management system leads to additional energy demand and decreases the total efficiency. Therefore, low charging power ranges are selected, where it is assumed that those do not enable thermal management systems. Among others, thermal management systems can be highly use case dependant as their operation varies for each vehicle, cell type, ambient weather conditions and pre-conditions of the vehicle.

The sensitivity analysis includes different ancillary services and the Dutch energy markets. Four ancillary services form the scope of this work regardless if they lead to financial income or not. One can roughly divide these services into two physical demands of the grid: active power and reactive power provision. To evaluate both, two simplified grids represented the demand for either active power or reactive power. Thus, a sensitivity analysis of various grid topologies can increase the complexity and demand of providing those services. Hence, it is possible that some hotspots exist, where weak nodes highly require voltage support, while others do not. Both, the day-ahead market and balancing market were used as a measure to evaluate the sensitivity on the possible share of participation for only one specific year. It should be noticed that a higher penetration of renewables and electric vehicles can lead to emerging markets and price changes. As the introduction already states based

on a paper, a higher penetration of electric vehicles can question if the vehicle participates as a price taker. Hence, a sensitivity analysis of the market can enhance the results made in this work as well.

To conclude, the model intends revealing the sensitivity of Vehicle-to-Grid by covering the vehicle's battery, the electric vehicle supply equipment as well as the power system. Because it is not possible to cover all types of batteries, the model represents only a specific type of battery. By interpreting the results of degradation, these limitations have to be considered. Nevertheless, most of the results are independent of the battery degradation and are valid regardless of the batter type. In example, the revealed sensitivity for the four ancillary services and the requirements for the supply equipment are still valid.

8

Conclusion, Outlook & Implications

This last chapter draws the main conclusion with respect to the research question. Based on that, a discussion and outlook will be given to emphasise recommendations and the impact of the result on stakeholders.

8.1. Conclusion

Based on the conducted work on Vehicle-to-Grid with respect to four ancillary services, the final conclusion can be drawn. To recap, the research question is defined as follows:

How sensitive are bidirectional charging capabilities
for Vehicle-to-Grid based ancillary services against vehicle characteristics?

Referring to the sensitivity in general terms, the capabilities are sensitive against: state of charge, open circuit voltage, discharging current, calendar aging, cycling losses, converter efficiency, thermal losses, standby losses, transformer loading, line loading, generation, load and bus voltages. These parameters include 34 dependencies (compare Table 5.1). However, their sensitivity varies, so considering the most dependent parameter, the sensitivity can be summarized as follows:

The Vehicle Battery's Role in the Context of Vehicle-to-Grid

The battery degradation as an indicator for the stress on the vehicle commonly forms the Vehicle-to-Grid basis for an economic analysis. Hence, the sensitivity of the component can be summarised in terms of favourable and avoidable conditions.

The operation conditions of the vehicle's battery are sensitive against temperature, applied charging rates, total energy throughput and state of charge. Firstly, deviations from an ideal cell temperature of 25 °C to ±20 °C increase the cycling costs by a factor of 9-10 for a charging rate of 0.1. Secondly, increasing charging rates from 0.1C increase the costs by 50 % to 100 % for temperatures above 25 °C, whereas low temperatures such as 5 °C increases the cost by a factor of 2.5. Thirdly, total energy throughout of a battery is linear, but the degradation subjects to the above discussed conditions. Therefore, one can obtain a 22 times higher energy throughput for batteries, which are cycled at 25 °C and 0.1C, compared to 5 °C and 2C, which would lead to the same degradation. Fourthly, discharging the selected battery type from states of charge above 70 % to a lower state of charge of less than 60 % can reduce the battery degradation if the battery is idle for a longer time (compare Section 6.1.3). Thus, operating conditions are present, which would allow use cases to not only minimise but also to avoid battery degradation.

Increasing the battery pack size can reduce cycling induced aging, but calendar aging is the unavoidable dominant loss. By scaling up the vehicle's battery pack size, calendar aging of each cell is unchanged. However, scaling the pack size leads to lowering charging rates for the same charging power, because the charging rate is relative to the capacity. While charging cycles result in losses that are accepted for either mobility purposes or financial incomes, calendar aging does not serve any needs. Calendar aging is unavoidable and subjects to the temperature, battery age and as already described to the state of charge. In example, while cycling conditions are favourable at 25 °C, a lower temperature of 5 °C halves the degradation. Furthermore, a battery on an early lifetime of four months has a 2.5 times higher calendar ageing induced degradation than a two-year-old battery. Calendar aging forms the dominant losses over the total lifetime of the battery [87]. Thus, cycling the battery may reduce battery degradation in several conditions, but idle times leads to degradation as well without providing any functionality.

Considering all operation conditions of the battery is crucial for determine the Vehicle-to-Grid costs. By taking the above mentioned operation ranges into account, degradation prices can be less than 0.01 €/kWh and higher than 0.10 €/kWh. Additionally and according to Preger et al. [65], the number of full cycles varies up to thousands of cycles based on different working conditions, which are within the operating limits of the manufacturer. Thus, Vehicle-to-Grid should be aligned to the outlined favourable conditions. Additionally, tracking those conditions could justify the vehicle degradation model of a vehicle by validating it with the results of the real degradation. Not only in the context of electric vehicles, but also for second life approaches, tracking those data becomes more important for selecting suitable second life batteries [53].

The Impact & Design of Electric Vehicle Supply Equipment

Beside focusing on the vehicle degradation, the sensitivity of bidirectional charging capabilities rely on the electric vehicle supply equipment as well.

The total discharging costs not only subject to the battery degradation but also to the non-linear efficiency of the converter. This work investigates converter with nominal efficiencies from 78 % to 98 % and power ratings up to 50 kW. Even if state-of-the-art power electronics tend to be highly efficient, minimising the production costs is currently prioritised over a high efficiency [42]. Reducing the component costs of bidirectional power electronics can lead to higher operating costs, because of energy losses. Additionally, operating the converter well below their nominal power ratings can further decrease the efficiency. By comparing two 11 kW converter with a nominal efficiency of 78 % and 98 %, charging and discharging with a power of 1 kW result in a full cycle efficiency of 30 % and 68 %, respectively. A maximum efficiency of 75 % and 93 % could be achieved if one charges and discharges with 11 kW. Moreover, increasing the nominal power can broadens the inefficient power region, that are likely to cover the power range of Vehicle-to-Home. Especially high charging prices and low efficiencies would increase the costs for discharging the vehicle.

This work argues that additional losses induced by enabling the thermal management system or further operation losses should be minimised. Even if in the scope of this work, the thermal management is not modelled, it is assumed that the investigated charging power do not require thermal control mechanism. By increasing the charging power to values, that require cooling or heating mechanism, the energy demand of the whole process increases. Thus, the energy demand inclines, while the efficiency declines and therefore discharging costs increase. Similar, further operation losses induced by controller, metering or communication purposes would further decrease the efficiency.

Grid components, degradation, battery capacity and Vehicle-to-Home mainly rise concerns regarding an increased nominal power of the electric vehicle supply equipment. If electric vehicles participate for grid supporting services to upstream or parallel networks, one has to consider the nominal power of the transformer and lines. Similar to the example of this work, 20 nodes, where each supply equipment would be increased to a nominal discharging power of 50 kW, would require a 1 MVA transformer in the distribution grid if all provide active power based services simultaneously. Additionally, a high

charging power becomes more cell temperature dependent and the cell degradation is increased. This mainly affects the preconditions of the battery for the grid services, because the battery management system prevents high discharging currents for certain cell temperatures. Furthermore and based on the temperature sensitivity, the resulting costs and degradation have to be determined for each condition separately. Besides, by discharging the vehicle with a higher power, the user has to accept a lower state of charge, if the battery capacity is not big enough.

Implications for Vehicle-to-Grid based Ancillary Services

The sensitivity of four ancillary services are analysed in this work, where only active power provision show present market structures.

Vehicle-to-Grid based active power provisions is possible for peak shaving and only limited by the network components. The example in this work highlighted that peak shaving through electric vehicles is possible. Rather than increasing the nominal power of the electric vehicle supply equipment, an increased fleet size was realised. The example network and its components limited the powerflow due to the transformer and line loading. Hence, for providing active power to upstream or parallel networks, the transformer rating is more important than the electric vehicle itself. In the overall context of peak shaving, electric vehicles were able to reduce component loading, increasing the maximum power provision within the distribution network and providing active power to upstream or parallel networks.

The volatile energy sources go along with active power ramps, where electric vehicles are able to flatten the power output. By taking renewable energies in the Dutch region as an example, power rampings per MW of installed capacity form the scope of the active power ramping demand. This work relies on solar, wind onshore and wind offshore and their power change within 15 minutes. The fleet size is highly sensitive against the amount of hours, where power output change should be compensated. In example, two vehicles per MW of installed solar capacity can compensate 80 % of the power ramps per year, regardless if actually demanded. Nevertheless, if all ramps should be compensated, one requires more than 30 vehicles per MW of installed capacity.

Beside injecting active power into the grid, reactive power provision is a further opportunity to increase power system stability. Uncoordinated charging rises concerns in terms of voltage stability [99]. Several configuration opportunities, that covers uncontrolled, partly controlled, fully controlled and bidirectional charging are investigated. The load flow analysis revealed that the grid services of a single vehicle depend on the whole fleet. Here, bidirectional charging capabilities and reactive power provision offer degrees of freedom for the grid operator to stabilise the voltage of all grid nodes locally.

Overall, by taking the Dutch energy market as an example, the revealed sensitivity of bidirectional charging capabilities lead to market potentials from 0 % to almost 90 %. In this work, the potential is defined as the maximum time per year in %, where the market price exceed the discharging costs. On the one hand, even if no driving patterns are considered, the discharging costs can exceed all revenues, which can be obtained in the day-ahead market if one charges with 0.3 €/kWh. For participating in the day-ahead market it is almost unavoidable to charge the vehicle for free or a few euro cent per kWh to be able to dispatch the energy from the vehicle. Even if Frequency Restoration Reserves in the balancing market rely on higher peak prices, high charging prices show a similar reduction of the market potential (from 45 % to 2 %). Note that the prices are above 0 €/MWh for 46 % of the time between 2020 and 2021. Furthermore, even the cell temperature's sensitivity has a noticeable market potential loss of around 70 % for the day-ahead market. Hereby, the balancing market potential was reduced by around 20 %. On the other hand, operating the battery in favourable conditions can lead to a market potential of almost 90 % for the day-ahead market, 60 % for Frequency Containment Reserves and 45 % for Frequency Regulation Reserves. All potentials subject to the use case dependent driving patter, levies and taxes. Thus, the sensitivity of bidirectional charging costs can influence the market potential significantly.

8.2. Outlook & Implications

Derived from the conclusion of the Vehicle-to-Grid based sensitivity analysis, this final section draws implications for stakeholder and use cases. To affiliate the implications to the stakeholders, the already introduced architecture model in Figure 8.1 will be applied.

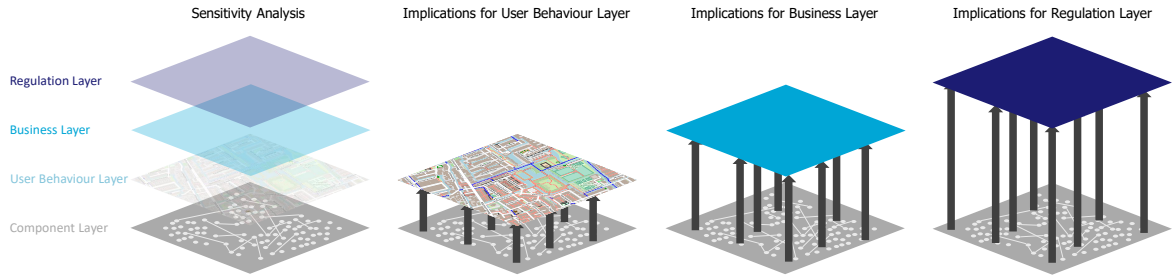

Figure 8.1: Outlook and implications based on the architecture model.

As the figure depicts, the sensitivity analysis on the component layer forms the basis in order to derive those implications. Hereby, stakeholder can identify themselves in the relevant layers. For instance, while aggregator have to consider all layers, car manufacturer may primarily identify themselves with the component layer. One has to note that the listed stakeholder of each layer are not limited to the given examples. Based on all implications, a last conclusion regarding use case will be given.

Component Layer

Grid operator can rely on an enhanced portfolio made available through Vehicle-to-Grid. The investigated ancillary services are namely frequency control, peak load leveling, active power ramping support and voltage control. A decentralised penetration of electric vehicles are an advantage to cope with local grid disturbances. Especially voltage control through transmitting reactive power over a long distance is physically limited, whereas electric vehicles can inject or absorb reactive power close to the disturbance. Compared to serve local disturbances, active power based services (frequency control, active power ramping support and peak load leveling) can be provided locally or in upstream and parallel networks as well. Mainly grid components, such as lines and transformers, are limiting Vehicle-to-Grid, because the fleet size and power provision can be adapted. Of course, this presupposes that an electric vehicle fleet is available. Besides, it can be beneficial for bidirectional charging capabilities to focus on emerging converter based ancillary services as well. As an example, the converter of a photovoltaic system may be capable of providing the same services as an electric vehicle. Strasser et al. [83] argue that power converter result in a higher automation degree. Hereby, system approaches like multiport converter with a shared converter can align a photovoltaic system with an electric vehicle. Different system architectures are presented in the work of Chandra Mouli et al. [54].

Electric vehicle supply equipment producer contribute to Vehicle-to-Grid by aiming a high energy efficiency, but should consider Vehicle-to-Home as well. The converter efficiency for both charging and discharging lead to energy losses for the overall cycling process. As stated and based on a literature review, the power electronics efficiency can be well below state-of-the-art efficiencies due to costs saving. Especially the non-linear efficiency curve can lead to a low efficiency in lower power ranges, which can be disadvantageous for Vehicle-to-Home. As the example shows, a converter with a nominal efficiency of 78 % lead to a maximum total efficiency of 30 % for operated below 1 kW. Thus, by adapting the nominal power and efficiency, it is recommended to consider both, the demand of Vehicle-to-Home and Vehicle-to-Grid.

Car manufacturer can promote the vehicle integration by providing ancillary services, but have to focus on energy efficiency and the battery's operation conditions. This work outlined that ancillary services can contribute to a stable and secure grid operation. However, the sensitivity revealed that efficiency is crucial for reducing the losses, as it was seen for the supply equipment as well. Beyond that, the operation conditions of the battery are non-linear and individual resulting in the requirement to know their characteristics comprehensively. Thus, it is recommended to consider all relevant data, which are state of charge, battery age, cell temperature, C-rate and total throughput to evaluate the degradation. Additionally, preheating and cooling strategies can lead to an increased energy demand. However, this work tends to recommend avoiding high currents and cell temperatures beyond ideal temperatures to avoid further energy losses. Generally, increasing the battery pack size tends to be an advantageous due to lowering C-rates and the increased capacity.

For further research, the sensitivity analysis revealed that operation conditions should not be neglected through simplifications. Especially degradation and non-linear behaviours can lead to increased losses or component stress. As an example for the degradation, this work refers to the work of Preger et al. [65], who investigated that the number of full cycles varies up to thousands of cycles based on different working conditions of the datasheet. Thus, by simplifications one can neither identify optimal working conditions, nor those who stresses the battery the most. Generally, battery degradation is a complex topic and requires further investigation to derive a comprehensive model.

As an aggregator, the overall system sensitivity makes it complex for identifying optimum working conditions for both, the grid and the vehicle. If an aggregator determines and scales the fleet size, the physical limits of the power system form constraints. Thus, an aggregator has to rely on information about the grid capabilities as well as the working conditions of the vehicle fleet. Furthermore, while frequency control can be provided on different busses, reactive power control for frequency regulation requires a short distance to the disturbance. Thus, it can be challenging to align the fleet size to the ancillary services needed by the power system.

User Behaviour Layer

For the user, it is crucial that one has to translate the technical complexity into an understandable unit. The technical driven sensitivity analysis revealed more than thirty technical dependencies, which define a Vehicle-to-Grid condition. However, not through simplifications, but translated into monetary terms can reflect those conditions. This goes along with the already made recommendations for the original equipment manufacturer to track all relevant data for determining the discharging costs and total component stress.

Aggregator have to consider the behaviour of the user, which individual potential for Vehicle-to-Grid can differ. As stated in the introduction, socio-technical researcher advise to individually analyse the user behaviour in the context of Vehicle-to-Grid. Based on the sensitivity analysis, this work supports this advice from a purely technical perspective. For instance the individual user defines and subjects to transformer limits, cable limits, demand for ancillary services, cell temperature, battery size, efficiency of the vehicle etc. Consequently, the technical capabilities vary, which sensitivity in terms of market potential was shown.

Business Layer

Original equipment manufacturer not only have to face an increased technical complexity, but also the opportunity to increase penetration and user acceptance. To cope with local grid disturbances like voltage drops, an electric vehicle that provides voltage control not only serves the grid needs but also allows charging without increasing the voltage deviations. Thus, by increasing the amount of electric vehicles which are able to provide ancillary services, one can argue that their penetration level can be increased. Besides and without further investigations, Vehicle-to-Gird and Vehicle-to-Home could be represented as benefit for the user. For instance, black start capabilities and islanding capability have the potential to protect against blackout or serve in off-grid locations.

Aggregator have to cope with the complexity of Vehicle-to-Grid in order to identify a suitable business model. Based on this work, the sensitivity analysis revealed the viability of cost, which depend on the working conditions. Ideally, the aggregator has direct access to the discharging costs, which are calculated dynamically considering all dependencies. Thus, if the user charges in example with 0.3 €/kWh and the cell temperature is 5 °C, the weak market potential can be identified. If the aggregator has no access to the working conditions of the battery, two other approaches may be interested as well. Firstly, as a further bidding strategy, average prices can be assumed which may overestimate oder underestimate the potential at a certain time. Secondly, by taking the maximum discharging costs as a reference, the price can cover all costs, but are likely to reduce the potential significantly. For both strategies, it can be beneficial to differentiate between locations and seasons. Ambient temperatures of around 25 °C are likely to result in better conditions than cold winter seasons. In addition to that, if one charges with domestic prices or at public charging stations, discharging costs can exceed market prices. Further information regarding fleet management can be found in the work of Hu et al. [33]. Further business models for electric vehicle are identified in the publication of Kley et al. [45].

Regulation Layer

For policymakers, it is crucial to derive a suitable regulation framework to enable ancillary services for electric vehicles. The technical sensitivity of discharging costs along with individual user behaviours result in different market potentials. Thus, remunerated ancillary services can result in complex market designs, which have to cope with the presented technical sensitivity. Hereby, it has to be considered that the power system limitations induced by transformer and lines determine the fleet size. Some ancillary services, like reactive power provision for voltage control, are beneficial for both, grid operator and electric vehicle user. Hence, reactive power provision contributes to a higher penetration. In all cases, standardisation are a key for providing interoperability. Therefore, it has to be decided how the information flow will be organised. For example, who receives information about the grid state and determines the operation condition of the vehicle.

Possible aggregator could form a bridge between the technical complexity and the regulation framework. Hereby, it needs to be investigated if an aggregator should aggregate charging stations or electric vehicles. This question considers that electric vehicles can enter a different control area, which subject to different contracts or registration processes. Compared to that, charging stations can be installed on a fixed location aligned with the demand and limit of the power system. Without going into further comparisons, regulation aspects are not only influenced, but also influencing the aggregation approach.

Use Cases

Lastly, implications for future use case can be made based on this work. Especially, the variety of cases from a niche use case to the average user are important to distinguish. Additionally, developments in technical terms emerge, which are driven by transitions in the energy and transport sectors.

Beside relying research on an average user, niche use cases should be investigated as well. While a user can subject to high costs and energy losses due to low temperatures or high charging costs, niche use cases can be suited to the favourable conditions of Vehicle-to-Grid. In example, low degradation costs at 25 °C are attractive. Thus, conditions where the ambient temperature provide similar temperatures are beneficial, which are already location and season dependent. Furthermore, in this work, very specific conditions can lead to a total degradation reduction (see Section 6.1.3). Moreover, low charging costs can occur if one charges energy from the photovoltaic system, while charging at public fast charging station can already induce high degradation and energy costs. Specific niche use cases, such as a company that needs ramping support may provide a financial attractive charging and discharging profile for their employees. Hereby, by scaling the vehicle fleet size, an aggregated vehicle fleet can be predicted more accurately [78]. Additionally, a study found that bidding at work places can be more reliable than at home [71]. Strategies that more vehicles are in the vehicle fleet than required, can overcome the situation that vehicles are not blocked anymore. Instead, other

vehicles can replace a vehicle, which is demanded for mobility.

Use cases not only subject to technical dependencies, but also to future developments like autonomous driving and new technologies. Latter technologies can be new battery types, such as solid state batteries. However, autonomous driving can be beneficial for participating during high market prices as well as reducing user induced uncertainties. For instance, companies can use their fleet to schedule the services at a given time and control the vehicle to participate at peak prices.

Bibliography

[1] Victor A. Agubra and Jeffrey W. Fergus. The formation and stability of the solid electrolyte interface on the graphite anode. *Journal of Power Sources*, 268:153–162, 2014. ISSN 0378-7753. doi: https://doi.org/10.1016/j.jpowsour.2014.06.024. URL https://www.sciencedirect.com/science/article/pii/S0378775314008775.

[2] Elpiniki Apostolaki-Iosifidou, Paul Codani, and Willett Kempton. Measurement of power loss during electric vehicle charging and discharging. *Energy*, 127:730–742, 2017. ISSN 0360-5442. doi: https://doi.org/10.1016/j.energy.2017.03.015. URL https://www.sciencedirect.com/science/article/pii/S0360544217303730.

[3] Ines Baccouche, Sabeur Jemmali, Bilal Manai, Noshin Omar, and Najoua Essoukri Ben Amara. Improved ocv model of a li-ion nmc battery for online soc estimation using the extended kalman filter. *Energies*, 10(6), 2017. ISSN 1996-1073. doi: 10.3390/en10060764. URL https://www.mdpi.com/1996-1073/10/6/764.

[4] Abdoulmenim Bilh, Kshirasagar Naik, and Ramadan El-Shatshat. Evaluating electric vehicles' response time to regulation signals in smart grids. *IEEE Transactions on Industrial Informatics*, 14(3):1210–1219, 2018. doi: 10.1109/TII.2017.2750638.

[5] Michael Birk, José Pablo Chaves-Ávila, Tomás Gómez, and Richard Tabors. Tso/dso coordination in a context of distributed energy resource penetration. *MIT Energy Initiative Reports*, 2017.

[6] Justin D.K. Bishop, Colin J. Axon, David Bonilla, and David Banister. Estimating the grid payments necessary to compensate additional costs to prospective electric vehicle owners who provide vehicle-to-grid ancillary services. *Energy*, 94:715–727, 2016. ISSN 0360-5442. doi: https://doi.org/10.1016/j.energy.2015.11.029. URL https://www.sciencedirect.com/science/article/pii/S0360544215015649.

[7] Gerald Broneske and David Wozabal. How do contract parameters influence the economics of vehicle-to-grid? *Manufacturing & Service Operations Management*, 19(1):150–164, 2017.

[8] Stephen Brown, David Pyke, and Paul Steenhof. Electric vehicles: The role and importance of standards in an emerging market. *Energy Policy*, 38(7):3797–3806, 2010. ISSN 0301-4215. doi: https://doi.org/10.1016/j.enpol.2010.02.059. URL https://www.sciencedirect.com/science/article/pii/S0301421510001631. Large-scale wind power in electricity markets with Regular Papers.

[9] Christian Bussar, Philipp Stöcker, Zhuang Cai, Luiz Moraes Jr., Dirk Magnor, Pablo Wiernes, Niklas van Bracht, Albert Moser, and Dirk Uwe Sauer. Large-scale integration of renewable energies and impact on storage demand in a european renewable power system of 2050—sensitivity study. *Journal of Energy Storage*, 6:1–10, 2016. ISSN 2352-152X. doi: https://doi.org/10.1016/j.est.2016.02.004. URL https://www.sciencedirect.com/science/article/pii/S2352152X16300135.

[10] TenneT TSO B.V. *Imbalance Pricing System*, 7 2020. URL https://www.tennet.eu/fileadmin/user_upload/SO_NL/Imbalance_pricing_system.pdf.

[11] Lisa Calearo and Mattia Marinelli. Profitability of frequency regulation by electric vehicles in denmark and japan considering battery degradation costs. *World Electric Vehicle Journal*, 11 (3), 2020. ISSN 2032-6653. doi: 10.3390/wevj11030048. URL https://www.mdpi.com/2032-6653/11/3/48.

[12] Lisa Calearo, Andreas Thingvad, and Mattia Marinelli. Modeling of battery electric vehicles for degradation studies. In *2019 54th International Universities Power Engineering Conference (UPEC)*, pages 1–6. IEEE, 2019.

[13] Gautham Ram Chandra Mouli, Pavol Bauer, Thiwanka Wijekoon, Ara Panosyan, and Eva-Maria Bärthlein. Design of a power-electronic-assisted oltc for grid voltage regulation. *IEEE Transactions on Power Delivery*, 30(3):1086–1095, 2015. doi: 10.1109/TPWRD.2014.2371539.

[14] Xiaopeng Chen, Weixiang Shen, Thanh Tu Vo, Zhenwei Cao, and Ajay Kapoor. An overview of lithium-ion batteries for electric vehicles. In *2012 10th International Power & Energy Conference (IPEC)*, pages 230–235. IEEE, 2012.

[15] NM Chivelet, F Chenlo, and MC Alonso. Analysis and modelling of dc/ac inverters with resistive and reactive loads for sand alone pv systems. In *12 European Photovoltaic solar energy conference*, page 1631, 1994.

[16] Sarp G. Cimen, Alexander Pfannkuchen, and Benedikt Schmuelling. Compensation considerations for bidirectional inductive charging systems of electric vehicles with coil positioning flexibility. *IEEE Transactions on Magnetics*, 52(3):1–4, 2016. doi: 10.1109/TMAG.2015.2497369.

[17] A Conejo, T Gomez, and JI De la Fuente. Pilot-bus selection for secondary voltage control. *European Transactions on Electrical Power*, 3(5):359–366, 1993.

[18] David Dallinger, Daniel Krampe, and Martin Wietschel. Vehicle-to-grid regulation reserves based on a dynamic simulation of mobility behavior. *IEEE Transactions on Smart Grid*, 2(2):302–313, 2011.

[19] Alfonso Damiano, Gianluca Gatto, Ignazio Marongiu, Mario Porru, and Alessandro Serpi. Vehicle-to-grid technology: State-of-the-art and future scenarios. 2014.

[20] Luis Davila-Gomez, Antonio Colmenar-Santos, Mohamed Tawfik, and Manuel Castro-Gil. An accurate model for simulating energetic behavior of pv grid connected inverters. *Simulation Modelling Practice and Theory*, 49:57–72, 2014. ISSN 1569-190X. doi: https://doi.org/10.1016/j.simpat.2014.08.001. URL https://www.sciencedirect.com/science/article/pii/S1569190X14001300.

[21] AN Dey. Electrochemical alloying of lithium in organic electrolytes. *Journal of The Electrochemical Society*, 118(10):1547, 1971.

[22] Dr. Ing. h.c. F. Porsche AG. Taycan: 800-volt system, 2019. URL https://newsroom.porsche.com/en/media-search.html?type=image&page=22&keyword=taycan.

[23] Mehrdad Ehsani, Milad Falahi, and Saeed Lotfifard. Vehicle to grid services: Potential and applications. *Energies*, 5(10):4076–4090, 2012.

[24] ENTSO-E. Balancing Report. Technical report, 2020. URL https://eepublicdownloads.entsoe.eu/clean-documents/Publications/Market%20Committee%20publications/ENTSO-E_Balancing_Report_2020.pdf.

[25] ENTSO-E. Transparency platform, 2021. URL https://transparency.entsoe.eu/.

[26] Hassan Farhangi. The path of the smart grid. *IEEE Power and Energy Magazine*, 8(1):18–28, 2010. doi: 10.1109/MPE.2009.934876.

[27] Joachim Geske and Diana Schumann. Willing to participate in vehicle-to-grid (v2g)? why not! *Energy Policy*, 120:392–401, 2018. ISSN 0301-4215. doi: https://doi.org/10.1016/j.enpol.2018.05.004. URL https://www.sciencedirect.com/science/article/pii/S0301421518302982.

[28] Felipe Gonzalez Venegas, Marc Petit, and Yannick Perez. Plug-in behavior of electric vehicles users: Insights from a large-scale trial and impacts for grid integration studies. *eTransportation*, 10:100131, 2021. ISSN 2590-1168. doi: https://doi.org/10.1016/j.etran.2021.100131. URL https://www.sciencedirect.com/science/article/pii/S2590116821000291.

[29] John B Goodenough. How we made the li-ion rechargeable battery. *Nature Electronics*, 1(3): 204–204, 2018.

[30] Yunpeng Guo, Weijia Liu, Fushuan Wen, Abdus Salam, Jianwei Mao, and Liang Li. Bidding strategy for aggregators of electric vehicles in day-ahead electricity markets. *Energies*, 10(1): 144, 2017.

[31] Hassan Haes Alhelou, Mohamad Esmail Hamedani-Golshan, Takawira Cuthbert Njenda, and Pierluigi Siano. A survey on power system blackout and cascading events: Research motivations and challenges. *Energies*, 12(4):682, 2019.

[32] Chioke B. Harris and Michael E. Webber. The sensitivity of vehicle-to-grid revenues to plug-in electric vehicle battery size and evse power rating. In *2014 IEEE PES General Meeting | Conference Exposition*, pages 1–5, 2014. doi: 10.1109/PESGM.2014.6939251.

[33] Junjie Hu, Hugo Morais, Tiago Sousa, and Morten Lind. Electric vehicle fleet management in smart grids: A review of services, optimization and control aspects. *Renewable and Sustainable Energy Reviews*, 56:1207–1226, 2016. ISSN 1364-0321. doi: https://doi.org/10.1016/j.rser.2015.12.014. URL https://www.sciencedirect.com/science/article/pii/S1364032115013970.

[34] Xiaosong Hu, Yusheng Zheng, David A. Howey, Hector Perez, Aoife Foley, and Michael Pecht. Battery warm-up methodologies at subzero temperatures for automotive applications: Recent advances and perspectives. *Progress in Energy and Combustion Science*, 77:100806, 2020. ISSN 0360-1285. doi: https://doi.org/10.1016/j.pecs.2019.100806. URL https://www.sciencedirect.com/science/article/pii/S0360128519301169.

[35] IRENA. Renewable power generation costs in 2019. URL https://www.irena.org/-/media/Files/IRENA/Agency/Publication/2020/Jun/IRENA_Power_Generation_Costs_2019.pdf.

[36] Patrick Jochem, Thomas Kaschub, and Wolf Fichtner. How to integrate electric vehicles in the future energy system? In *Evolutionary paths towards the mobility patterns of the future*, pages 243–263. Springer, 2014.

[37] Abhimanyu Kaushal and Dirk Van Hertem. An overview of ancillary services and hvdc systems in european context. *Energies*, 12(18), 2019. ISSN 1996-1073. doi: 10.3390/en12183481. URL https://www.mdpi.com/1996-1073/12/18/3481.

[38] Peter Keil, Simon F. Schuster, Jörn Wilhelm, Julian Travi, Andreas Hauser, Ralph C. Karl, and Andreas Jossen. Calendar aging of lithium-ion batteries. *Journal of The Electrochemical Society*, 163(9):A1872–A1880, 2016. doi: 10.1149/2.0411609jes. URL https://doi.org/10.1149/2.0411609jes.

[39] Willett Kempton and Jasna Tomić. Vehicle-to-grid power fundamentals: Calculating capacity and net revenue. *Journal of Power Sources*, 144(1):268–279, 2005. ISSN 0378-7753. doi: https://doi.org/10.1016/j.jpowsour.2004.12.025. URL https://www.sciencedirect.com/science/article/pii/S0378775305000352.

[40] Georg Kerber and Rolf Witzmann. Statistical distribution grid analysis and reference network generation; statistische analyse von ns-verteilungsnetzen und modellierung von referenznetzen. netzklassen mit quantitativen unterscheidungsmerkmalen. *EW*, 107, 2008.

[41] P Kessel and H Glavitsch. Estimating the voltage stability of a power system. *IEEE Transactions on power delivery*, 1(3):346–354, 1986.

[42] Andreas Kieldsen, Andreas Thingvad, Sergejus Martinenas, and T Meier Sørensen. Efficiency test method for electric vehicle chargers. In *Proceedings of EVS29-International Battery, Hybrid and Fuel Cell Electric Vehicle Symposium*, 2016.

[43] Jaewan Kim, Jinwoo Oh, and Hoseong Lee. Review on battery thermal management system for electric vehicles. *Applied Thermal Engineering*, 149:192–212, 2019. ISSN 1359-4311. doi: https://doi.org/10.1016/j.applthermaleng.2018.12.020. URL https://www.sciencedirect.com/science/article/pii/S135943111835614X.

[44] Benedikt Kirpes, Philipp Danner, Robert Basmadjian, Hermann De Meer, and Christian Becker. E-mobility systems architecture: a model-based framework for managing complexity and interoperability. *Energy Informatics*, 2(1):1–31, 2019.

[45] Fabian Kley, Christian Lerch, and David Dallinger. New business models for electric cars—a holistic approach. *Energy Policy*, 39(6):3392–3403, 2011. ISSN 0301-4215. doi: https://doi.org/10.1016/j.enpol.2011.03.036. URL https://www.sciencedirect.com/science/article/pii/S0301421511002163.

[46] Katarina Knezović and Mattia Marinelli. Phase-wise enhanced voltage support from electric vehicles in a danish low-voltage distribution grid. *Electric Power Systems Research*, 140:274–283, 2016. ISSN 0378-7796. doi: https://doi.org/10.1016/j.epsr.2016.06.015. URL https://www.sciencedirect.com/science/article/pii/S0378779616302231.

[47] Long Lam and Pavol Bauer. Practical capacity fading model for li-ion battery cells in electric vehicles. *IEEE Transactions on Power Electronics*, 28(12):5910–5918, 2013. doi: 10.1109/TPEL.2012.2235083.

[48] Yunjian Li, Kuining Li, Yi Xie, Jiangyan Liu, Chunyun Fu, and Bin Liu. Optimized charging of lithium-ion battery for electric vehicles: Adaptive multistage constant current–constant voltage charging strategy. *Renewable Energy*, 146:2688–2699, 2020. ISSN 0960-1481. doi: https://doi.org/10.1016/j.renene.2019.08.077. URL https://www.sciencedirect.com/science/article/pii/S0960148119312649.

[49] Kuo-Yuan Lo, Yaow-Ming Chen, and Yung-Ruei Chang. Bidirectional single-stage grid-connected inverter for a battery energy storage system. *IEEE Transactions on Industrial Electronics*, 64(6):4581–4590, 2017. doi: 10.1109/TIE.2016.2559453.

[50] João A Peças Lopes, Filipe Joel Soares, and Pedro M Rocha Almeida. Integration of electric vehicles in the electric power system. *Proceedings of the IEEE*, 99(1):168–183, 2010.

[51] Nic Lutsey and Michael Nicholas. Update on electric vehicle costs in the united states through 2030. *The International Council on Clean Transportation*, 2, 2019.

[52] E. Martinez-Laserna, I. Gandiaga, E. Sarasketa-Zabala, J. Badeda, D.-I. Stroe, M. Swierczynski, and A. Goikoetxea. Battery second life: Hype, hope or reality? a critical review of the state of the art. *Renewable and Sustainable Energy Reviews*, 93:701–718, 2018. ISSN 1364-0321. doi: https://doi.org/10.1016/j.rser.2018.04.035. URL https://www.sciencedirect.com/science/article/pii/S1364032118302491.

[53] Egoitz Martinez-Laserna, Elixabet Sarasketa-Zabala, Igor Villarreal Sarria, Daniel-Ioan Stroe, Maciej Swierczynski, Alexander Warnecke, Jean-Marc Timmermans, Shovon Goutam, Noshin Omar, and Pedro Rodriguez. Technical viability of battery second life: A study from the ageing perspective. *IEEE Transactions on Industry Applications*, 54(3):2703–2713, 2018. doi: 10.1109/TIA.2018.2801262.

[54] G. R. Chandra Mouli, P. Bauer, and M. Zeman. Comparison of system architecture and converter topology for a solar powered electric vehicle charging station. In *2015 9th International Conference on Power Electronics and ECCE Asia (ICPE-ECCE Asia)*, pages 1908–1915, 2015. doi: 10.1109/ICPE.2015.7168039.

[55] Valentin Muenzel, Anthony F Hollenkamp, Anand I Bhatt, Julian de Hoog, Marcus Brazil, Doreen A Thomas, and Iven Mareels. A comparative testing study of commercial 18650-format lithium-ion battery cells. *Journal of The Electrochemical Society*, 162(8):A1592, 2015.

[56] Jeremy Neubauer, Aaron Brooker, and Eric Wood. Sensitivity of battery electric vehicle economics to drive patterns, vehicle range, and charge strategies. *Journal of Power Sources*, 209:269–277, 2012. ISSN 0378-7753. doi: https://doi.org/10.1016/j.jpowsour.2012.02.107. URL https://www.sciencedirect.com/science/article/pii/S0378775312005290.

[57] Lance Noel, Gerardo Zarazua De Rubens, and Benjamin K Sovacool. Optimizing innovation, carbon and health in transport: Assessing socially optimal electric mobility and vehicle-to-grid pathways in denmark. *Energy*, 153:628–637, 2018.

[58] M. Noori, Y. Zhao, N. Onat, Stephanie Gardner, and O. Tatari. Light-duty electric vehicles to improve the integrity of the electricity grid through vehicle-to-grid technology: Analysis of regional net revenue and emissions savings. *Applied Energy*, 168:146–158, 2016.

[59] Pedro Nunes, Tiago Farias, and Miguel C Brito. Day charging electric vehicles with excess solar electricity for a sustainable energy system. *Energy*, 80:263–274, 2015.

[60] European Statistical Office. Electricity prices for household consumers - bi-annual data (from 2007 onwards), 06 2021. URL https://ec.europa.eu/eurostat/databrowser/view/nrg_pc_204/default/table?lang=en.

[61] Konstantinos Oureilidis, Kyriaki-Nefeli Malamaki, Konstantinos Gallos, Achilleas Tsitsimelis, Christos Dikaiakos, Spyros Gkavanoudis, Milos Cvetkovic, Juan Manuel Mauricio, Jose Maria Maza Ortega, Jose Luis Martinez Ramos, George Papaioannou, and Charis Demoulias. Ancillary services market design in distribution networks: Review and identification of barriers. *Energies*, 13(4), 2020. ISSN 1996-1073. doi: 10.3390/en13040917. URL https://www.mdpi.com/1996-1073/13/4/917.

[62] Peter Palensky and Friederich Kupzog. Smart grids. *Annual Review of Environment and Resources*, 38:201–226, 2013.

[63] Peter Palensky, Edmund Widl, Matthias Stifter, and Atiyah Elsheikh. Modeling intelligent energy systems: Co-simulation platform for validating flexible-demand ev charging management. *IEEE Transactions on Smart Grid*, 4(4):1939–1947, 2013.

[64] Jayakrishnan Radhakrishna Pillai and Birgitte Bak-Jensen. Integration of vehicle-to-grid in the western danish power system. *IEEE transactions on sustainable energy*, 2(1):12–19, 2010.

[65] Yuliya Preger, Heather M. Barkholtz, Armando Fresquez, Daniel L. Campbell, Benjamin W. Juba, Jessica Romàn-Kustas, Summer R. Ferreira, and Babu Chalamala. Degradation of commercial lithium-ion cells as a function of chemistry and cycling conditions. *Journal of The Electrochemical Society*, 167(12):120532, sep 2020. doi: 10.1149/1945-7111/abae37. URL https://doi.org/10.1149/1945-7111/abae37.

[66] G.A. Rampinelli, A. Krenzinger, and F. Chenlo Romero. Mathematical models for efficiency of inverters used in grid connected photovoltaic systems. *Renewable and Sustainable Energy Reviews*, 34:578–587, 2014. ISSN 1364-0321. doi: https://doi.org/10.1016/j.rser.2014.03.047. URL https://www.sciencedirect.com/science/article/pii/S1364032114002081.

[67] Eduardo Redondo-Iglesias, Pascal Venet, and Serge Pelissier. Calendar and cycling ageing combination of batteries in electric vehicles. *Microelectronics Reliability*, 88-90:1212–1215, 2018. ISSN 0026-2714. doi: https://doi.org/10.1016/j.microrel.2018.06.113. URL https://www.sciencedirect.com/science/article/pii/S0026271418305377. 29th European Symposium on Reliability of Electron Devices, Failure Physics and Analysis (ESREF 2018).

[68] Eduardo Redondo-Iglesias, Pascal Venet, and Serge Pelissier. Modelling lithium-ion battery ageing in electric vehicle applications—calendar and cycling ageing combination effects. *Batteries*, 6(1), 2020. ISSN 2313-0105. doi: 10.3390/batteries6010014. URL https://www.mdpi.com/2313-0105/6/1/14.

[69] F. Saidani, F. X. Hutter, R.-G. Scurtu, W. Braunwarth, and J. N. Burghartz. Lithium-ion battery models: a comparative study and a model-based powerline communication. *Advances in Radio Science*, 15:83–91, 2017. doi: 10.5194/ars-15-83-2017. URL https://ars.copernicus.org/articles/15/83/2017/.

[70] Gaizka Saldaña, Jose Ignacio San Martin, Inmaculada Zamora, Francisco Javier Asensio, and Oier Oñederra. Electric vehicle into the grid: Charging methodologies aimed at providing ancillary services considering battery degradation. *Energies*, 12(12), 2019. ISSN 1996-1073. URL https://www.mdpi.com/1996-1073/12/12/2443.

[71] Siyamak Sarabi, Arnaud Davigny, Vincent Courtecuisse, Yann Riffonneau, and Benoît Robyns. Potential of vehicle-to-grid ancillary services considering the uncertainties in plug-in electric vehicle availability and service/localization limitations in distribution grids. *Applied Energy*, 171:523–540, 2016. ISSN 0306-2619. doi: https://doi.org/10.1016/j.apenergy.2016.03.064. URL https://www.sciencedirect.com/science/article/pii/S0306261916303841.

[72] Lip Huat Saw, Yonghuang Ye, and Andrew A.O. Tay. Integration issues of lithium-ion battery into electric vehicles battery pack. *Journal of Cleaner Production*, 113:1032–1045, 2016. ISSN 0959-6526. doi: https://doi.org/10.1016/j.jclepro.2015.11.011. URL https://www.sciencedirect.com/science/article/pii/S0959652615016406.

[73] Team SCE-Cisco-IBM SGRA. Smart grid reference architecture. *Using Information and Communication Services to Support a Smarter Grid*, 2011.

[74] Pieter Schavemaker and Lou Van der Sluis. *Electrical Power System Essentials*. John Wiley & Sons, 2017. ISBN 978-1-118-80347-9.

[75] Florian Schloegl, Sebastian Rohjans, Sebastian Lehnhoff, Jorge Velasquez, Cornelius Steinbrink, and Peter Palensky. Towards a classification scheme for co-simulation approaches in energy systems. In *2015 International Symposium on Smart Electric Distribution Systems and Technologies (EDST)*, pages 516–521. IEEE, 2015.

[76] Karl Schwenk, Stefan Meisenbacher, Benjamin Briegel, Tim Harr, Veit Hagenmeyer, and Ralf Mikut. Integrating battery aging in the optimization for bidirectional charging of electric vehicles. *arXiv preprint arXiv:2009.12201*, 2020.

[77] Angshuman Sharma and Santanu Sharma. Review of power electronics in vehicle-to-grid systems. *Journal of Energy Storage*, 21:337–361, 2019. ISSN 2352-152X. doi: https://doi.org/10.1016/j.est.2018.11.022. URL https://www.sciencedirect.com/science/article/pii/S2352152X1830481X.

[78] Rob Shipman, Julie Waldron, Sophie Naylor, James Pinchin, Lucelia Rodrigues, and Mark Gillott. Where will you park? predicting vehicle locations for vehicle-to-grid. *Energies*, 13(8):1933, 2020.

[79] Ramteen Sioshansi, Paul Denholm, Thomas Jenkin, and Jurgen Weiss. Estimating the value of electricity storage in pjm: Arbitrage and some welfare effects. *Energy Economics*, 31(2):269–277, 2009. ISSN 0140-9883. doi: https://doi.org/10.1016/j.eneco.2008.10.005. URL https://www.sciencedirect.com/science/article/pii/S0140988308001631.

[80] Tirupati Uttamrao Solanke, Vigna K. Ramachandaramurthy, Jia Ying Yong, Jagadeesh Pasupuleti, Padmanathan Kasinathan, and Arul Rajagopalan. A review of strategic charging–discharging control of grid-connected electric vehicles. *Journal of Energy Storage*, 28:101193, 2020. ISSN 2352-152X. doi: https://doi.org/10.1016/j.est.2020.101193. URL https://www.sciencedirect.com/science/article/pii/S2352152X19311302.

[81] Benjamin K Sovacool, Jonn Axsen, and Willett Kempton. The future promise of vehicle-to-grid (v2g) integration: a sociotechnical review and research agenda. *Annual Review of Environment and Resources*, 42:377–406, 2017.

[82] Benjamin K Sovacool, Lance Noel, Jonn Axsen, and Willett Kempton. The neglected social dimensions to a vehicle-to-grid (v2g) transition: a critical and systematic review. *Environmental Research Letters*, 13(1):013001, 2018.

[83] Thomas Strasser, Filip Andrén, Johannes Kathan, Carlo Cecati, Concettina Buccella, Pierluigi Siano, Paulo Leitão, Gulnara Zhabelova, Valeriy Vyatkin, Pavel Vrba, and Vladimír Mařík. A review of architectures and concepts for intelligence in future electric energy systems. *IEEE Transactions on Industrial Electronics*, 62(4):2424–2438, 2015. doi: 10.1109/TIE.2014.2361486.

[84] Bjorn CP Sturmberg, Laura Jones, Kathryn Lucas-Healey, Monirul Islam, and Hugo Temby. Niche to normality–an interdisciplinary review of vehicle-to-grid. *arXiv preprint arXiv:2106.05837*, 2021.

[85] Kang Tan, Vigna K. Ramachandaramurthy, Jia Ying Yong, P. Sanjeevikumar, Lucian MIHET-POPA, and F. Blaabjerg. Minimization of load variance in power grids—investigation on optimal vehicle-to-grid scheduling. *Energies*, 10:1–20, 11 2017. doi: 10.3390/en10111880.

[86] Henning Thiesen, Clemens Jauch, and Arne Gloe. Design of a system substituting today's inherent inertia in the european continental synchronous area. *Energies*, 9(8), 2016. ISSN 1996-1073. doi: 10.3390/en9080582. URL https://www.mdpi.com/1996-1073/9/8/582.

[87] Andreas Thingvad, Lisa Calearo, Peter Bach Andersen, and Mattia Marinelli. Empirical capacity measurements of electric vehicles subject to battery degradation from v2g services. *IEEE Transactions on Vehicular Technology*, 70(8):7547–7557, 2021. doi: 10.1109/TVT.2021.3093161.

[88] L. Thurner, A. Scheidler, F. Schäfer, J. Menke, J. Dollichon, F. Meier, S. Meinecke, and M. Braun. pandapower — an open-source python tool for convenient modeling, analysis, and optimization of electric power systems. *IEEE Transactions on Power Systems*, 33(6):6510–6521, Nov 2018. ISSN 0885-8950. doi: 10.1109/TPWRS.2018.2829021.

[89] Anna Tomaszewska, Zhengyu Chu, Xuning Feng, Simon O'Kane, Xinhua Liu, Jingyi Chen, Chenzhen Ji, Elizabeth Endler, Ruihe Li, Lishuo Liu, Yalun Li, Siqi Zheng, Sebastian Vetterlein, Ming Gao, Jiuyu Du, Michael Parkes, Minggao Ouyang, Monica Marinescu, Gregory Offer, and Billy Wu. Lithium-ion battery fast charging: A review. *eTransportation*, 1:100011, 2019. ISSN 2590-1168. doi: https://doi.org/10.1016/j.etran.2019.100011. URL https://www.sciencedirect.com/science/article/pii/S2590116819300116.

[90] Anastasios Tsakalidis and Christian Thiel. Electric vehicles in europe from 2010 to 2017: is full-scale commercialisation beginning. *Joint Research Centre*, 2018.

[91] Harun Turker and Seddik Bacha. Optimal minimization of plug-in electric vehicle charging cost with vehicle-to-home and vehicle-to-grid concepts. *IEEE Transactions on Vehicular Technology*, 67(11):10281–10292, 2018.

[92] Harun Turker and Ilhami Colak. Multiobjective optimization of grid-photovoltaic-electric vehicle hybrid system in smart building with vehicle-to-grid (v2g) concept. In *2018 7th International Conference on Renewable Energy Research and Applications (ICRERA)*, pages 1477–1482. IEEE, 2018.

[93] Thierry Van Cutsem and Costas Vournas. *Voltage stability of electric power systems*, volume 441. Springer Science & Business Media, 1998.

[94] Thierry Van Cutsem, Mevludin Glavic, William Rosehart, Claudio Canizares, Marios Kanatas, Leonardo Lima, Federico Milano, Lampros Papangelis, Rodrigo Andrade Ramos, Jhonatan Andrade dos Santos, et al. Test systems for voltage stability studies. *IEEE Transactions on Power Systems*, 35(5):4078–4087, 2020.

[95] Mart van der Kam and Wilfried van Sark. Smart charging of electric vehicles with photovoltaic power and vehicle-to-grid technology in a microgrid; a case study. *Applied Energy*, 152:20–30, 2015. ISSN 0306-2619. doi: https://doi.org/10.1016/j.apenergy.2015.04.092. URL https://www.sciencedirect.com/science/article/pii/S0306261915005553.

[96] Koen van Heuveln, Rishabh Ghotge, Jan Anne Annema, Esther van Bergen, Bert van Wee, and Udo Pesch. Factors influencing consumer acceptance of vehicle-to-grid by electric vehicle drivers in the netherlands. *Travel Behaviour and Society*, 24:34–45, 2021. ISSN 2214-367X. doi: https://doi.org/10.1016/j.tbs.2020.12.008. URL https://www.sciencedirect.com/science/article/pii/S2214367X20302519.

[97] Wiljan Vermeer, Gautham Ram Chandra Mouli, and Pavol Bauer. Real-time building smart charging system based on pv forecast and li-ion battery degradation. *Energies*, 13(13), 2020. ISSN 1996-1073. doi: 10.3390/en13133415. URL https://www.mdpi.com/1996-1073/13/13/3415.

[98] Dai Wang, Jonathan Coignard, Teng Zeng, Cong Zhang, and Samveg Saxena. Quantifying electric vehicle battery degradation from driving vs. vehicle-to-grid services. *Journal of Power Sources*, 332:193–203, 2016. ISSN 0378-7753. doi: https://doi.org/10.1016/j.jpowsour.2016.09.116. URL https://www.sciencedirect.com/science/article/pii/S0378775316313052.

[99] Jingyuan Wang, Guna R. Bharati, Sumit Paudyal, Oğuzhan Ceylan, Bishnu P. Bhattarai, and Kurt S. Myers. Coordinated electric vehicle charging with reactive power support to distribution grids. *IEEE Transactions on Industrial Informatics*, 15(1):54–63, 2019. doi: 10.1109/TII.2018.2829710.

[100] John Wang, Ping Liu, Jocelyn Hicks-Garner, Elena Sherman, Souren Soukiazian, Mark Verbrugge, Harshad Tataria, James Musser, and Peter Finamore. Cycle-life model for graphite-lifepo4 cells. *Journal of Power Sources*, 196(8):3942–3948, 2011. ISSN 0378-7753. doi: https://doi.org/10.1016/j.jpowsour.2010.11.134. URL https://www.sciencedirect.com/science/article/pii/S0378775310021269.

[101] John Wang, Justin Purewal, Ping Liu, Jocelyn Hicks-Garner, Souren Soukazian, Elena Sherman, Adam Sorenson, Luan Vu, Harshad Tataria, and Mark W. Verbrugge. Degradation of lithium ion batteries employing graphite negatives and nickel–cobalt–manganese oxide + spinel manganese oxide positives: Part 1, aging mechanisms and life estimation. *Journal of Power Sources*, 269:937–948, 2014. ISSN 0378-7753. doi: https://doi.org/10.1016/j.jpowsour.2014.07.030. URL https://www.sciencedirect.com/science/article/pii/S037877531401074X.

[102] Martin Winter, Jürgen O Besenhard, Michael E Spahr, and Petr Novak. Insertion electrode materials for rechargeable lithium batteries. *Advanced materials*, 10(10):725–763, 1998.

[103] Shujie Wu, Rui Xiong, Hailong Li, Victor Nian, and Suxiao Ma. The state of the art on preheating lithium-ion batteries in cold weather. *Journal of Energy Storage*, 27:101059, 2020. ISSN 2352-152X. doi: https://doi.org/10.1016/j.est.2019.101059. URL https://www.sciencedirect.com/science/article/pii/S2352152X19307728.

[104] Guodong Xia, Lei Cao, and Guanglong Bi. A review on battery thermal management in electric vehicle application. *Journal of Power Sources*, 367:90–105, 2017. ISSN 0378-7753. doi: https://doi.org/10.1016/j.jpowsour.2017.09.046. URL https://www.sciencedirect.com/science/article/pii/S0378775317312557.

[105] Gang Xu, Bingxu Zhang, Le Yang, and Yi Wang. Active and reactive power collaborative optimization for active distribution networks considering bi-directional v2g behavior. *Sustainability*, 13(11), 2021. ISSN 2071-1050. doi: 10.3390/su13116489. URL https://www.mdpi.com/2071-1050/13/11/6489.

[106] Fangfang Yang, Dong Wang, Yang Zhao, Kwok-Leung Tsui, and Suk Joo Bae. A study of the relationship between coulombic efficiency and capacity degradation of commercial lithium-ion batteries. *Energy*, 145:486–495, 2018. ISSN 0360-5442. doi: https://doi.org/10.1016/j.energy.2017.12.144. URL https://www.sciencedirect.com/science/article/pii/S0360544217321874.

[107] Low Wen Yao, J. A. Aziz, Pui Yee Kong, and N. R. N. Idris. Modeling of lithium-ion battery using matlab/simulink. In *IECON 2013 - 39th Annual Conference of the IEEE Industrial Electronics Society*, pages 1729–1734, 2013. doi: 10.1109/IECON.2013.6699393.

[108] Jia Ying Yong, Vigna K Ramachandaramurthy, Kang Miao Tan, and N Mithulananthan. Bi-directional electric vehicle fast charging station with novel reactive power compensation for voltage regulation. *International Journal of Electrical Power & Energy Systems*, 64:300–310, 2015.

[109] Masaki Yoshio and Hideyuki Noguchi. A review of positive electrode materials for lithium-ion batteries. *Lithium-Ion Batteries*, pages 9–48, 2009.

[110] Xiang Zhang, Ernst Gockenbach, Volker Wasserberg, and Hossein Borsi. Estimation of the lifetime of the electrical components in distribution networks. *IEEE Transactions on Power Delivery*, 22(1):515–522, 2006.

[111] Xin Zhao, Liuchen Chang, Riming Shao, and Katelin Spence. Power system support functions provided by smart inverters—a review. *CPSS Transactions on Power Electronics and Applications*, 3(1):25–35, 2018. doi: 10.24295/CPSSTPEA.2018.00003.

[112] Yuejiu Zheng, Minggao Ouyang, Languang Lu, Jianqiu Li, Zhendong Zhang, and Xiangjun Li. Study on the correlation between state of charge and coulombic efficiency for commercial lithium ion batteries. *Journal of Power Sources*, 289:81–90, 2015. ISSN 0378-7753. doi: https://doi.org/10.1016/j.jpowsour.2015.04.167. URL https://www.sciencedirect.com/science/article/pii/S0378775315008356.

[113] Ghassan Zubi, Rodolfo Dufo-López, Monica Carvalho, and Guzay Pasaoglu. The lithium-ion battery: State of the art and future perspectives. *Renewable and Sustainable Energy Reviews*, 89:292–308, 2018. ISSN 1364-0321. doi: https://doi.org/10.1016/j.rser.2018.03.002. URL https://www.sciencedirect.com/science/article/pii/S1364032118300728.